

**DEVELOPING NEW ANALYTICAL AND NUMERICAL MODELS FOR MR FLUID
DAMPERS AND THEIR APPLICATION TO SEISMIC DESIGN OF BUILDINGS**

Kambiz Esteki

A Ph.D. Thesis

The Department of Building, Civil, and Environmental Engineering

Concordia University

Montréal, Québec, Canada

June 2014

CONCORDIA UNIVERSITY
SCHOOL OF GRADUATE STUDIES

This is to certify that the thesis prepared

By: **Kambiz Esteki**

Entitled: **DEVELOPING NEW ANALYTICAL AND NUMRICAL MODELS FOR MR
FLUID DAMPERS AND THEIR APPLICATION TO SEISMIC DESIGN OF
BUILDINGS**

and submitted in partial fulfillment of the requirements for the degree of
DOCTOR OF PHILOSOPHY (Civil Engineering)

Complies with the regulations of the University and meets the accepted standards with
respect to originality and quality. Signed by the final examining committee:

Dr.I.Stiharu, MIE _____	Chair
Dr.Najib Bouaanan, École Polytechnique de Montréal _____	External Examiner
Dr.A.Youssef, CIISE _____	External to Program
Dr.O.Pekau, BCEE _____	Examiner
Dr.K.Galal, BCEE _____	Examiner
Dr.A.Bagchi, BCEE _____	Thesis Supervisor
Dr.R.Sedaghati, MIE _____	Thesis Co-Supervisor

Approved by

_____ Chair of department or graduate program director

_____ Dean of faculty

ABSTRACT

Magnetorheological (MR) and Electrorheological (ER) fluid dampers provide a fail-safe semi-active control mechanism for suppressing vibration response of structures as these smart fluids can change their apparent viscosity immediately under the influence of magnetic and electrical fields, respectively. MR based damping devices have recently received appropriate attention as they have less power demand, provide better dynamic range and are less sensitive to the temperature and external contaminants as compared to their ER counterparts.

This thesis studies physics-based modeling of MR fluid dampers and their application in seismic design of buildings. In the first part of thesis, MR damper modeling and its related subject are studied, while in the second part of the thesis, application of MR dampers in tuned mass damper and bracing system is investigated.

The existing models, namely the phenomenological models for simulating the behavior of MR and ER dampers rely on various parameters determined experimentally by the manufacturers for each damper configuration. It is of interest to develop mechanistic models of these dampers which can be applied to various configurations so that their fundamental characteristics can be studied to develop flexible design solutions for smart structures. This research presents a formulation for dynamics analysis of ER and MR fluid dampers in flow and mix mode configurations under harmonic and random excitations. The procedure employs the vorticity transport equation and the regularization function to deal with the unsteady flow and nonlinear behaviour of ER/MR fluid in general motion. Using the developed approach, the damping force of ER/MR damper can be evaluated under any type of excitations.

While tuned mass dampers are found to be effective in suppressing vibration in a tall building, integrating them with semi-active MR based control system enables them to perform more efficiently under varying external excitations. To study the application of MR damper in tuned mass damper, a forty-storey tall steel-frame building assumed to be located in the Pacific Coast region of Canada (Vancouver), designed according to the relevant Canadian code and standard, has been studied with and without semi-active and passive tuned mass dampers. The response of the structure has been studied under a variety of ground motions with low, medium and high frequency contents to investigate the performance of the optimally designed semi-active MR based tuned mass damper in comparison to that of a passive tuned mass damper. It has been shown that the semi-active MR based system modifies structural response more effectively than the conventional passive tuned mass damper in both mitigation of the maximum displacement and reduction of the settling time of the building.

Finally, the effectiveness of MR damper in structural bracing has been examined. Two steel building structures, five and twenty-storey building designed according to Canadian national building code, have been modeled using the finite element method. These building structures have been equipped with MR dampers in different floors appropriately based on the seismic floor-shear distribution. The governing equations of motion of the structures integrated with MR dampers have been cast into the state space representation for the implementation of the full state LQR combined with clipped optimal control strategies. The response of building structures under passive on and active controlled modes have been obtained for low, medium and high frequency content seismic records and compared.

Table of Contents

Chapter 1: Introduction

1.1	Background and motivation	1
1.2	Problem statements.....	5
1.3	Research objectives.....	6
1.4	Organization of the thesis.....	6

Chapter 2: Background and Literature Review.....9

2.1	Introduction.....	9
2.2	Common lateral load resisting systems for buildings.....	9
2.2.1	Moment-resisting frame.....	9
2.2.2	Centrally braced frame.....	10
2.2.3	Eccentrically braced frame.....	11
2.2.4	Shear wall system.....	13
2.3	Passive energy-dissipation system.....	13
2.3.1	Tuned mass damper.....	13
2.3.2	Tuned liquid damper.....	15

2.3.3	Upper storey isolation system.....	16
2.3.4	Friction damper.....	17
2.3.5	Metallic yield damper.....	19
2.3.6	Viscoelastic damper.....	21
2.3.7	Viscous fluid damper.....	22
2.3.8	Base-isolation system.....	25
2.4	Active control energy-dissipation systems	28
2.4.1	Active mass damper system.....	28
2.4.2	Active tendon system.....	29
2.4.3	Active brace system.....	30
2.4.4	Pulse Generation System.....	31
2.5	Semi active energy-dissipation system.....	32
2.5.1	Semi active tuned mass damper.....	33
2.5.2	Semi active stiffness control device.....	34
2.5.3	Semi-active viscous fluid damper.....	35
2.5.4	MR/ER damper.....	35
2.5.5	Flow mode (Valve mode) dashpot damper.....	38

2.5.6	Mixed mode (Shear mode) dashpot damper.....	39
2.6	MR Damper modeling.....	39
2.6.1	Phenomenological model.....	40
2.6.2	Physics-based or Mechanistic model.....	45
2.7	Application of MR damper in bracing system.....	47
2.8	Application of MR damper in tuned mass damper.....	51
2.9	Summary and discussion.....	53
 Chapter 3: Methodology		
3.1	Introduction.....	55
3.2	Analytical quasi-static model of ER/MR damper, Bingham plastic formulation.....	59
3.3	Dynamics model of ER/MR damper.....	62
3.4	Mechanistic model of ER/MR damper.....	62
3.5	A new phenomenological model for random loading in ER/MR damper.....	69
3.6	Modeling of MR-based TMD and MR damper braces in building structure.....	75
3.7	Control algorithms for semi-active system.....	86
3.8	Summary.....	94
 Chapter 4: MR Damper Modeling		

4.1	Introduction.....	95
4.2	Results of the Duct-Flow model.....	95
4.2.1	Case study and numerical analysis.....	96
4.3	Results of the simple Phenomenological model.....	115
4.3.1	Case study 1.....	115
4.3.2	Case study 2.....	117
4.4	Summary.....	125
 Chapter 5: Seismic Response of a Building with Semi-active TMD		
5.1	Introduction.....	127
5.2	Response of the 40-storey building equipped with SATMD.....	128
5.3	Control system tuning.....	140
5.4	Mass ratio effect on response of SATMD system.....	142
5.5	Summary.....	143
 Chapter 6 : Seismic Response of Building with Semi-Active Bracing System		
6.1	Introduction.....	145
6.2	Response of the twenty and the five storey buildings.....	146
6.2.1	Response to seismic record.....	148

6.3	Summary.....	165
Chapter 7: Summary and Conclusion		
7.1	Summary.....	166
7.2	Conclusions.....	167
7.3	Contribution and achievements.....	168
7.4	Limitation.....	170
7.5	Scope for future research.....	171
	References.....	172
	Appendix A: List of Publications based on the present thesis.....	188
	Appendix B: Analytical model of ER/MR damper	190
	Appendix C:TMD design.....	203

List of Figures

Figure 2-1: Concentrically Braced Frames.....	11
Figure 2-2: Eccentrically Braced Frames.....	12
Figure 2-3: Different TMD system configuration.....	14
Figure 2-4: Sloshing damper with meshes, Column damper with orifice.....	15
Figure 2-5: Upper storey isolation systems.....	17
Figure2-6: Damper installation.....	18
Figure 2- 7: Friction damper detail.....	18
Figure 2-8: Metallic yield damper device	20
Figure 2-9: The installation configuration of viscoelastic dampers.....	21
Figure 2-10: Viscous fluid dampers configuration.....	23
Figure 2-11: Viscous fluid damper installation arrangement.....	23
Figure 2-12: Elastomeric bearing with steel shims.....	26
Figure 2-13: Lead plug bearing.....	27
Figure 2-14: Friction pendulum bearing.....	28
Figure 2-15: Passive tuned mass damper versus active tuned mass damper.....	29

Figure 2-16: Schematic diagram of active tendon system.....	30
Figure 2-17: Active bracing system with hydraulic actuator.....	31
Figure 2-18: Pulse generation systems:	32
Figure 2-19: Semi-active tuned mass dampers.....	33
Figure 2-20: Semi active variable-stiffness device.....	34
Figure 2-21: Configuration of semi active viscous fluid damper.....	35
Figure 2-22: Magnetorheological damper configuration.....	36
Figure 2-23: Three operating modes of MR damper.....	37
Figure 2-24: MR damper arrangement installation.....	37
Figure 2-25: Flow mode dashpot damper.....	38
Figure 2-26: Mixed mode dashpot damper.....	39
Figure 3-1:MR fluid polarization.....	56
Figure 3-2: MR damper stress-strain rate relation with and without magnetic field.....	57
Figure 3-3:MR fluid in duct of flow mode damper.....	58
Figure 3-4: Typical velocity profile of MR/ER.....	60
Figure 3-5: Flow mode of ER damper	61
Figure 3-6: Mix mode of ER damper.....	61

Figure 3-7: Approximation of generalizing function for Bingham model.....	65
Figure 3-8: One-dimensional finite-difference grid	67
Figure 3-9: Schematic configuration of the ER damper.....	70
Figure 3-10: The variation of the damping force versus yield stress in ER fluid.....	71
Figure 3-11: The damping force versus yield stress	72
Figure 3-12: Damping force versus strut velocity for different value of α	73
Figure 3-13: Structure and its TMD.....	75
Figure.3-14: Beam frame plan and elevation of 40 storey building.....	77
Figure.3-15: 40 Storey building mode shapes.....	79
Figure 3-16: 40 storey building torsional vibration mode shape.....	80
Figure.3-17: Beam frame plan and elevation of 5 storey building.....	82
Figure.3-18: Beam frame plan and elevation of 20 storey building.....	83
Figure 3-19: State space flow chart for SATMD and TMD analysis.....	91
Figure 4-1: Schematic diagram of the ER damper.....	96

Figure 4-2: Damping force versus piston velocity and displacement of ER damper due to sinusoidal motion of the piston at medium frequency (frequency: 10 Hz, amplitude: 10 mm, $\tau_y = 600 \text{ Kg/cm}^2$).....101

Figure 4-3: Damping force versus piston velocity and displacement of ER damper due to sinusoidal motion of the piston at medium frequency (frequency: 20 Hz, amplitude: 10 mm, $\tau_y = 600 \text{ Kg/cm}^2$).....102

Figure 4-4: Damping force versus piston velocity and displacement of ER damper due to sinusoidal motion of the piston at medium frequency (frequency: 10 Hz, amplitude: 10 mm, $\tau_y = 2500 \text{ Kg/cm}^2$).....103

Figure 4-5: Damping force versus piston velocity and displacement of ER damper due to sinusoidal motion of the piston at medium frequency (frequency: 20 Hz, amplitude: 10 mm, $\tau_y = 2500 \text{ Kg/cm}^2$).....104

Figure 4-6: Damping force versus piston velocity and displacement of MR damper due to sinusoidal motion of the piston at medium frequency in MR damper (frequency: 10 Hz, amplitude: 10 mm, $\tau_y = 350 \text{ Kg/cm}^2$, MR fluid type; MRF-122EG).....105

Figure 4-7: Damping force versus piston velocity and displacement of MR damper due to sinusoidal motion of the piston at medium frequency in MR damper (frequency: 20 Hz, amplitude: 10 mm, $\tau_y = 350 \text{ Kg/cm}^2$, MR fluid type; MRF-122EG).....106

Figure 4-8: Damping force versus piston velocity and displacement of MR damper due to sinusoidal motion of the piston at medium frequency in MR damper (frequency: 10 Hz, amplitude: 10 mm, $\tau_y = 600 \text{ Kg/cm}^2$, MR fluid type; MRF-140CG).....107

Figure 4-9: Damping force versus piston velocity and displacement of MR damper due to sinusoidal motion of the piston at medium frequency in MR damper (frequency: 20 Hz, amplitude: 10 mm, $\tau_y = 600 \text{ Kg/cm}^2$, MR fluid type; MRF-140CG).....108

Figure 4-10: Pseudo-random excitation (combination of 10 and 20 Hz sinusoidal motion) (Top) and damping force (Bottom) in ER damper with $\tau_y = 2500 \text{ Kg/cm}^2$;.....109

Figure 4-11: Random excitation (Top) and damping force (Bottom) in ER damper with $\tau_y = 2500 \text{ Kg/cm}^2$110

Figure 4-12: Random excitation (Top), velocity of random motion (Middle) and damping force (Bottom) in ER damper with $\tau_y = 2500 \text{ Kg/cm}^2$ between 1.5 and 3 second.....111

Figure 4-13: Velocity of random motion of ER damper strut (Blue solid line) and ER damper force (Red dash line) with $\tau_y = 2500 \text{ Kg/cm}^2$ between 2.5 to 2.8 second.....112

Figure 4-14:a)Velocity profile of Newtonian fluid b)Velocity profile of Bingham fluid
c)Velocity profile of Bingham fluid in unstable solution(large diffusion number).....112

Figure 4-15: Snapshots of velocity profile for unidirectional flow; the blue Figure is a manifestation of numerical instability $\alpha \geq 0.005$, while the red curve shows stability in velocity profile.113

Figure 4-16: Maximum damping force in ER/MR damper versus duct length.....114

Figure 4-17: Maximum damping force in ER/MR damper versus duct gap.....114

Figure 4-18: Comparing analytical model (blue) with the proposed model (red); Right -up (frequency=10HZ, $\tau_y = 1500kg/cm^2$).Left-down (frequency=15HZ, $\tau_y = 1500kg/cm^2$).Left-up (frequency=20HZ, $\tau_y = 2500kg/cm^2$).....116

Figure 4-19: Schematic of the full-scale 20-ton MR fluid damper.....117

Figure 4-20: Mechanical model of MR damper118

Figure 4-21: Random excitation (Top) and MR damper models predictions (Bottom) at constant current of I=1 amp.....121

Figure 4-22: Random excitation (Top) and MR damper models predictions (Bottom) at constant current of I=1 amp.....122

Figure 4-23: Random excitation (Top) and MR damper models predictions (Bottom) at constant current of I=1 amp.....123

Figure 4-24: Random excitation (Top) and MR damper models predictions (Bottom) at constant current of I=0 amp.....125

Figure 5-1: Kobe ground acceleration record and its FFT diagram.....130

Figure 5-2: Roof top response of the structure due to Kobe ground motion in time domain.....131

Figure 5-3: Roof top response of the structure due to Kobe ground motion in frequency domain.....131

Figure 5-4: Irpinia ground acceleration record and its FFT in frequency domain.....131

Figure 5-5: Roof top response of the structure due to Irpinia ground motion in time domain.....132

Figure 5-6: Roof top response of the structure due to Irpinia ground motion in frequency domain; TMD effect.....133

Figure 5-7: Kocaeli ground acceleration record and its FFT diagram.....133

Figure 5-8: Roof top response of the structure due to Kocaeli ground motion in time domain.....134

Figure 5-9: Roof top response of the structure due to Kocaeli ground motion in frequency domain; TMD effect.....134

Figure 5-10: Tabas ground acceleration record and its FFT diagram.....136

Figure 5-11: Roof top response of the structure due to Tabas ground motion in time domain.....139

Figure 5-12: Roof top response of the structure due to Tabas ground motion in frequency domain.....137

Figure 5-13: Nahanni ground acceleration record and its FFT diagram.....137

Figure 5-14: Roof top response of the structure due to Nahanni ground motion in time domain.....138

Figure 5-15: Roof top response of the structure due to Nahanni ground motion in frequency domain.....138

Figure 5-16: Upland ground acceleration record and its FFT diagram.....	139
Figure 5-17: Roof top response of the structure due to Upland ground motion in time domain.....	139
Figure 5-18: Roof top response of the structure due to Upland ground motion in frequency domain.....	140
Figure 5-19: Roof top response of the structure with different Q weighting matrix due to Kobe ground motion in frequency domain.....	142
Figure 5-20: Roof top response of structure with different mass ratio for SATMD due to Kobe ground motion in frequency domain.....	143
Figure 6-1:Schematic MR brace location in five storey building.....	146
Figure 6-2: Schematic MR brace location in twenty storey building	147
Figure 6-3: Response of five storey building under KOBE record ground excitation.....	150
Figure 6-4: Response of five storey building under Irpinia record ground excitation.....	151
Figure 6-5: Semi active ON and OFF control command for first floor MR damper up to 50second.....	152
Figure 6-6: Break down of semi active control percentage of ON command for first floor MR damper in five storey building under Irpinia seismic record.....	153
Figure 6-7: Response of twenty storey building under KOBE record ground excitation (1).....	155

Figure 6-8: Response of twenty storey building under Irpinia record ground excitation (1).....156

Figure 6-9: Response of twenty storey building under KOBE record ground excitation (2).....157

Figure 6-10: Response of twenty storey building under Irpinia record ground excitation (2).....158

Figure 6-11: Response of five storey building under Kocaeli record ground excitation(1).....159

Figure 6-12: Response of twenty storey building under Kocaeli record ground excitation(2).....160

Figure 6-13: Response of five storey building under Tabas record ground excitation.....162

Figure 6-14: Response of five storey building under Nahanni record ground excitation.....163

Figure 6-15: Response of five storey building under Upland record ground excitation.....164

List of Tables

Table 2-1: Summary of passive energy dissipation devices in seismic application.....	24
Table3-1: Summary of tall building columns and beams sections.....	78
Table 3-2: 40 storey building vibration frequency and modal participation.....	80
Table3-3: 40 storey building torsional vibration frequency and modal participation.....	81
Table3-4: Summary of twenty storey building columns and beams sections.....	83
Table3-5: Summary of 5 storey building columns and beams sections.....	84
Table3-6: Twenty storey building vibration frequency and modal participation.....	86
Table 3-7: Five storey building vibration frequency and modal participation.....	86
Table 4-1: Configuration parameters of the prototype ER damper.....	98
Table 4-2: Model parameters identified for the large-scale 20-ton MR damper	119
Table5 -1: The name, location and occurrence name of seismic design used in analysis.....	129
Table5-2: Maximum displacements reduction and settling time.....	134
Table 5-3: Maximum displacements reduction and settling time	135

List of Symbols

ω	Vorticity
ρ	Density
σ	Stress
τ	Shear stress
ψ	Stream function
μ	Absolute viscosity
$\dot{\gamma}$	Strain rate
$\tau_{_y}$	Yield stress in ER/MR fluid
α	Dimensionless numerical diffusion number
ν	Kinematic viscosity
γ	Thermal expansion coefficient
L	Length of duct in MR/ER damper
n	Stress growth exponent
N	Number of nodes in finite different grid
F_d	Damping force in ER/MR damper
u	Velocity
t	Time

Sign	Sign function
h	High of the Chanel
U	Velocity of Chanel wall
Q	Volumetric flow rate
g	Gravity
p	Pressure
A_p	Piston area
A_s	cylinder area
h	plug thickness
e	base of the natural logarithm
k	stiffness
m	mass
c	damping coefficient
ω	structural frequency
I	electric current, unity matrix

List of Abbreviations

MR damper.....	Magnetorheological damper
ER damper.....	Electrorheological damper
TMD.....	Tuned mass damper
SATMD.....	Semi active tuned mass damper
CFD.....	Computational fluid dynamics

Chapter 1: Introduction

1.1. Background and motivation

Earthquakes are very destructive and devastating natural hazards. During the last decade, earthquakes have taken a heavy toll on lives which shocked the world (United States Geological Survey, 2013). For example, in Japan, 2011 earthquake, at least 15,550 people were killed, 5,344 missing, 5,314 injured, 130,927 displaced and at least 332,395 buildings, 2,126 roads, 56 bridges and 26 railways were destroyed or damaged by the earthquake and accompanying tsunami. The total economic loss in Japan was estimated at 309 billion US dollars. Recently, the 8.2 magnitude quake that shook northern Chile in 2014 killed six people and caused a tsunami with 2-meter waves. In addition, 900,000 people had evacuated and more than 2,600 homes were damaged. In Haiti, 2010 earthquake, according to official estimates, 316,000 people were killed, 300,000 injured, 1.3 million displaced, 97,294 houses destroyed and 188,383 damaged in the Port-au-Prince area and in much of southern Haiti. In China, 2008 earthquake, at least 69,195 people were killed, 374,177 injured and 18,392 missing and presumed dead in the Chengdu-Lixian-Guangyuan area. More than 45.5 million people in 10 provinces and regions were affected. At least 15 million people were evacuated from their homes and more than 5 million were left homeless. An estimated 5.36 million buildings collapsed and more than 21 million buildings were damaged. The total economic loss was estimated at 86 billion US dollars. In Pakistan, 2005

earthquake, at least 86,000 people were killed, more than 69,000 were injured, and extensive damage occurred in northern Pakistan. In Sumatra, 2004 earthquake, in total of 227,898 people were killed or were missing and presumed dead and about 1.7 million people were displaced by the earthquake and subsequent tsunami in 14 countries in South Asia and East Africa. In Iran, 2003 earthquake, about 31,000 people were killed, 30,000 were injured, 75,600 were rendered homeless and 85 percent of buildings were damaged or destroyed in the Bam area. The maximum acceleration of 0.98g was recorded in Bam that was believed to be the largest earthquake in this area in more than 2000 years.

In the face of such an unpredictable, imminent and enormous human tragedy, earthquake engineering plays an important role. Over the past few decades, earthquake engineering has developed as a branch of engineering concerned with reduction of earthquake risks. It has become an interdisciplinary subject including information technology, urban planning, structural, seismologists and geotechnical engineering, architects and social scientist. In the context of earthquake engineering, structural engineering plays an important role which concerns with designing structural systems and technologies that can withstand vertical and lateral seismic loading and to prevent buildings and structures from collapsing during earthquake.

The following four different approaches have been developed to dissipate the vibratory energy due to lateral seismic loadings on structures and building: 1) Passive systems, 2) Active systems, 3) Semi active systems, and 4) Hybrid systems. Conventional seismic design of a structure mainly relies on the ductility of the structure to dissipate seismic-generated vibration energy while accepting a certain level of structural damage. Passive system is the most widely used system. Passive systems apply forces on the structure by reacting to the motion of the structure to dissipate vibration energy. The drawback of passive system is that they cannot be adapted to

varying loading conditions but they are usually simple in design, cheap in cost and very reliable and robust in performance. Example of a passive system is hydraulic damper. Passive system is considered as stable system because they don't induce energy into structure and they do not need extra power source during operation time.

In recent years a more versatile and more sophisticated system called active control system was introduced for vibration mitigation of the structure. Active control system measure the vibration disturbance of the structure (such as accelerations) and compute the proper counteracting forces to reduce the vibration effect (displacement, velocity or acceleration) according to a specified control system strategy. These forces as determined by the control system are then applied by the actuators connected to the system. The advantage of active control system is that they can adjust applied forces to accommodate different environmental changes such as seismic event. On the other hand, these active forces that are supposed to be applied in proper position to decrease a structure's response may initiate instability in the structure. Furthermore, generating control forces requires large power supply, which cannot be guaranteed during an earthquake. In addition, active systems are not as robust or reliable as passive systems. The technology and equipment that are used in active control are still in preliminary stages and not readily adopted for structural applications with seismic loading yet.

Semi-active systems offer another alternative in control of structural response. The concept of semi-active control is to adjust system vibration characteristics (mass, damping or stiffness) to minimize the response of the structure under seismic loading. The manipulation of the mass of a structure as with Tuned Mass Damper (TMD) can be accomplished by moving (or prevent from moving) auxiliary masses during earthquake occurrence to mitigate the structural response (e.g., Semi active TMD, Active TMD and Hybrid TMD). The variable damping system

is feasible by using variable orifice hydraulic jack or Magneto-Rheological (MR) damper. Semi active systems are usually activated with very small power supply as compared to those associated with active control systems. They also do not cause structural instability as they do not introduce extra energy to the structure. The function of a semi-active system during loading is controlled by a control system and the level of performance achieved is between that of corresponding active system (upper band) and a passive system (lower band).

Between different semi-active devices, MR dampers have attracted significant attention recently due to their high dynamic range and less power consumption. MR damper has two main parts in addition to a regular damper, which are MR fluid and an electromagnetic coil that generates the magnetic field. MR fluid consists of tiny iron particle suspended in a carrier fluid. If a magnetic field is applied to the MR fluid, the suspended iron particles will form a chain like structure that can change the apparent viscosity of the MR fluid and transform the liquid to semi solid. The change in the apparent viscosity can significantly affect the damping force in MR damper. Thus, by varying the level of magnetic field applied to the MR damper, a variable damping force can be produced. MR damper reacts to magnetic field in a millionth of a second make it a unique device for real-time vibration control applications. It should be noted that the MR damper damping force depends on not only the viscosity of the fluid but also on the velocity of the damper strut.

MR-based energy absorption devices provide the reliability and fail-safe feature of the passive systems while maintaining the adaptability of active systems with minimal power requirements. Thus they can be effectively utilized for vibration control of civil infrastructures under varying environmental changes.

1.2. **Problem statement**

This research concerns with analysis, optimization and control of buildings integrated with MR based semi-active devices. For this purpose, initially it is required to develop a mathematical model for the MR damper to effectively predict its behaviour under different magnetic field intensities and varying external excitations. Phenomenological models are widely used to characterize MR damper behaviour. These models are experiment-based in which a volume of experimental data is required to identify the characteristic parameters of the model. While, phenomenological models are simple and may be easily used for control applications, their characteristic parameters are tuned to a particular damper and external excitation. Moreover, phenomenological model cannot be used to design a new MR damper where no experimental data exists. Considering the above, a physics-based model, which considers material and geometrical properties of MR fluid and dampers, respectively, is required to effectively predict the dynamic characteristics of any type of MR damper under any external excitations.

Integration of multiple MR dampers into the structural systems and development of a model to predict the overall system response under random external excitations are important issues that need to be addressed. It should be noted that most of the research works on MR damper in civil engineering structures are mainly limited to small scale or prototype lab scale structures. In addition, the use of MR dampers in these research works is mostly limited to one or two MR damper in one or two floors, which may not represent practical applications. Furthermore, ground motion records, which are utilized in most previous works, are very limited. Further studies are required with more complex applications and a wide range of ground motion records for seismic analysis of buildings and bridges.

1.3. Research objectives

The proposed research has the following three main objectives:

- To develop a physics-based or mechanistic model of MR fluid dampers that can be used for studying the behaviour of such dampers of different sizes and capacities, subjected to harmonic and random excitations.
- To study the effectiveness of MR fluid dampers in building structures utilizing tuned mass dampers to improve their seismic performance.
- To study the effectiveness of MR fluid dampers integrated in the bracing systems of building structures to improve their seismic performance.

1.4. Organization of the thesis

Chapter one is dedicated to motivation, problem statement, research objectives and thesis organization. Chapter two covers passive, semi-active and active systems in building structures and review of pertinent literature on the subject including MR damper modeling, MR damper application in bracing systems, and MR damper application in TMD systems. Chapter three addresses the development of a new physical and phenomenological models for ER/MR damper and analysis of application of MR damper in TMD systems and in bracing systems, respectively. The developed physic-based model for ER/MR damper can estimate dynamic behaviour of

MR/ER damper in both flow and shear modes. Although proposed physic-based model is versatile and accurate, it may not be suitable and practical to be incorporated into complex structural numerical model for the simulation analysis. For this purpose, a new phenomenological model has been proposed based on the results of the developed physic-based model in chapter three. Due to its simplicity, the model can be easily integrated into the numerical analysis. The relevant parameters of this model have been estimated for a MR damper with 200 kN capacity.

The results of the proposed MR damper models are presented in Chapter four. First, the proposed physic-based model has been evaluated and compared to another model along with available experimental results. The proposed phenomenological model has also been evaluated versus Bou-Wen model for harmonic and random vibration.

The results of application of MR dampers in tuned mass damper for tall building structures have been presented in Chapter five. A forty-storey building has been designed according to National Building Code of Canada (NBCC). The behaviour of building with passive tuned mass damper and semi-active MR based tuned mass damper has been studied under low, medium and high frequency content seismic records.

Chapter six addresses the application of MR dampers in bracing system for medium and short buildings. Two building structures, five and twenty-storey high, integrated with MR dampers in bracing configuration and designed according to NBCC provisions have been investigated for passive and semi-active modes.

Finally Chapters 7 summarizes the most important achievements and conclusions on results. Limitations of the present research and scope for further research have also been identified in this Chapter.

Chapter 2: Background and Literature Review

2.1. Introduction

This chapter presents some fundamental discussion on supplemental damping systems utilized in structures to control their dynamic response. Supplemental damping system used in structures can be of the following types: passive, semi active and hybrid energy dissipation systems. A state-of-the art literature review pertaining to the current research covering MR damper modelling techniques and application of MR damper in tuned mass and bracing system in multi-storey buildings are provided in this chapter. Commonly used lateral load resisting systems in buildings are also discussed in this chapter.

2.2. Common lateral load resisting systems for buildings

2.2.1. Moment-resisting frame

Steel moment-resisting frames are assemblies of columns and beams that are typically connected by welding or bolting. In Reinforced Concrete (RC) frames, the beam-column joints are specially detailed to transfer moments. Resistance to lateral loads is provided by flexural and shearing actions in the beams and the columns. The design of the connection in moment-resistance frame

should be such that cause formation of the plastic hinge in beam during the earthquake. The plastic hinge in the beam provides an energy dissipation mechanism. To form and use such an energy dissipation mechanism, a designer should prevent formation of the plastic hinge in the connection or column. Formation of plastic hinges in columns (except at bottom of the ground floor columns) will jeopardize the structural stability and could trigger collapse. On the other hand, plastic hinge in a connection appear to damage and destroy the connection.

2.2.2. Concentrically braced frame

Concentrically braced frames are used to provide lateral resistance and stiffness to steel frame buildings in order to resist wind and earthquake loading. A correctly designed brace can provide plastic deformations and dissipate hysteretic energy in a sustained manner through sequential buckling in compression and yielding in tension.

The design philosophy is to ensure that plastic deformations only happen in the braces, leaving the columns, beams, and connections intact. Braces can be design as tension only or tension-compression member. Tension-compression braces have larger hysteresis loop, and as a result a large amount of vibration energy can be dissipated. Braces can have very versatile installation arrangement but usually they are installed between beams and columns as shown in Figure 2-1.

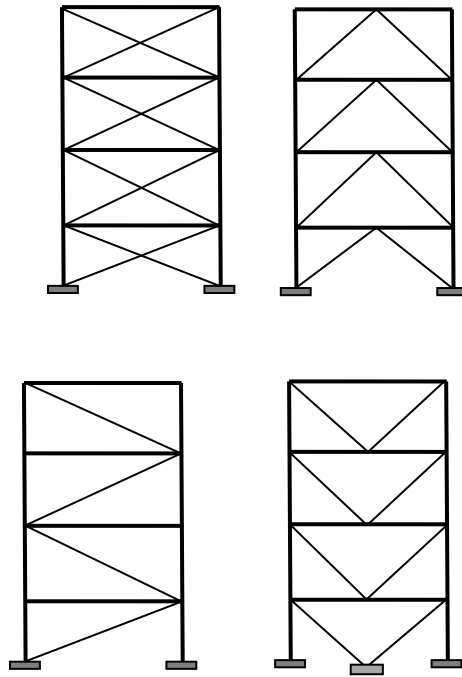


Figure 2-1: Concentrically Braced Frames

2.2.3. **Eccentrically braced frame**

Concentric brace frame have a large lateral stiffness but their energy dissipation capacity is rather limited by buckling of the braces. On the other hand, a moment resisting frame has higher energy dissipation mechanism but they do not provide adequate lateral stiffness for a structure. Eccentrically Braced Frame has the advantages of both the steel moment frame and braced frame.

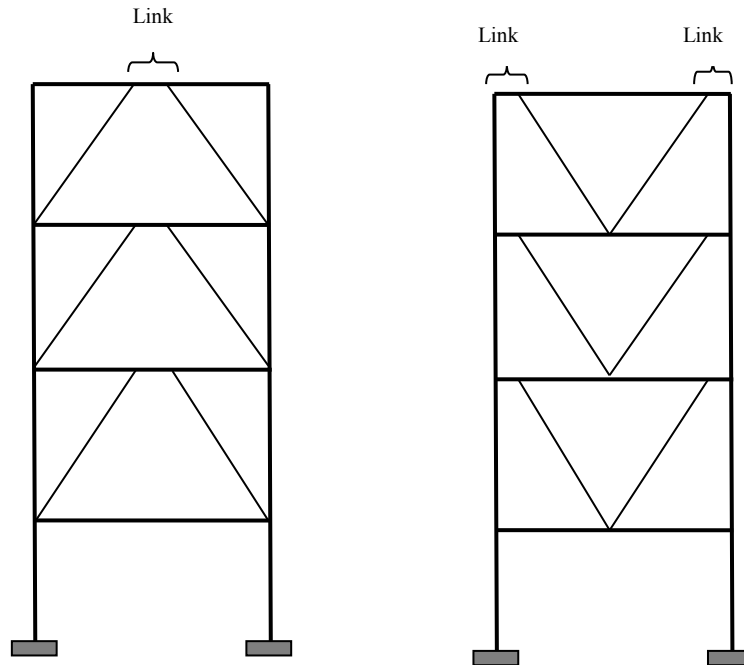


Figure 2-2: Eccentrically Braced Frames

An eccentrically braced frame is a framing system in which the axial force induced in the braces are transferred through shear and bending in a small segment of the beam which is called Link. Links in EBFs act as structural fuses to dissipate the earthquake vibration energy in a structure in a sustained manner. A link needs to be properly designed and detailed to have adequate strength and stable energy dissipation. All other structural elements should remain essentially elastic during seismic event. Eccentric brace frames installation arrangements and their links are demonstrated in Figure 2-2.

2.2.4. Shear wall system

Shear wall are stiff vertical panels in structure that transfer lateral load from upper floors of buildings to lower floors and foundation of the buildings. Shear walls can be made of concrete or steel but comparing to other structural elements and components, they should have relatively much higher lateral stiffness so that they can absorb lateral forces induced by wind or seismic loading. Shear wall are usually used in medium to high rise concrete structure as primary lateral resistance system. The amount of energy that a concrete shear wall can dissipate during lateral loading depends on level of ductility of concrete walls. Dissipation energy can be quite large for a well-designed ductile concrete shear wall.

2.3. Passive energy-dissipation system

Passive energy-dissipating systems are external add-on damping devices which commonly utilized to dissipate structural vibration energy without requiring external power sources to operate. They basically react to the structural deformation through resisting damping forces to suppress vibration. Examples of dissipation devises include tuned mass dampers, tuned liquid dampers, viscous-elastic dampers, metallic yield devices, friction devices, and viscous fluid dampers, which will be briefly described in the subsequent sections.

2.3.1. Tuned mass damper

A tuned mass damper (TMD) is a passive damping device that consists of a mass, a spring, and a damper. TMD is mainly attached to the main structure to reduce its dynamic response. Different configurations of the TMD are shown in Figure 2-3. The frequency of tuned mass damper is

usually tuned to fundamental (first) natural frequency. Thus when the structure is excited at a frequency close to its fundamental frequency, the TMD will generate the counteracting out-of-phase damping force to dissipate the energy in case of severe vibration in resonance condition. . TMD's overall effect can be considered as increasing the equivalent damping ratio of the main structure. The restoring force can be produced by a spring (Fig. 2-3c,d,e), by a bearing shape or by a gravity load in a pendulum type TMD (Fig. 1-1 a,b). The damping force can be generated by a dashpot damper (Fig. 2-3 a,c,d,e) or by viscoelastic type materials such as rubber (Fig. 2-3 f). There are some disadvantages in TMD applications though. TMDs are mainly effective on their tuned frequency. Thus they may not be very effective for ground excitation which usually contains many different frequencies. They are also very sensitive to de-tuning. Moreover, they typically occupy large space and contain large mass.

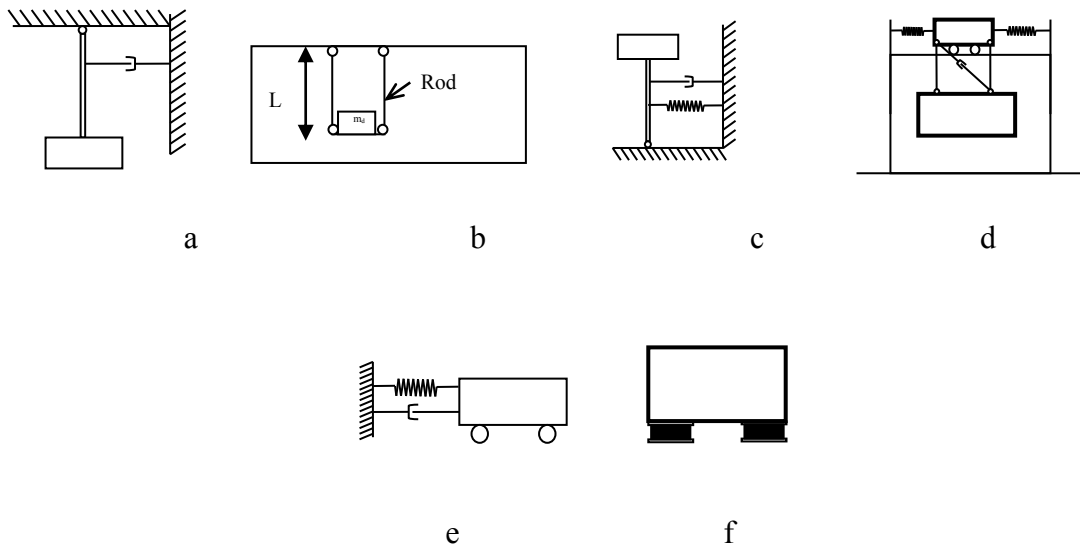


Figure 2-3: Different TMD system configuration (Cheng et al,2008)

2.3.2. Tuned liquid damper

In Tuned Liquid Dampers as shown in Figure 2-4, water acts as the mass in motion and the restoring force is produced by gravity. The building vibration rocks the container which causes water movement inside the container. The turbulence of water flow and the friction between water and the container convert the dynamic energy of water flow to heat, thus dissipate structural vibration energy. Installing sloshing damper with meshes and rods and or column damper with orifice will help absorbing structural energy as shown in Figure 2-4. It is interesting to note that all three components of a typical TMD system (i.e., mass, damping, and restoring mechanisms) are provided by water.

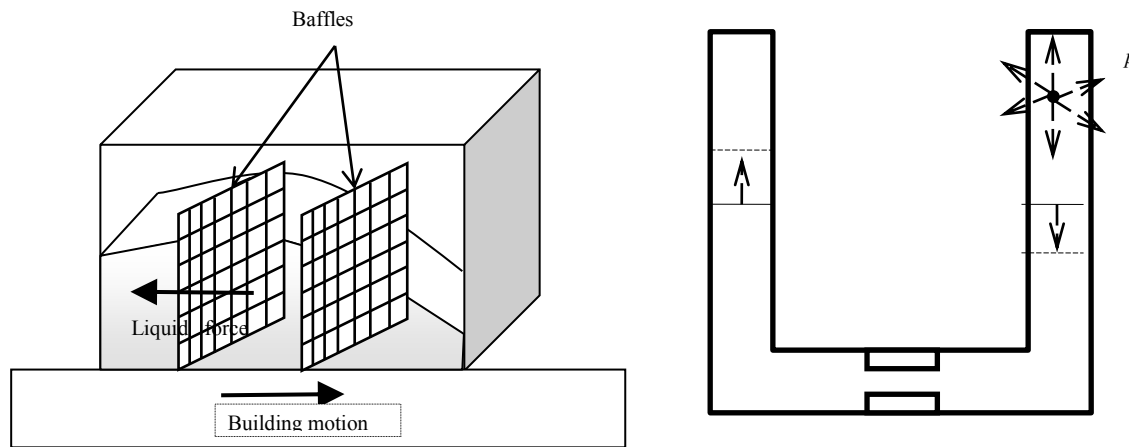


Figure 2-4: Sloshing damper with meshes, Column damper with orifice (Cheng et al,2008)

2.3.3. **Upper storey isolation system**

The mechanism of decreasing structural vibrations by attaching a TMD to the structure is to transfer the vibration energy of the structure to the TMD and to dissipate the energy in the damper of the TMD. However, overall performance is limited by the weight of the auxiliary mass (normally about 1% to 3% of building weight). To increase the performance of the TMD without increasing structural weight, a portion of the building itself can be used as a mass damper. For example, the building's top storey may be used as a tuned mass damper. The concept of an 'expendable top storey' was introduced by Jagadish et al. (1979), and the 'energy absorbing storey' was presented by Miyama (1992). As it is illustrated in Figure 2-5, top 4 floors of the building are used as TMD. To adjust the stiffness of top floors to TMD stiffness requirement, columns are discontinued at the top floor and the top floors are supported on a base isolation system which reduces and adjusts the stiffness of the top floors. Energy dissipation capacity of this configuration can be enhanced by interdicting viscous damper as illustrated in Figure 2-5.

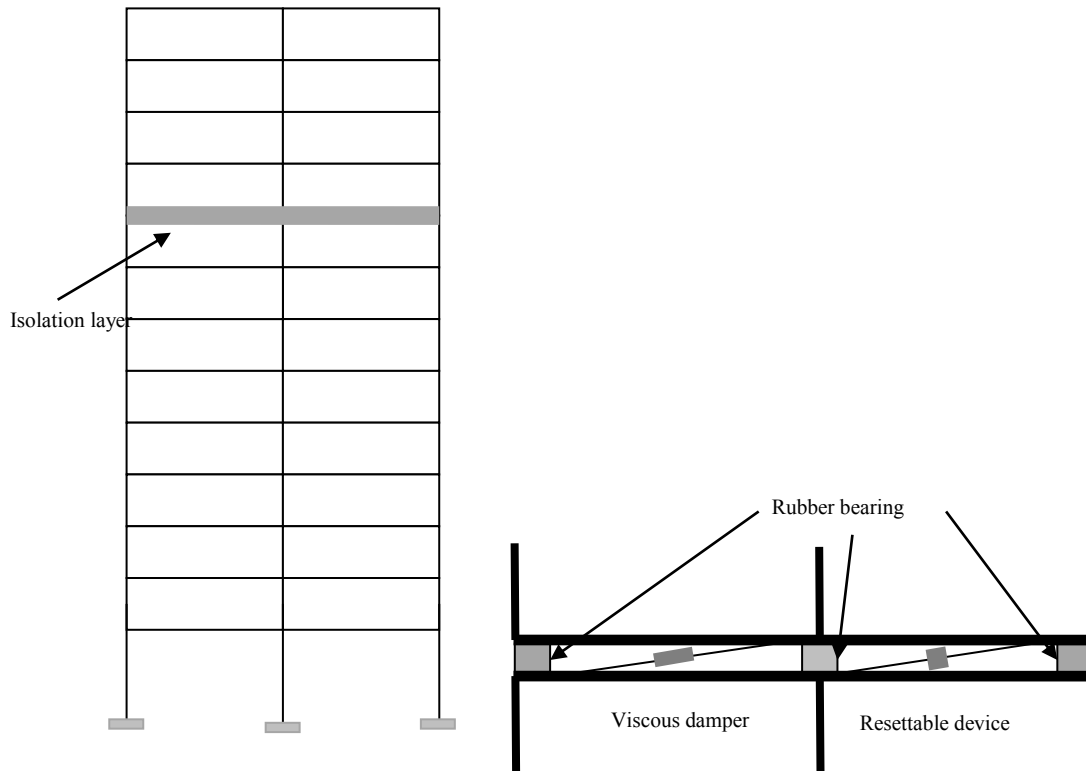


Figure 2-5: Upper storey isolation systems (Cheng et al. 2008)

2.3.4. Friction damper

Friction dampers are devices which depend on the friction developed between two solid interfaces sliding relative to one another to dissipate structural vibration. During severe earthquakes, the device starts slipping at a predetermined load and thus generating energy dissipation by friction. Another feature of friction damped buildings is that their natural period varies with the amplitude of vibration. Hence during a seismic event, a friction damper device shifts the fundamental frequency of a structure away from the earthquake's resonant frequency. Friction dampers have large rectangular hysteresis loops which indicate their capacity to

dissipate vibration energy. The performance of friction dampers depend on velocity and temperature. Friction dampers are designed not to slip during wind. Another advantage of friction dampers apart from being reliable and inexpensive is that they do not need regular inspection, maintenance or repair after installation. The friction damper installation arrangement and detail are depicted in Figure 2-6 and 2-7, respectively.

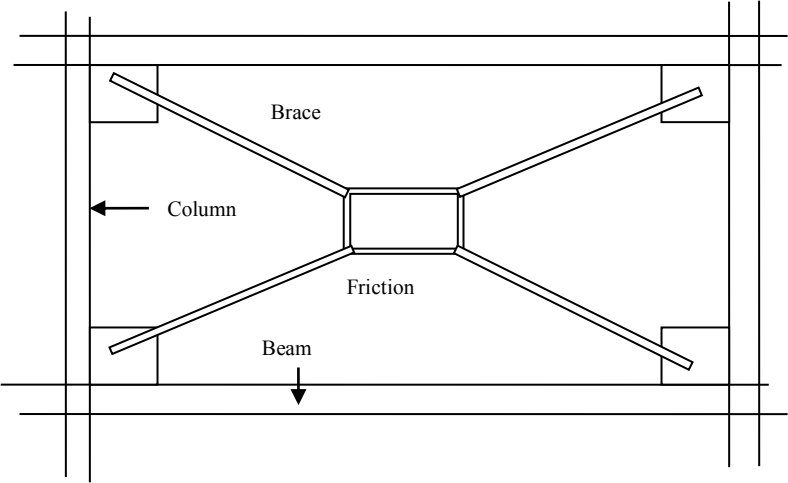


Figure 2-6: Damper installation

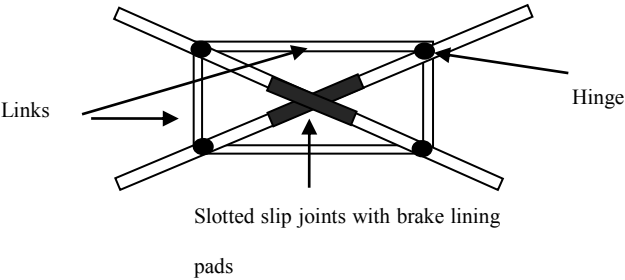
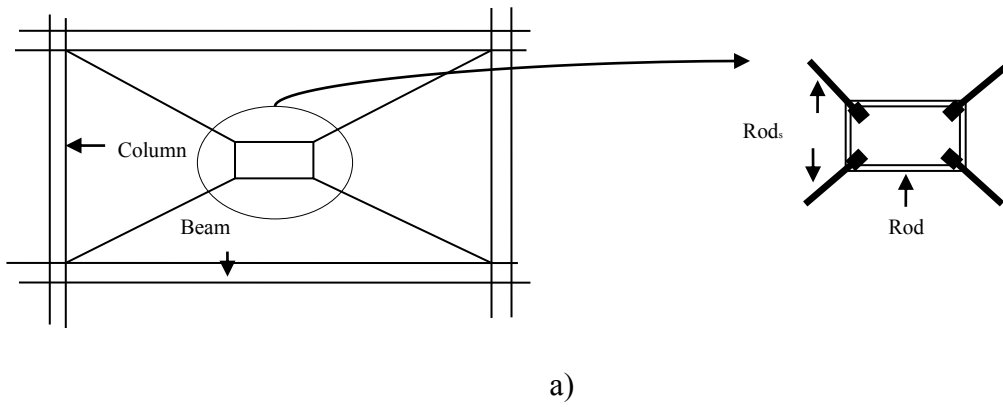


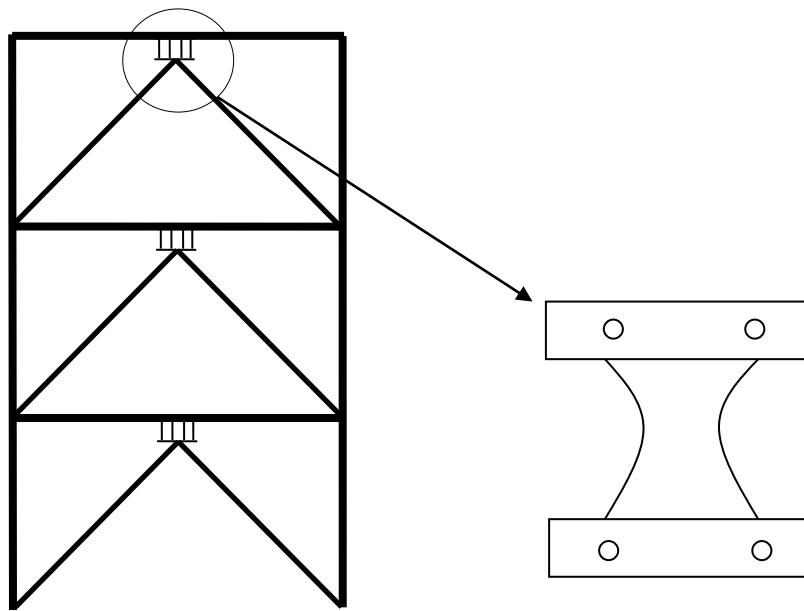
Figure 2- 7: Friction damper detail (Cheng et al, 2008)

2.3.5. **Metallic yield damper**

Plastic deformation of metallic materials is an effective phenomenon for vibration energy dissipation. The classic earthquake design of structures depends on plastic behaviour and ductility of structural members to dissipate seismic vibration energy. Many kinds of metallic yield devices have been invented. For example in Figure 2-8, the mechanism dissipates energy by hysteretic behaviour in plastic tensile deformation of the rectangular steel frame in tension brace. The other device (Figure 2-8 b) consists of multiple plates, and yielding occurs over the entire X like portion of the device. Moment-resisting frame, concentric brace and eccentrically brace discussed before may be considered as the classical metallic yield systems.



a)



b)

Figure 2-8: a) Metallic yield damper device installation arrangement and detail b) Metallic yield damper device installation arrangement and detail (Cheng et al, 2008)

2.3.6. Viscoelastic damper

A viscoelastic material is characterized by possessing both viscous and elastic behaviour. An elastic material is one in which all the energy stored in material during loading is recovered once the load is removed. On the contrary, a viscoelastic material returns the energy stored during loading phase with a delay or out of phase angle, θ . The magnitude of angle θ provides an indication of the damping level of the materials. A larger magnitude of θ would mean a larger value of damping in the material. Viscoelastic solid dampers usually consist of elastomeric viscoelastic pads attached to steel plates. The steel plates can be attached to a structure by a bracing system. Viscoelastic dampers generally behave linearly which simplifies the analysis and design for seismic application.

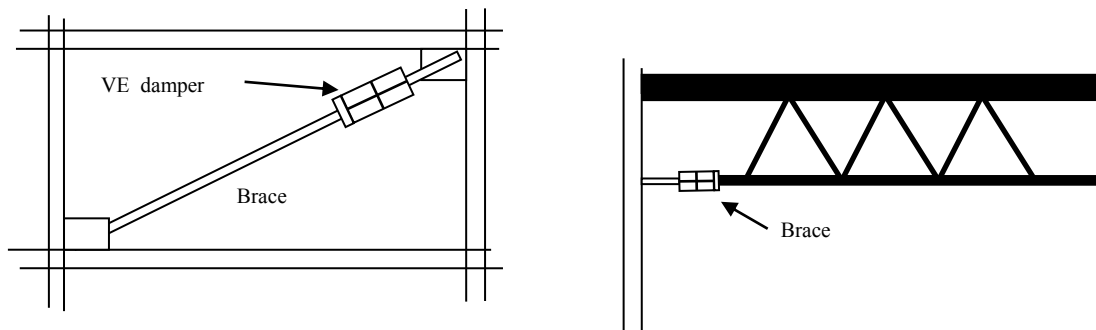


Figure 2-9: The installation configuration of viscoelastic dampers (Cheng et al,2008)

One obvious disadvantage of viscoelastic devices is that their properties are influenced by many parameters including frequency, static pre-loading condition, temperature, dynamic strain rate, aging, creep, relaxation, and other effects. Visco-elastic devices exhibit a behaviour which is

somewhere between that of a damper and a spring; and unfortunately, under a high level of seismic vibration, the spring behaviour dominates the response of a viscoelastic damper. The installation configuration of viscoelastic dampers is shown in Figure 2-9.

2.3.7. **Viscous fluid damper**

Viscous fluid dampers are commonly used as passive energy dissipation devices for mechanical systems. Automotive shock absorbers are example of viscous fluid dampers system. Viscous fluid dampers as shown in Figure 2-10 consist of a hollow cylinder filled with silicone-based fluid. As the damper piston rod and piston head are stroked, fluid is forced to flow through an orifice. This movement causes differential pressure across the piston head, which can subsequently generate very large forces to prevent the relative motion of the damper. In the other words, the energy is dissipated by the friction between the fluid and the orifice. The biggest advantage of the viscous fluid damper is its reliability. Because of their extensive usage in mechanical system and long history of successful application since early 1900, there is no mystery in their behaviour and applications. They are rather inexpensive, reliable, easy to use and very high capacity (up to 40-50% of critical damping). The viscous fluid damper is usually integrated with the bracing system as shown in Figure 2-11.

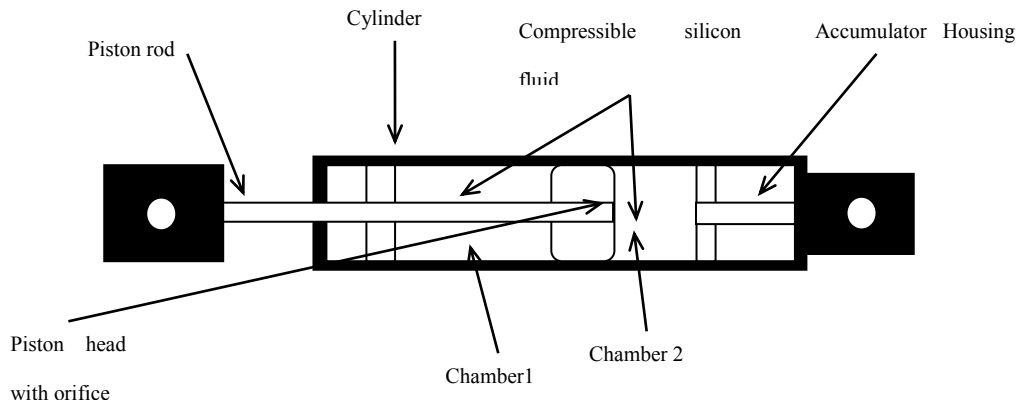


Figure 2-10: Viscous fluid dampers configuration (Cheng et al, 2008)



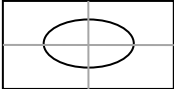
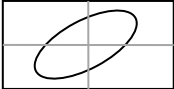
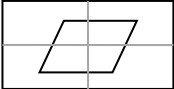
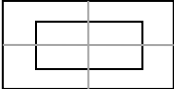
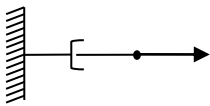
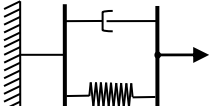
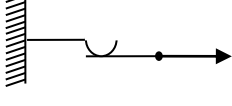
Figure 2-11: Viscous fluid damper installation arrangement (Symans et al, 2008)

Experimental testing has demonstrated that a mathematical model of a viscous fluid damper can be described using Eq. (2-1), in which u is velocity, and C and α are constant parameters to be determined by experiments.

$$P(t) = C|u(\dot{t})|^\alpha \text{sgn}[u(\dot{t})] \quad (2.1)$$

Summary energy dissipation devices are provided in Table 2-1.

Table 2-1: Summary of passive energy dissipation devices in seismic application (Symans et al, 2008).

	Viscous fluid damper	Viscoelastic solid damper	Metallic damper	Friction damper
Idealized hysteresis behaviour				
Idealized mechanical model			Idealized model not available	
Advantage	Active at low displacements Minimal restoring force Easy modeling Properties largely independent of frequency and temperature Proven record of performance	Activated at low displacements Provide restoring force Linear behaviour and easy modeling	Stable hysteresis behaviour Long term reliability Insensitive to ambient temperature Material and behaviour familiar to practicing engineers	Large energy dissipation per cycle Insensitive to ambient temperature
Disadvantage	Possible fluid seal leakage	Limited deformation capacity Properties largely dependent on frequency and temperature. Possible deboning and tearing of VE material	Device damaged after earthquake Nonlinear behaviour and may need nonlinear behaviour	Permanent displacements if no restoring force mechanism provided Strongly nonlinear behaviour and required nonlinear analysis Sliding interface conditions may change with time

2.3.8. **Base-isolation system**

Base isolation of structures is one of the most widely used methods of protecting structures against seismic loads. It is a passive control device that is installed between the foundation and the base of the building. The base isolation device provides flexibility in the base of a structure in lateral direction (instead of fixed) which increases the first period of the structure. It is noted that the buildings with large time periods attract less seismic force. In addition, the base isolation itself dissipates large amount of induced energy because of its non-linear behaviour and hysteresis loop.

The main effect of base isolation system is altering the fundamental period of a structure. Therefore, base isolation is an effective tool for providing seismic protection for low- and middle-rise structures because these types of buildings have high frequencies. There are two major base-isolation systems: Elastomeric Bearing and Friction Bearing.

Elastomeric Bearing

Elastomeric bearings were originally made from natural rubber and then their properties were improved by adding steel plates as shown in Figure 2-12. Owing to the flexibility of rubber properties, elastomeric bearings will prolong fundamental period of the structure but because of low critical damping, elastomeric bearings have little resistance to lateral service load. Consequently, additional damping devices are required in order to control higher lateral loads otherwise it may cause structural instability.

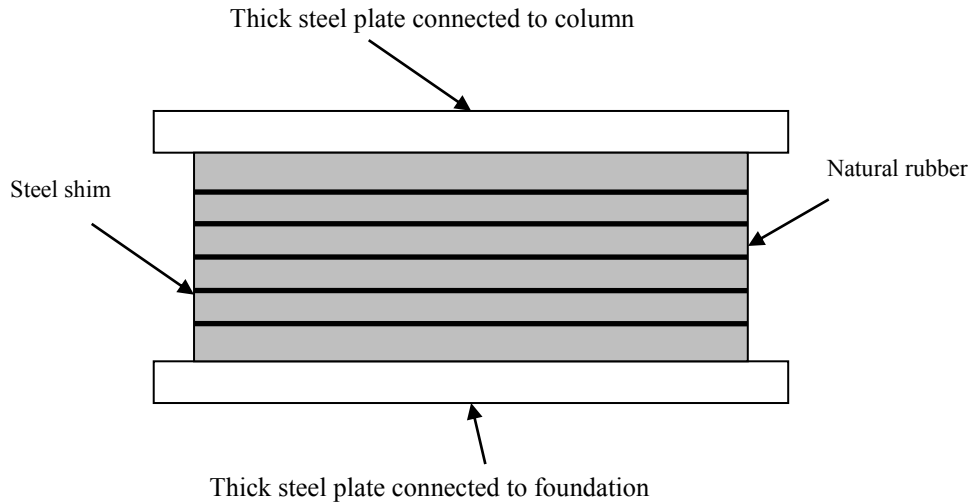


Figure 2-12: Elastomeric bearing with steel shims (Cheng et al, 2008)

Lead-Plug Bearing

The low-damping properties of the elastomeric bearings can be resolved by plugging a lead core into the bearing as shown in Figure 2-13. The performance of the lead-plug bearing depends on the induced lateral force. When the lateral force is small, the movement of the steel shims is prevented by the lead core, and the bearing demonstrates higher lateral stiffness. As the lateral force increases, lead core will yield. Yielding of lead provides hysteretic damping which dissipate the vibration energy. As the results of the yielding of lead core, the lateral stiffness of the bearing will be reduced.

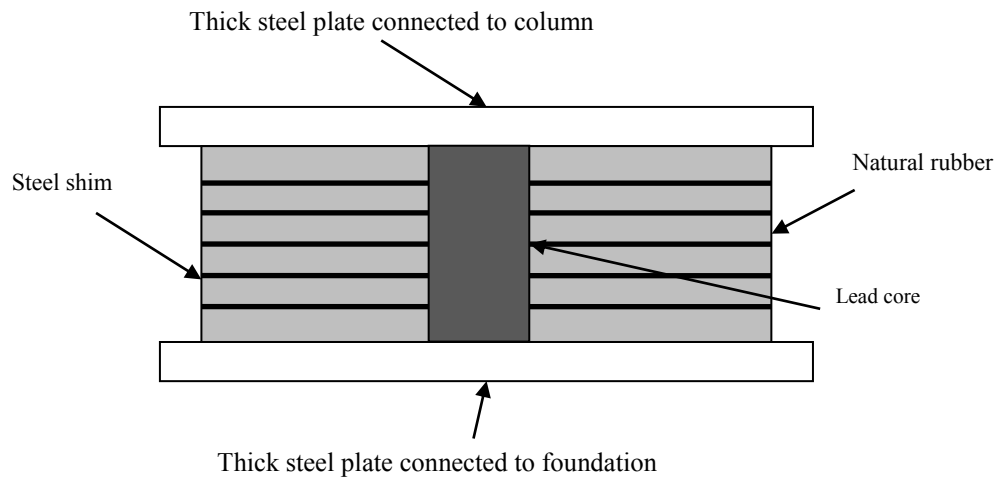


Figure 2-13: Lead plug bearing (Cheng et al, 2008)

Friction Pendulum Bearing

The original friction bearing has flat sliding surfaces. The induced lateral force is resisted by the product of the friction coefficient and the vertical load applied on the bearing. The major disadvantage of the friction bearing with flat sliding surfaces is that the building structure is unable to return to its original position after an earthquake. This disadvantage has been overcome by the development of modified friction pendulum bearing systems. In the modified friction pendulum bearing systems, spherical or concave sliding surface help structure to maintain its initial position after seismic event. A friction bearing with a spherical or concave sliding surface is shown in Figure 2-14. The Teflon coat provides a coefficient of friction of 3% and protects the sliding surface from corrosion. The bearings have a very low maintenance as they slide only during an earthquake. The coated Teflon can basically last for the entire design life span of the structure.

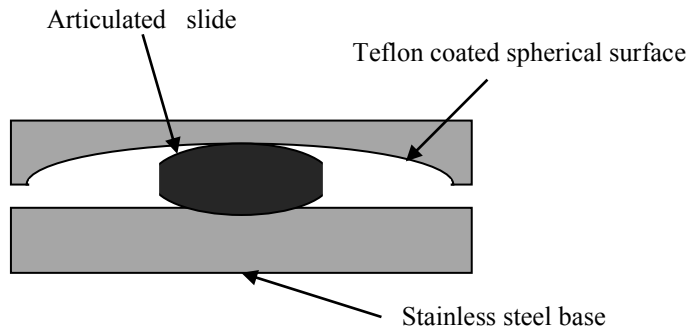


Figure 2-14: Friction pendulum bearing (Cheng et al. 2008)

2.4. Active control energy-dissipation systems

In active control systems, the external forces are exerted to the structures using actuators in order to damp out the excessive vibration. Basically structural responses are measured using sensors, and then using pre-defined control strategy, the required counteracting forces to damp out the vibration are evaluated. The actuators are then commanded to exert these forces. While active control dissipation systems can adapt themselves to the varying environmental changes, they require large power sources, complex and expensive hardware. In addition, as they induce energy to the system using active forces, they may destabilize the structure if not properly designed. In the following, the most common active control system used in structures is discussed.

2.4.1. Active mass damper system

As discussed before, the passive tuned mass dampers are mainly effective for structural vibration control when the first mode is dominant, such as wind loading. On the other hand, active tuned mass dampers can adapt themselves to the varying frequency and thus they are very effective for

control of structural response in an earthquake with a wide frequency band. In active tuned mass damper systems as shown in Figure 2-15, an actuator is placed between the structure and the auxiliary mass. The movement of auxiliary mass can be controlled by the actuator to increase structural control effectiveness. The function of actuator itself is controlled by a control system that is designed to minimize the structural vibration.

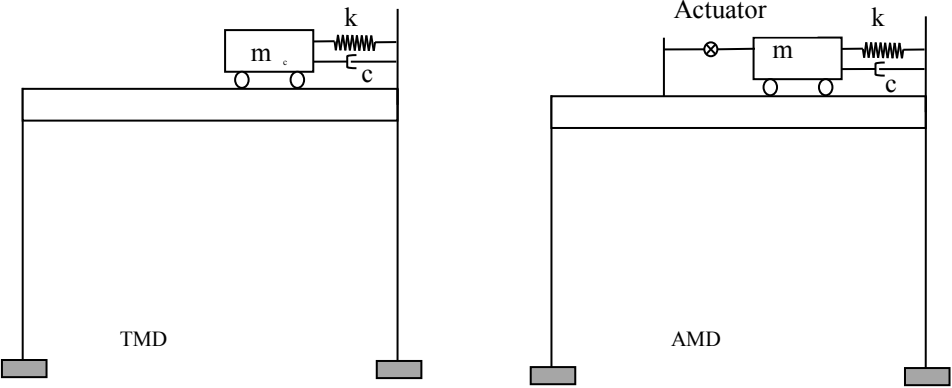


Figure 2-15: Passive tuned mass damper versus active tuned mass damper

2.4.2. **Active tendon system**

Active tendons are installed between two storeys of a building structure and are a system of pre-stressed tendons in which the tension is controlled by an actuator as shown in Figure 2-16.

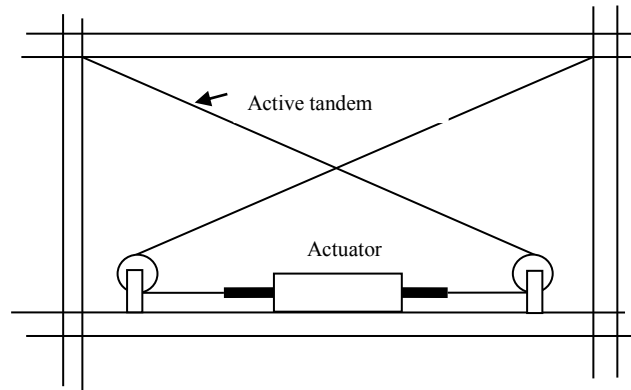


Figure 2-16: Schematic diagram of active tendon system (Cheng et al,2008)

The actuator is connected on the lower floor and one end of the tendon is connected to the upper-floor and the other end to the actuator. Under the structural disturbance, the structural vibration produces inter-storey drift that changes the tension in the pre-stressed tendons. This change in the tendon stress can be adjusted with actuators pulling or releasing tendons. Active tendons can function in both the pulsed- and the continuous-time modes.

2.4.3. Active brace system

Active Brace Systems consist of an actuator which is installed on the bracing system between two floors. Actuator piston is connected to bracing system while actuator itself is attached to a floor as shown in Figure 2-17. The direction and magnitude of actuator force is determined by control system to minimize the structural vibration.

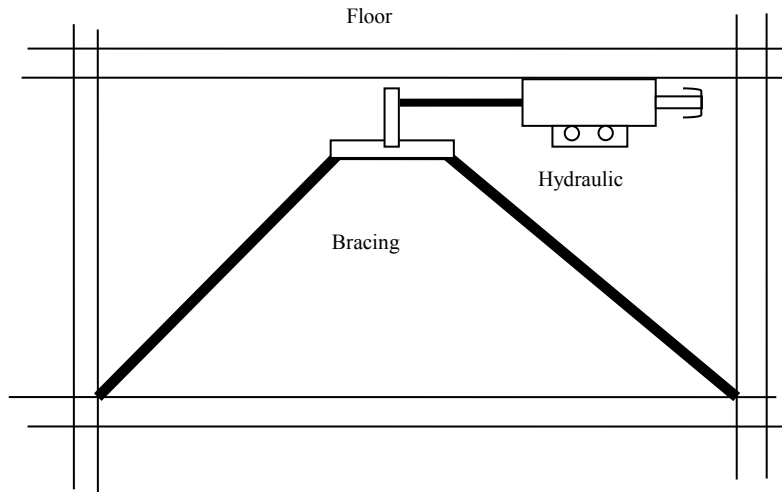


Figure 2-17: Active bracing system with hydraulic actuator

2.4.4. **Pulse generation system**

Pulse generators (Miller et al, 1988) use pneumatic mechanisms to generate pulse-type actuation force instead of hydraulic pressure. The adaptive structure is typically equipped with several of this pulse generation system. When a large relative velocity is detected at the location of Pulse generation equipment, the pneumatic actuator at this location is activated, and a pneumatic force opposite to the velocity is exerted in to the structure. The pulse generation system is cheaper than hydraulic system. Sensors measure structure motion due to the earthquake excitation. The controller processes these measurements and generates the required control signal. The servo valve then uses the control signal to regulate flow direction and intensity, which yields a pressure difference in the two actuator chambers. The control force is thus generated by the pressure difference to resist seismic loads applied on the structure. A schematic of pulse generation system is illustrated in Figure 2-18.

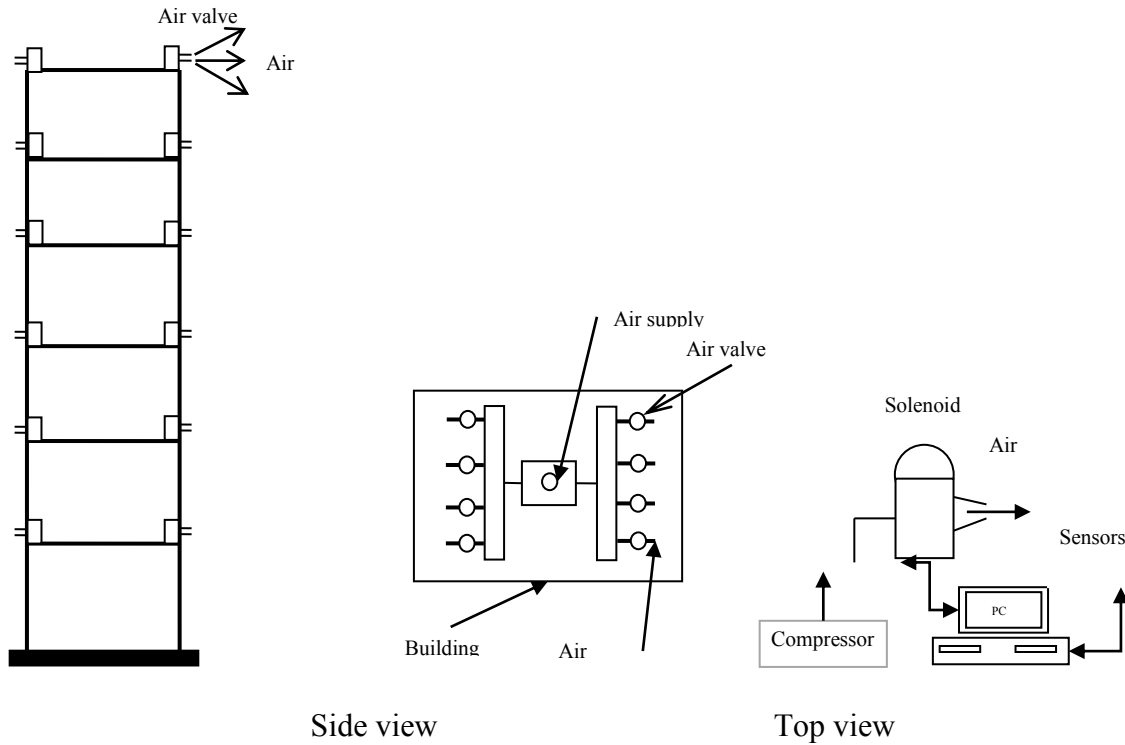


Figure 2-18: Pulse generation systems

2.5. Semi active energy-dissipation system

Semi-active control systems represent a class of systems for which energy is used to change the mechanical properties of the device (Casciati et al, 2006). These systems have adaptability of the fully active systems and fail-safe feature of the passive systems. They are sometimes referred to as controllable passive systems. Semi active control system requires much smaller amount of energy compared with active control system. They can be typically operated with a battery power. Moreover, since semi-active control devices do not add mechanical energy to the structural system, the stability of the structure is guaranteed. In the following some semi-active devices used typically in structural systems are discussed.

2.5.1. Semi-active tuned mass damper

In 1983, Hrovat et al (1983) proposed Semi-active Tuned Mass Damper (SATMD) for control of wind-induced vibrations in tall buildings. This system consists of a Tuned Mass Damper (TMD) and an actuator installed on top of the main structure (Figure 2-19). Unlike a conventional passive TMD system, an SATMD system can employ a controllable semi-active damping device or variable stiffness spring or variable pendulous length instead of a passive damping device, constant stiffness spring or fixed pendulum length. This flexibility in damping, stiffness or length in pendulum can be used for tuning the TMD system by semi active control system.

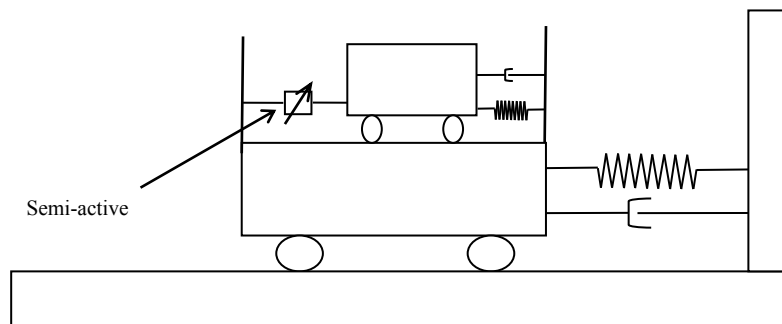


Figure 2-19: Semi-active Tuned Mass Dampers

2.5.2. Semi-active stiffness control device

Semi active stiffness is installed on a bracing system of the structure. The Variable Stiffness Device (VSD) as shown in Figure 2-20 consists of a hydraulic cylinder, a piston rod, a solenoid control valve, and a tube connecting the two cylinder chambers. The solenoid valve can be opened or closed. When the valve is open, fluid flows freely and releases the beam–brace connection, thus decreases the structural stiffness. When the valve is closed, the fluid cannot flow, and attaches the beam to the brace, thus increases the structural stiffness. A VSD adjusts the stiffness of the structure’s bracing system according to the control system strategy to minimize the structural responses during a seismic event.

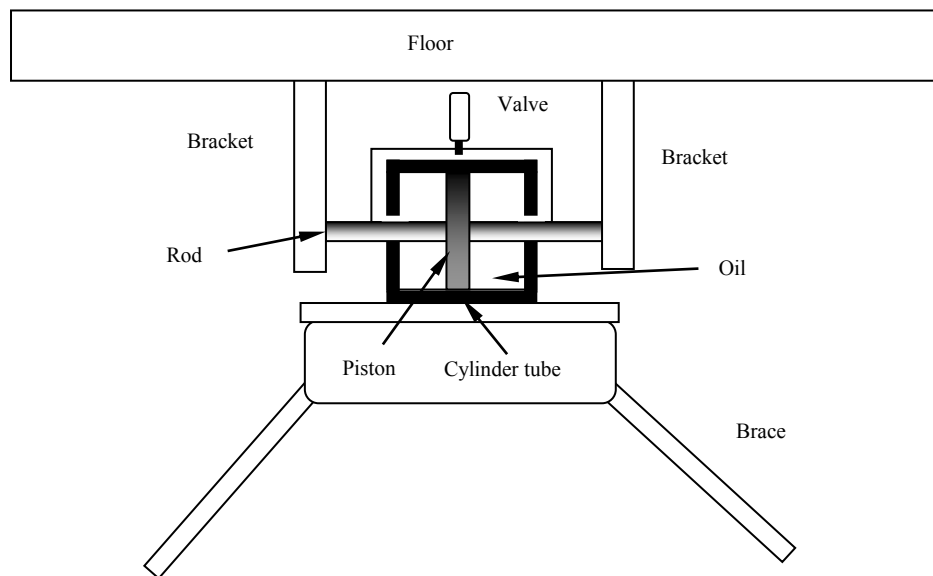


Figure 2-20: Semi active variable-stiffness device (Cheng et al, 2008)

2.5.3. **Semi-active viscous fluid damper**

Semi-active Viscous Fluid uses a closed solenoid valve to control the volume of the flow of the fluid through a bypass loop (Figure 2-21). When the opening of the valve is large, the fluid can easily flow through the valve, and a low damping force develops. When the opening is small, the fluid cannot easily flow through the valve, and the damper generates bigger control force. Damper behaviour is controlled by adjusting the valve opening according to the control system command to minimize structural response.

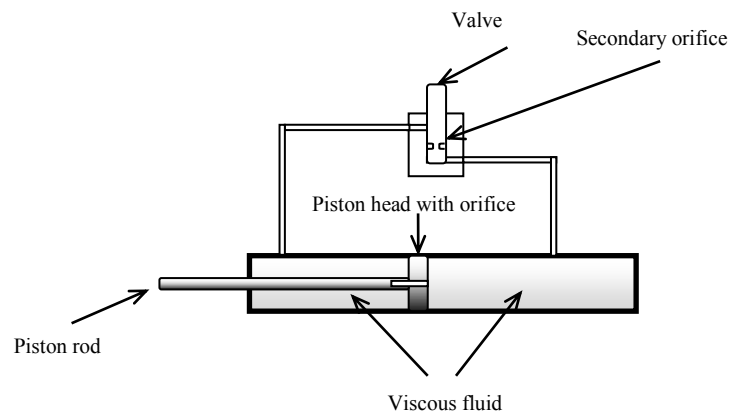


Figure 2-21: Configuration of semi active viscous fluid damper

2.5.4. **MR/ER damper**

Magnetorheological (MR) and Electrorheological (ER) fluid dampers represent a category of controllable fluid dampers where shear force of the fluid (viscosity of the fluid) is adjusted by an external magnetic or electric field, respectively. MR/ER dampers are like viscous fluid damper except they have a mechanism to change the apparent viscosity of their fluid. The MR/ER fluid is a suspension of oil, additives and iron particles whose polarization can be influenced by an

external magnetic/electric field. Hence, the control input variable of MR / ER dampers is current and voltage. Thus, according to the applied current/voltage, the viscosity of the MR/ER fluid and consequently the dampening force can be controlled.

A prototype of MR damper is illustrated in Figure 2-22. As damper strut moves, it pushes MR fluid through the orifice. In the orifice, MR fluid is magnetized by a very powerful but concentrated magnetic field which makes suspended iron particles to polarize along the magnetic field and form a series of chains. These chains and polarization of iron particles change the MR fluid form from liquid to semi solid instantly. By altering the magnetic field in orifice area, polarization of iron particles and consequently viscosity of MR damper fluid and damping force can be adjusted.

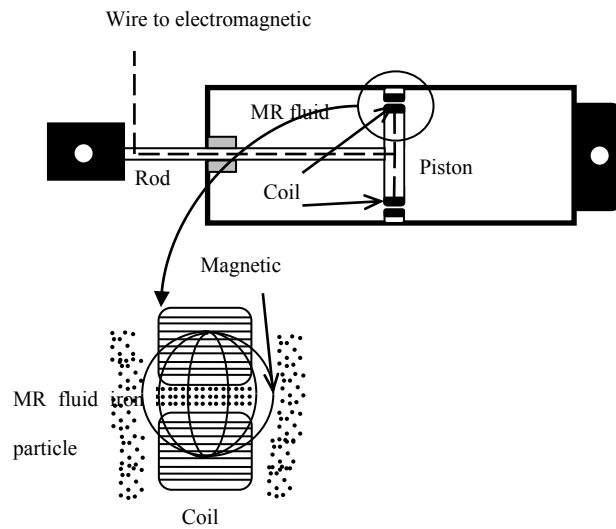


Figure 2-22: Magnetorheological damper configuration

Figure 2-23 illustrates the three operating modes of controllable fluids: flow mode, direct shear mode and squeeze mode. The flow mode is the normal operating mode of MR dampers and shock absorbers; the direct shear mode is that of clutches and brakes.

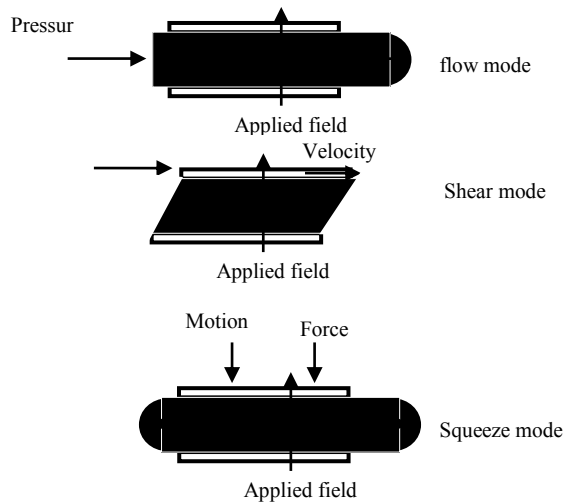


Figure 2-23: Three operating modes of MR damper

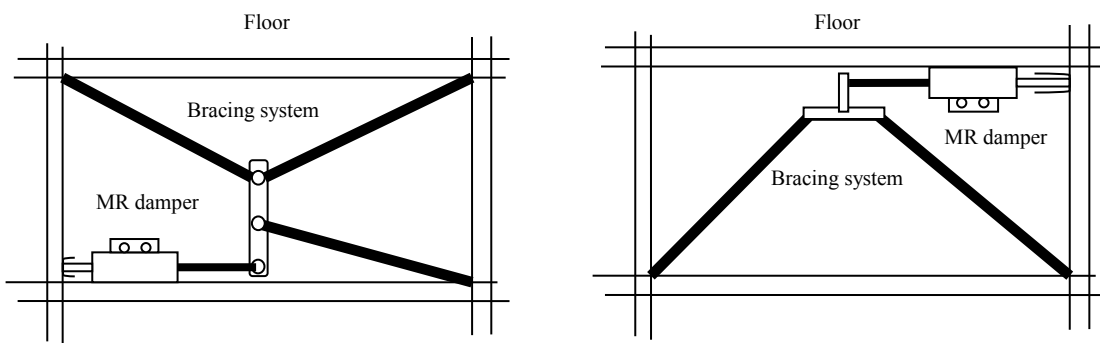


Figure 2-24: MR damper arrangement installation

MR damper can be used as a part of the bracing system as shown in Figure 2-24 or can be implemented in base isolation systems and tuned mass damper as semi active systems. Based on operating mode of MR damper two major MR damper configurations can be defined as: 1) Flow mode (Valve mode) dashpot damper; and 2) Mixed mode (Flow and Shear modes) dashpot damper

2.5.5. Flow mode (Valve mode) dashpot damper

In this damper arrangement, there is a hollow duct around the damper (Figure 2-25). When piston is moving inside the cylinder forces the MR fluid to move inside the duct. Here both walls of MR flow duct are stationary.

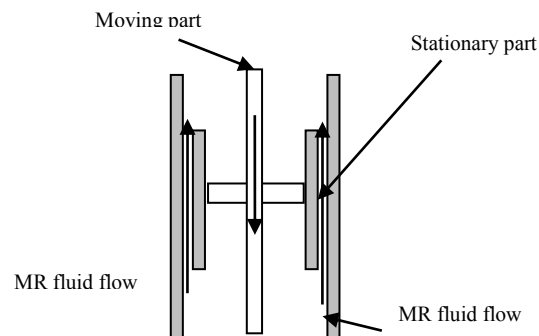


Figure 2-25: Flow mode dashpot damper

2.5.6. **Mixed mode (Flow and Shear modes) dashpot damper**

In this arrangement of MR damper, outer cylinder is stationary and inner one is moving with piston inside the damper as shown in Figure 2-26. Here, MR flow duct contains a stationary and moving walls. .

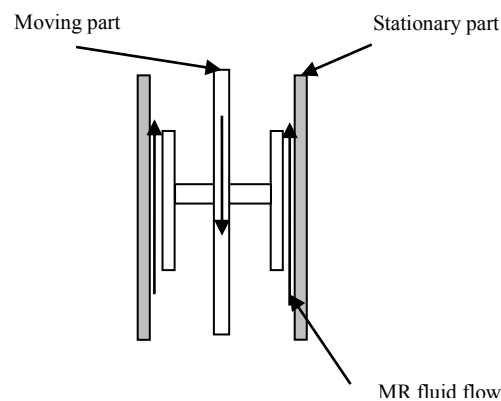


Figure 2-26: Mixed mode dashpot damper

2.6. **MR damper modeling**

The modeling of MR or ER dampers is mainly divided into two main categories; Phenomenological Model (parametric and non-parametric modeling) and Physical or Mechanistic Model. In phenomenological method, the model is based on the data and results of experiments. Phenomenological models are typically simple and computationally efficient; however they depend on experimental data for the identification of the model parameters. Thus characteristic parameters of phenomenological model should be re-evaluated or updated based

on loading conditions. For example, a phenomenological model that is based on quasi-static test of MR or ER damper may not work for high frequency vibration. To design a MR damper, one should actually use a mechanistic model, as initially there is no experimental data available. On the other hand, mechanistic models are based on principles of physics, which are capable of predicting the MR damping force using geometrical parameters of damper, and material characteristics. Here in this section pertinent literature on these models are systematically reviewed.

2.6.1. **Phenomenological model**

Iskandarani et al (2012) proposed an iterative approach based on Particle Swarm Optimization to estimate Bouc-Wen model hysteresis parameters when data from tests are not sufficient or missing. They investigated the impact of the number of iterations, the number of particles and the initial guess in the estimation of the parameters.

Jiang and Christenson (Jiang and Christenson, 2011; Jiang and Christenson, 2012) proposed a new fully dynamic magneto-rheological fluid damper model. They divide the MR damper dynamics model into three parts. 1) Nonlinear force behaviour of the MR damper for a constant level of current 2) the dynamic response of the current being commanded through the Pulse-Width Modulated (PWM) amplifier and (3) the dynamics of the inductance in the damper. For nonlinear force behaviour of an MR damper, they applied the hyperbolic tangent model proposed by Bass and Christenson (2007). The hyperbolic tangent model which was first invented by Gamato and Filisko (1991) consists of a series of springs, viscous and Coulomb dampers, and a mass that are connected (six characteristics parameters in total). They validated the model for the large-scale 200 kN MR damper. In another experiment, they utilized a simple

linear three degree-of-freedom three storey single bay model to examine the relative performance of four frequently used damper models: Hyperbolic tangent model, Bouc–Wen model, algebraic model and viscous plus Dahl model. The four models were evaluated for speed, accuracy stability, and convergence.

A static model for MR damper based on artificial neural networks was proposed by Martinez et al(2012).They compared the proposed ANN model with the three parameters of the classical Bingham model. The ANN-based MR damper model showed very good results in comparison to the corresponding Bingham model.

Parametric identification of the Dahl model for three large scale MR dampers was investigated by Aguirre et al (2012). The proposed Dahl model had eleven characteristics parameters for each damper, which was determined by experimental and analytical procedures. It was experimentally proven that the Dahl model described the behaviour of the MR dampers under random loading reasonably well.

A new MR damper model, called the Maxwell Nonlinear Slider (MNS) model, was developed based on the characterization tests reported by Chae and Sause (2012a, 2012b). The MNS model describes separately the pre-yield and post-yield behaviour of the MR damper. The MNS model uses Hershel–Bulkley visco-plasticity to explain the post-yield non-Newtonian fluid behaviour, that is, shear thinning and thickening behaviour, of the MR fluid. The MNS model has eleven characteristics parameters, which should be identified by experiments. The model was examined by comparing response of the MR damper MNS model to the measured damper response from experiments. Very satisfactory agreement was observed between MNS model and experimental results. In addition, in the second paper Chae and Sause (2012b), the authors investigated MNS MR damper model in a prototype building structure. The experiments

included a real-time hybrid simulation of a three-storey building structure with a large-scale MR damper under design earthquake loading. Two MR dampers were installed in the 3rd storey in each direction of the prototype building structure. The authors ascertained the robustness and the accuracy of the variable current MNS model from the good agreement observed between the predicted and experimental results.

Spaggiari and Dragoni (2012) proposed parameter estimation for magnetorheological fluid damper using Bouc-Wen model. They proposed an easy procedure to implement in an automatic system which can directly retrieve Bouc-Wen model parameters of MR damper with a few experimental tests. As author correctly mentioned, the new model was less precise than the previous models but it was fast and inexpensive. Boada et al (2011) investigated the application of recursive lazy learning based on neural networks to model the MR damper behaviour.

Guan et al (2011) proposed a parametric MR damper model which was developed by considering the compressibility of MR fluid. The model was capable of predicting the damping force-velocity hysteresis of MR dampers under sinusoidal displacement excitation. The model consisted of a friction element and a parallel-connected viscous element in combination with a spring simulating the compression of the MR fluid.

Truong and Ahn (2010) proposed a self-tuning fuzzy technique based on this fact that the damping force of the MR fluid damper depends on the displacement/velocity of the damper rod and the applied current. Their proposed black box model had two parts: the first part was the neural-fuzzy inference which was applied to estimate the damping force caused by the displacement of the damper strut, and the second part was a gain fuzzy inference that was employed to switch between different damping force levels with respect to the applied.

Metered et al (2010) proposed another feed-forward and recurrent neural networks to predict MR damper behaviour. In the model, they considered the time-histories of the relative displacement across the MR damper and the voltage applied to the coil as input and the damper force as output. They used these data to train and validate the feed-forward and recurrent neural networks model. At the end, they validated their model by evaluating the model's predicted damping force against the experimental test for LORD RD-1005-3 damper under random relative displacements.

Shivaram and Gangadharan (2007) investigated the statistical modeling of a magnetorheological fluid damper. They did an experimental study to identify the factors that have a significant influence on damping force of the MR damper. It was determined that the magnetic field strength and volume fraction of particles in the fluid, had the largest effect on the MR damping force.. In addition, significant correlation between vibration frequency and RMS damping force was observed. A statistical modeling equation was developed based on the experimental data, which could predict the damping force of the MR damper.

Soeiro et al (2008) presented an implicit formulation for the characterization of MR dampers using the Bouc-Wen model. The method was based on stochastic methods, Simulated Annealing, and Genetic Algorithms, as well as, hybridizations of these methods. In addition, the sensitivity analysis was shown to be an important tool to verify which parameters could be more easily identified.

Guo et al. (2005) and Guan et al (2011) proposed a model for dynamic modeling of magnetorheological damper behaviour. The proposed model had a simple form, which was an extended Bingham model by using a shape function of hyperbolic tangent and new term for

velocity. For harmonic excitation, the proposed model had only four parameters. It is noted that the model was only developed and validated for harmonic motion.

Powell (1994) adopted a mathematical model of the MR fluid damper for Harmonic analysis of a magnetorheological damper. In their paper, the energy dissipated and equivalent damping coefficient of the MR damper in terms of input voltage, displacement and frequency were studied. The model predicted the MR damper behaviour through updating the equivalent damping coefficient of MR damper.

Du et al (2006) presented a model for dynamic behaviour of a magneto-rheological damper by using evolving radial basis function networks. A radial basis function network is an artificial neural network that uses radial basis functions as activation functions. The radial basis function network is also been known to be universal function approximator. The model was validated for harmonic and random vibration. Dominguez et al (2006) proposed a new hysteresis model based on the Bouc–Wen model to better characterize the hysteresis phenomenon of the MR damper. The proposed model incorporated the frequency, amplitude and current excitation as variables and thus enabled prediction of the damping force due to changing excitation conditions. Giuclea et al (2004) proposed genetic algorithms for modeling the dynamic behaviour of magnetorheological dampers which was proved to be very efficient. The method was experimentally validated for constant levels of the applied magnetic field and harmonic imposed motion.

Sodeyama et al (2003) designed and developed (in collaboration with Lord Corporation) three different capacities of MR dampers. One of 200 kN MR dampers ended up to be installed in a building. According to their study, MR dampers without magnetic field show similar dynamic behaviour as typical viscous dampers. By applying the magnetic field, the MR damping

force is increased according to the strength of the applied magnetic field and can be simply modeled by the Bingham plastic model.

Ahn et al (2009) proposed self-tuning fuzzy (STF) method based on neural technique for modeling of a magneto-rheological (MR) fluid damper. In this research work, a back propagation and a gradient descent method were used to train the fuzzy parameters to minimize the model error function. It should be added that although the fuzzy system is an intelligent tool mimicking the rational thinking of humans, there is no systematic method to design and determine input space partitions and the number of rules, and membership functions. The STF model was observed to predict the force-displacement behaviour of the MR damper with very good precision.

2.6.2. **Physics-based or Mechanistic model**

Kamath et al (1996) investigated the Mechanistic modeling of ER damper in 1996. They tried to address quasi-steady model of ER dampers by solving simultaneously conservation of mass, conservation of momentum and equation of equilibrium. They proposed two sets of equations for flow mode damper and shear mode dampers. However, the model did not correlate well with the experimental data.

Wereley and Li Pang (1998) classified the MR/ER damper configuration and corresponding boundary conditions and used the momentum equation (pressure-velocity formulation) for MR/ER damper vibration analysis. Since then different researchers attempted to develop different analytical based models to predict the damping force (Wereley and Lee, 1999; Wereley and Lindler, 1999, 2003; Honga et al 2000; Dimock et al 2002; Wereley, 2008). The

common ground for the above mentioned works is the use of direct momentum equation (pressure-velocity formulation) to analyze the MR/ER dampers in the quasi-static range.

Chen et al (2004) investigated the solution for velocity profile and pressure gradient of the unsteady state unidirectional flow of Bingham fluid between parallel plates by solving the momentum equation of the ER fluid flow using the Laplace transform technique. The analytical solutions were proposed for Bingham fluid flow between two stationary plates under different flow rate that represented different motion types. Although, the solution had a closed form, it was restricted to a well-defined motion like harmonic motion.

Perhaps the most comprehensive paper on mechanistic modeling of MR/ER damper is by Nguyen and Choi (2009). Their paper is based on mathematical solution on “Unsteady unidirectional flow of Bingham fluid between parallel plates with different given volume flow-rate conditions” by Chen et al.(2004). Nguyen and Choi (2009) used the closed-form mathematical solution proposed by Chen et al. (2003), and adjusted and validated it for MR/ER damper for harmonic motion. Although, their model was very comprehensive and precise, it was constrained by the following assumptions: (a) the Bingham fluid flow is between stationary annular duct (flow mode), and (b) the Bingham fluid flow rate is limited to certain kinds of motion such as harmonic motion.

Wang and Gordaninejad et al. (2009, 2011) investigated steady-state analysis of ER and MR fluid flow through pipes or parallel plates using the Herschel-Bulkley model. They proposed a simplified closed-form expression for determining the pressure drop as a function of material properties, geometry and volume flow rate. In addition, the effect of fluid compressibility on the equation of the MR fluid damper was considered. They validated their model for harmonic motion.

2.7. Application of MR damper in bracing system

The research on potential application of MR damper in civil application is numerous. The research in structural engineering application is focused on base isolation system (Johnson et al. 1998; Yoshioka et al. 2000; Kim et al. 2006;), bridge engineering (Jung et al. 2006; Bani, 2006; Sanjay and Nagarajaiah, 2005; Erkus et al., 2002), cable vibration control (Jung et al. 2003; Duan et al. 2006; Cai et al. 2007), tuned mass damping system (Pinkaw and Fujino, 2001; Rulin et al. 2002; Lin and Chung, 2005) and bracing system (Dyke et al., 1998; Kim et al. 2009). The subject of the current research is the application of MR dampers in bracing system in building frames as adaptive or intelligent damper for suppressing vibration.

Dyke and Spencer (1997) investigated the performance of a three storey building model (98.3Kg mass in each floor) under NS component of the 1940 El Centro earthquake. This building model was equipped with a single MR damper in the first floor. Five control methods: Decentralized Bang-Bang Control, Lyapunov Control, Clipped-Optimal Control, Modulated Homogeneous Friction and Passive control were implemented in the study. The results demonstrated that each control system can be more effective in controlling of displacements, drift or acceleration of one floor than others. In other words, one control strategy can be best in reducing acceleration of one floor but not so good in reducing the drift. On the other hand, another control method can be more effective in reducing the response of a specific floor than other floors. Dyke et al. (1998) expanded the above experiment for high (120%) and low amplitude of 1940 El Centro earthquake record. Dyke and Caicedo (1999) investigated the response of six-storey test building (equipped with MR dampers in first two floors) under seismic loading. They compared clip optimal semi active control strategy versus passive on

method and it was shown that optimal control system can reduce the floor displacements and drift by 17% more than that by passive on control method.

Jason and Dyke (2000) conducted a comparative study between different MR damper semi-active control strategies. In the study, a six-storey model structure was controlled using MR dampers on the lower two floors. The responses of the structure to El-Centro earthquake excitation were found for each controller. Based on these results, three of these control algorithms were found to be most capable for use with MR dampers in structural system. The Lyapunov controller algorithm, the clipped-optimal algorithm, and the modulated homogeneous friction algorithm yield considerable reductions in the responses of the structure in seismic event.

Xu et al. (2000) proposed two new optimal displacement control strategies for semi-active control of seismic response of frame structures using MR damper. In their research the stiffness of the bracing system supporting the MR damper was taken into account. Wereley et al. (1999, 2003) studied the effectiveness of MR braces in earthquake hazard reduction. They used a single-bay, three storey, and 60 inch tall steel frame as their scaled experimental model structure with only one MR damper mounted in the first floor. They examined three control system strategies; sky hook LQR and CSM and concluded that all three worked very well (numerically and experimentally) as compared to passively damped case (damper with field OFF).

The implementation of MR damper in real building was described by Sodeyama et al(2004). In this study, it is explained how two 300 kN MR dampers were developed, designed, tested, modeled, and installed in National Science and Innovation Museum of Emerging in Japan in 2001. Renzi and Serino (2004) investigated MR damper application in mitigation of seismic load by using the shaking table tests performed on a four storey, large-scale, steel frame equipped with a bracing system including MR dampers operating both in passive and semi-active

and ON–OFF mode. In their test, two MR dampers were positioned between the ground and second floor and between the second and fourth floor. A reduction of 30-35% have been obtained in terms of peak relative structural displacements of second-floor for both the natural seismic inputs and about 10% for the ‘synthetic’ seismic input relative to passive configuration. However, the reduction in peak displacement for first, third and fourth floor were not discussed clearly.

The study on MR dampers application to reduce the response of irregular buildings was done by Yoshida and Dyke (2005). They observed that in reducing inter-storey drift responses, the clipped-optimal and passive-on controls are comparable to each other. Gattulli et al. (2009) examined the application of MR damper in the lateral-torsional seismic response of a prototype frame structure with asymmetric mass distribution. They concluded that clipped optimal semi-active control law, based on a H2/LQG optimization criterion, efficiently mitigate the peak response and enhance the passive control performance. Chae et al. (2010) in Lehigh University did an extensive research on a three-storey actual size building (45.72x45.72x12.2) to verify the application of MR damper. The experiment was a real-time hybrid simulation to compute the structural response based on the feedback restoring forces from the experimental and analytical substructures. The structure was subjected to six different ground accelerations. Two different control strategies: LQR and SMC (Sliding mode control) were implemented in the research work. Based on the storey drift of the structure in elastic range, it was concluded that the overall performance of semi-active controllers is similar to the passive controller for the 3-storey structure. It is added that the research results can be attractive to design engineers since a passive controller does not require any sensors for feedback data, as well as control algorithms and hardware for supplying the command current to the damper.

Lee and et al. (2010) investigated quantitative evaluation of the seismic performance of a building structure equipped with a MR damper. The building model was a full scale five-storey tower (one bay in each direction) with one MR damper in the first floor. They came to a conclusion that the semi-active control produces an insignificant control performance as compared to the passive control system. They explained that the passive control forces of the MR damper already reached the optimal damping force as compared to the shear force in the first floor and to accomplish a better performance for semi-active control algorithms, further loading capacity is required.

Lee et al. (2007) showed analytically and experimentally using toggle bracing system in structure that a MR damper could produce larger effective control force due to its response amplification mechanism.

In another research, Bitaraf et al. (2010) investigated MR damper application for earthquake excitation. In their case study, they used a six-storey building model with MR damper installed in the first two floors. They concluded that semi-active operation of MR dampers using proposed control systems can improve the response of a structure under seismic excitation. Although, the study results show MR damper in passive on mode can achieve similar results in reducing structural displacements.

Mohajer Rahbari et al. (2012) studied the semi-active direct control method for seismic alleviation of structures using MR dampers. They introduced two case studies: a three-storey building with two 1000 kN MR dampers installed in the first floor and an eleven storey building with three 1000 kN MR dampers installed at the top three stories. They established three performance criteria for comparing semi-active control and passive on mode: displacement,

storey drift and acceleration. Passive on mode control generates very good results in reduction of structural displacement.

2.8. Application of MR damper in tuned mass damper

The history of using TMD system goes back to 1928 (Ormondroyd and Hartog, 1928) but the concept of semi-active tuned mass damper came much later in 1986. In 1986, Hrovat et al. (1986) introduced semi-active TMD concept in structural control. In this approach, a TMD is armed with the so-called SA damper which is basically a time-varying damper and requires only a small amount of energy to change the damping. The so-called SA was a control-valve damper. Thus, by controlling valve orifice diameter, the damping can be controlled. For wind induced motion of tall buildings (one degree of freedom), the semi-active TMD results indicate substantial improvements in RMS of building displacement, with respect to conventional passive TMD's.

Weber and Maslanka (2012) described a new type of semi-active tuned mass damper with a magnetorheological damper to alleviate single harmonic vibrations of the main structure with varying frequencies. They utilized rotational MR damper in TMD arrangement as damping system for a 15.6 m spam bridge. The MR damper assisted TMD to shift its resonance frequency from -12.2% to +10.4% away from its nominal value and effectively outperformed passive TMD up to 63%.

Kang et al. (2011) investigated the effectiveness of semi-active tuned mass dampers for the response control of a wind-excited tall building. In their case study the 76-storey building proposed for the city of Melbourne, Australia was used. The research demonstrated that the performance of the MR-SATMD was superior to that of the passive TMD. Zemp et al. (2011a

2011 b) studied the seismic and harmonic response of a tall building equipped with two tuned pendular inertial masses and magnetorheological (MR) dampers. The building was reinforced concrete structure with 21-storey and a total height of 90 m. The masses were hanged from the roof and two MR dampers were installed at the bottom of the masses so that MR dampers could manipulate the movement of the masses. The building model consisted of 20 Ritz-vectors and the TMDs were modeled considering two-horizontal displacements for each mass as the degrees of freedom. The authors concluded that TMD improved the peak structure displacements from 5% to 18% relative to the bare structure. On the other hand, the MR-damper with LQR control showed 16 to 39% larger reductions for peak and RMS displacement values than TMD with the optimal viscous damper.

Chey et al. (2010a, 2010b) examined the behaviour of multi-storey passive and semi-active tuned mass dampers under seismic loading. The building was a 12-storey moment frame structure in which the top 2 or 4 floors could act as the mass for a TMD system. In other words, instead of mounting a small extra mass at the top of the building, the researchers used the building's own mass to act as the mass needed in the tuned mass system. The results implied that SATMD systems can effectively reduce seismic response for multi-degree-of freedom systems across a broad range of ground motions in comparison to a passive system.

In the event of an earthquake, the fundamental frequency of structure can be altered due to damage or deterioration. Nagarajaiah (2009) investigated semi-active or smart tuned mass dampers (SATMD) using semi-active variable stiffness systems. In this research, it was shown that TMD lost its effectiveness even with just 5% mistuning while SATMD retuned and reduced the response of the structure. The problem of de-tuning in TMDs is an important problem that needs practical solution. Roffel et al. (2010) proposed an adaptive pendulum tuned mass which is

capable of adjusting its length and two air dampers connected to the mass to compensate for the de-tuning.

Although, LQR and LQG are the most used control algorithm in ATMD and SATMD systems, several control algorithm are proposed to improve the SATMD performance (Rulin et al. 2002; Koo, 2003; Lienes, 2010). Ji et al. (2005) compared four different control algorithms in SATMD and concluded that among the four control algorithms, DBG (displacement based ground-hook) and clipped optimal algorithm show the best performance under the earthquake loading. Yang, et al. (2010) also investigated vibration suppression of a structure model under random based excitation using MR based SATMD system. They developed an inverse MR-damper model based on improved LuGre friction model, and then combined with a H2/Linear-H2/LQG controller, in order to control the command current of the MR damper to suppress structural vibration levels, effectively.

2.9. Summary and discussion

It can be observed from the literature review that most of the research is based on the laboratory-scale or small-scale structures. Few studies investigated the behaviour of MR damper implemented in real size structures with limited number of MR dampers. It is also noted that none of research works available on semi-active dampers is based on real size tall structures with existing MR damper and real seismic records used for the seismic analysis. In other words, the research results are not yet extendable to practical usage. In addition, using unreasonable auxiliary mass may lead to good results but it may not be practical.

Phenomenological models dominate the research on MR damper modeling, but they have several drawbacks. First. they do not provide any information about how the physical and

geometric properties of an MR damper are related to the damper behaviour. The designer of a new MR damper cannot simulate the behaviour of the damper during its design as the phenomenological models are not applicable in this case due to the unavailability of test data. In addition, accuracy of the prediction of MR damping behaviour using a phenomenological model mainly depends on how well the model parameters are identified and estimated from the experimental data. Thus, a phenomenological model can only predict the MR damper behaviour in a range in which model parameters are tuned. For example phenomenological model of which parameters are tuned and estimated for quasi-static loadings may not be used for estimating the dynamic behaviour of MR damper under random loadings. Furthermore, some phenomenological models (including Boc-Wen, Dahl, LuGre) have very complicated form which make them very hard to determine their parameters from experiment. It should be added that although complexity and sensitivity of equations in phenomenological MR damper models help in predicting the behaviour of a damper accurately, it may eventually cause instability in the solution when the model is used for high frequency motion or when the damper model is coupled with the structural model. Thus there is a need for developing an accurate mechanistic model that is not dependent on the estimation of the parameters from the experimental data. The model can then be used for the design of a MR damper and also can be easily integrated to a structural model to determine the seismic or wind-induced vibration response of a structure utilizing such dampers.

Chapter 3: Methodology

3.1. Introduction

This chapter discusses the methods developed here to study the performance of MR-damper integrated buildings subjected to seismic excitations. In order to achieve the goals of the present research the following methods have been developed: (a) a physics-based or mechanistic model of Magnetorheological (MR) dampers, (b) a simplified phenomenological model of MR dampers for easy integration to a structural model of a building, and (c) modeling MR damper applications in building frames to conduct study on the seismic performance of buildings. The following forms of MR damper integration to building structures have been considered: semi-active tuned mass damper (SATMD) and semi-active bracing system (SBS). As mentioned earlier, MR dampers are filled with MR fluid instead of normal hydraulic oil. MR fluid is a fluid consists of micron-size, magnetically polarizable particles (like iron) dispersed in a viscous fluid, such as silicone oil. When MR fluid is exposed to magnetic field, micron –size iron particles form a chain between two poles of magnetic field as shown in Figure 3-1.

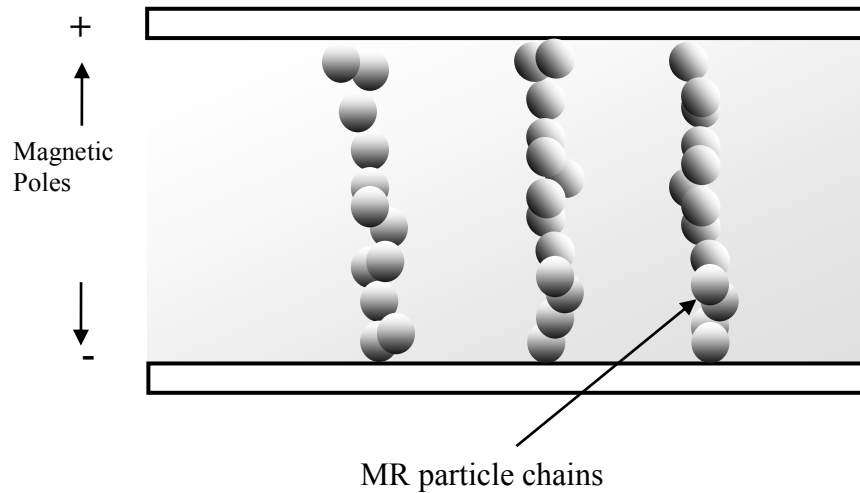


Figure 3-1: MR fluid polarization.

These iron chains prevent any fluid motion between two magnetic fields. These chains can resist fluid motion up to a certain limit which is known as MR fluid yield point. After reaching the yielding point, the iron chains in an MR fluid break apart, and the fluid flows like a normal (Newtonian) one. The yielding point in an MR damper mainly depends on the strength of the magnetic field and the amount of iron particles. Therefore, before yielding, MR fluid demonstrates a rigid body behaviour which means the fluid experiences no deformation. After yielding, MR fluid shows the Newtonian fluid behaviour with a linear relationship between the shear stress and the strain rate. This behaviour of MR fluid can be expressed using a bi-linear model which is called the Bingham model. As shown in Figure 3-2, MR fluid demonstrates no deformation under applied shear stress prior to yielding (τ_y); but after yielding, it acts as a Newtonian fluid with a linear relation between shear stress (τ) and strain rate ($\dot{\gamma}$).

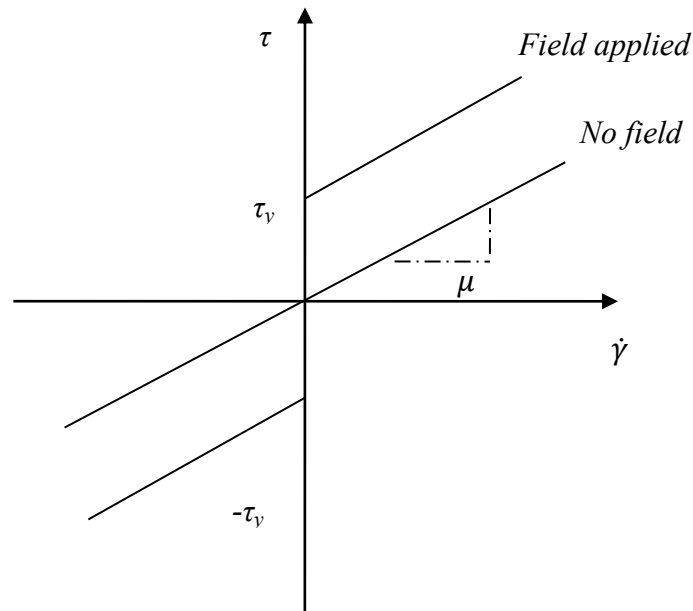


Figure 3-2: MR damper stress-strain rate relation with and without magnetic field.

Bingham model can be mathematically expressed as:

$$\tau = \tau_y \text{sgn}(\dot{\gamma}) + \mu \dot{\gamma} \quad |\tau| > |\tau_y| \quad (3-1)$$

$$\dot{\gamma} = 0 \quad |\tau| < |\tau_y|$$

The MR fluid behaviour in flow mode damper is illustrated in Figure 3-3. MR fluid flows like a Newtonian fluid where shear stress exceeds yielding stress (Region 2 &3) and remains solid where shear stress is less than yielding stress (Region 1)

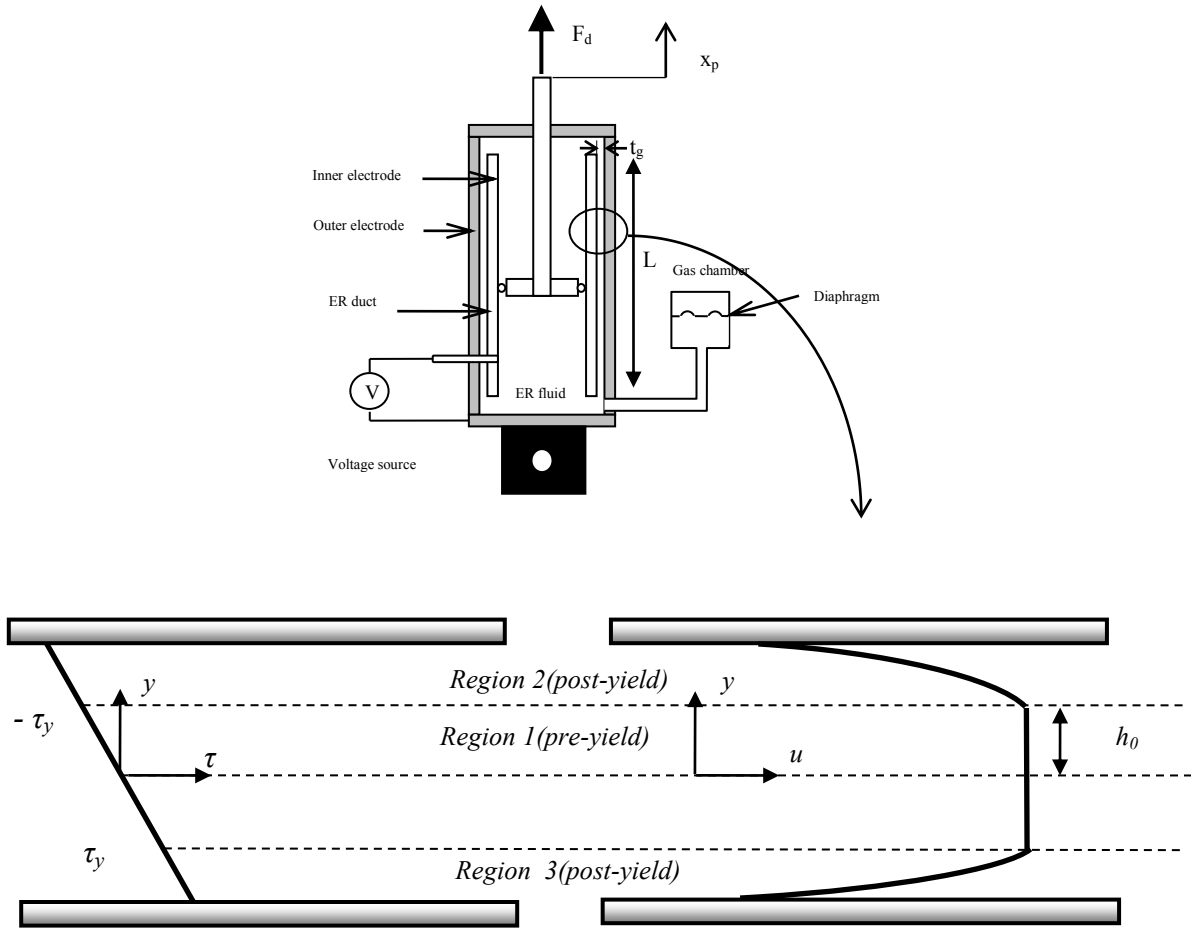


Figure 3-3: MR fluid in duct of flow mode damper.

Determining the point where shear stress exceeds yielding stress is the main challenge in the analysis of MR fluid. MR fluid is categorized as Non-Newtonian fluid or more specifically Non Newtonian fluid with yield point which makes the analysis nonlinear.

Section 3.2 of this chapter is dedicated to MR damping modeling methods and the proposed Mechanistic model. Simplified phenomenological model for random loading is presented in Section 3.3. The modelling of building frames integrated with MR dampers in TMD and bracing systems are presented in Sections 3.4 and 3.5. The design and modeling details of a set of three building structures (tall, medium and short) are presented in Sections 3.3 and 3.4.

These buildings are analyzed for their seismic responses to evaluate the effectiveness of the MR dampers used in them.

3.2. Analytical quasi-statics model of ER/MR damper- Bingham plastic formulation

In this formulation the governing equation is the equation of equilibrium of momentum (Eq. 3-2).

$$\rho \frac{\partial u}{\partial t} + \frac{\partial \tau}{\partial r} + \frac{\tau}{r} = \frac{\partial p}{\partial z} \quad (3-2)$$

In which, u is velocity, ρ is the fluid density, τ is the shear stress, p is fluid pressure, and r and z are the coordinates. The term quasi-static analysis means that for simplicity the inertia of MR/ER fluid is neglected as fluid is in steady-state condition. The equation of equilibrium of momentum can be rewritten for quasi-static condition as:

$$\frac{d\tau}{dr} + \frac{\tau}{r} = \frac{\Delta P}{L} \quad (3-3)$$

where, L is the MR/ER damper duct length, and it is assumed that pressure varies along the length L . The above mentioned equation is the benchmark equation for quasi-static formulation of MR/ER damper. In this section, the Bingham plastic formulation of ER/MR damper as presented in Kamath et al. (1996) has been discussed.

Bingham plastic model can be used to explain the MR/ER fluid behaviour. Bingham plastic model describes shear stress and strain rate (du/dr) relation in MR/ER fluid as follow:

$$\tau = \tau_y sgn\left(\frac{du}{dr}\right) + \mu \frac{du}{dr} \quad |\tau| > |\tau_y| \quad (3-4)$$

$$\frac{du}{dr} = 0$$

$$|\tau| < |\tau_y|$$

where, τ_y is the yield point of MR/ER fluid which is a function of magnetic field or current. A typical velocity profile of MR/ER fluid in an annular duct is shown in Figure 3-4. Region 2 in Figure 3-4 is pre-yield region and Regions 1 & 3 are post-yield region where shear stress exceeds the yield stress of the MR/ER fluid. The depth or thickness of the post-yield region (plug) is denoted by δ_p and R_{po} and R_{pi} represent the outer and inner radii of the plug (post-yield) region. The details of the formulation for MR dampers the flow-mode (Figure 3-5) and mixed-mode (Figure 3-6) operations are provided in Appendix-B. In Figures 3-4 to 3-6, R_1 and R_2 indicate the outer radius of the inner plate and the inner radius of the outer plate, respectively.

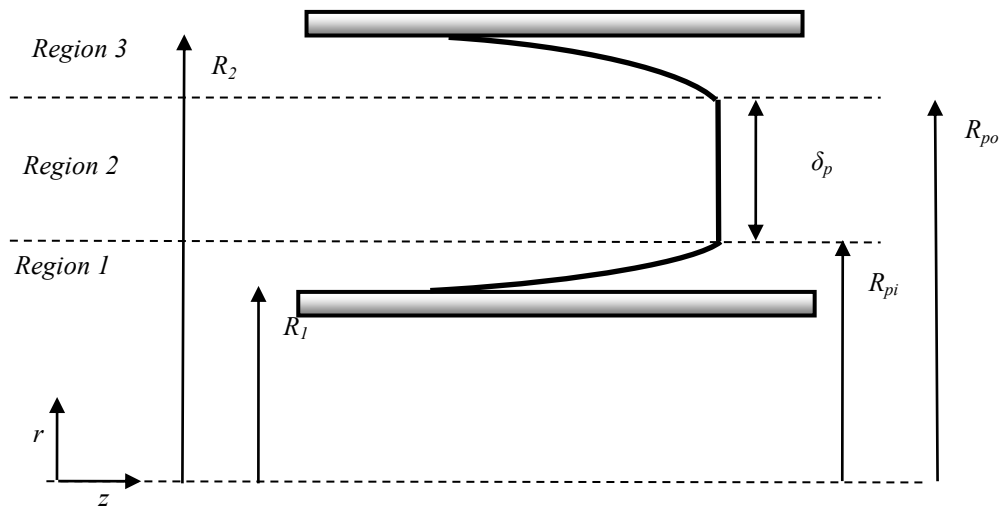


Figure 3-4: Typical velocity profile of MR/ER fluid in annular duct MR/ER damper

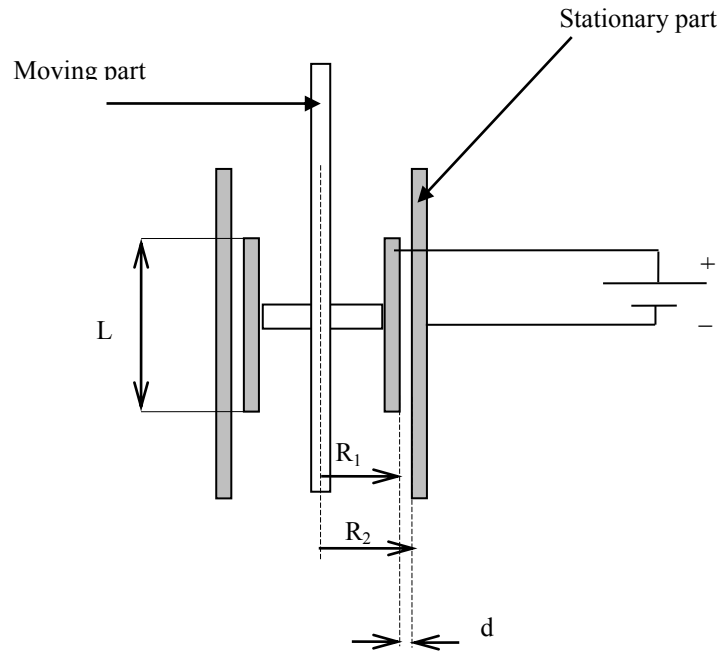


Figure 3-5: Flow mode of ER damper

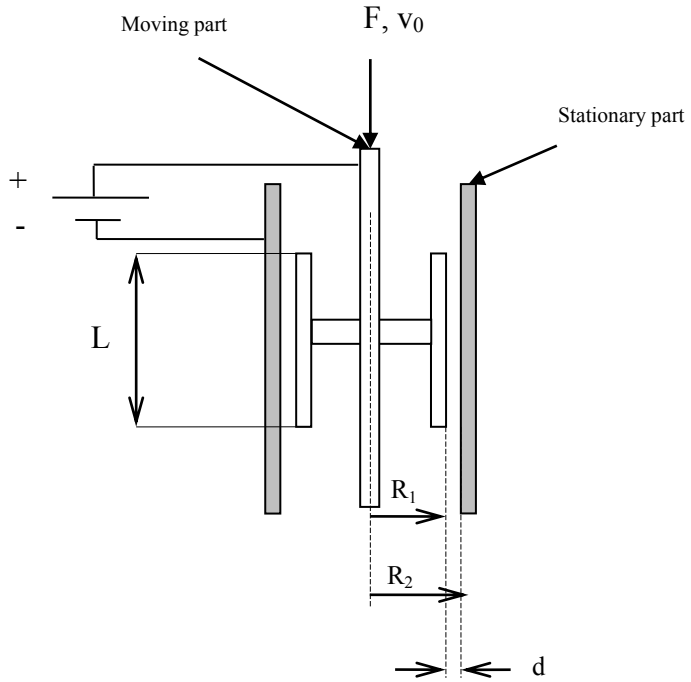


Figure 3-6: Mixed mode of ER damper.

3.3. Dynamic model of ER/MR damper

In the previous section ER/MR damper formulations have been established based on the assumption of steady-state behaviour of ER flow in a duct. This assumption is valid only in low frequency motion and small stroke. In high frequency motion and large stroke, dynamic and unsteady flow behaviour of ER/MR fluid should be taken in to account. In this section, the dynamic behaviour of ER/MR damper under harmonic excitation for flow mode damper according to Nguyen and Choi (2009) is presented.

3.4. Mechanistic model of ER/MR damper

The dynamic behaviour of MR/ER fluid damper can be expressed using the momentum equation, which can be formulated in the following two ways. In the first formulation, which is called velocity/pressure formulation, conservation of momentum equation is expressed using velocity and pressure terms. In this case, both pressure and velocity profile are unknown, and as found out by other researchers, this formulation is limited in scope and may not be very useful. In the second formulation, namely the stream function/vorticity formulation, the conservation of momentum is expressed using a stream function (volumetric flow rate) and vorticity (could be related to the velocity profile in the flow). In dynamic analysis of MR/ER damper, the volumetric flow rate of the fluid is known and it could be used to calculate the stream function. The proposed method in the present study follows this approach, which was not attempted earlier for modelling MR/ER fluid dampers.

The vorticity transport equation of motion in 2-D can be written as follows (Pozrikidis, 2009);

$$\frac{\partial \omega_z}{\partial t} = \frac{1}{\rho} \left(\frac{\partial^2 \tau_{xy}}{\partial x^2} - \frac{\partial^2 \tau_{xy}}{\partial y^2} + \frac{\partial^2 (\sigma_{yy} - \sigma_{xx})}{\partial y \partial x} \right) \quad (3-5)$$

In this research it is assumed that the environmental temperature has no effect in MR damper behaviour. For MR damper application in outdoor in extreme cold or extreme heat, environment temperature should be considered. Also, increase in temperature of MR fluid during its operation has been ignored here. However, in the practical applications, the piston movement in an MR damper may produce heat which may influence characteristics of the fluid. In developing the proposed mechanistic model of MR dampers, it is assumed that the MR fluid is incompressible.

In this study, one dimensional, axi-symmetric geometry of MR/ER damper with an annular duct is approximated by two parallel plates (Gavin, 2001) so that the vorticity transport equation of motion can be simplified as:

$$\frac{\partial \omega_z}{\partial t} = \frac{1}{\rho} \left(- \frac{\partial^2 \tau_{xy}}{\partial y^2} \right) \quad (3-6)$$

The following assumptions have been made to simplify the analysis: MR/ER fluid is incompressible, the yield stress of MR/ER fluid is constant across the gap between two plates, the fluid is in the laminar regime, and MR/ER fluid is in immediate contact with plate (no slippage with the boundary). The relation between the velocity and the vorticity and between the velocity and the stream function are expressed as (Pozrikidis, 2009):

$$\omega_z = -\frac{\partial u_x}{\partial y} \quad (3-7)$$

$$u_x = \frac{\partial \psi}{\partial y} \quad (3-8)$$

Thus, ω_z can be stated as:

$$\omega_z = -\frac{\partial^2 \psi}{\partial y^2} \quad (3-9)$$

MR/ER fluids are non-Newtonian fluids and their behaviour can be fairly approximated by Bingham model described as:

$$\begin{cases} \tau < \tau_{yield} & \dot{\gamma} = 0 \\ \tau > \tau_{yield} & \tau = \tau_{yield} \text{sign}(\dot{\gamma}) + \mu \dot{\gamma} \end{cases} \quad (3-10)$$

Bingham constitutive relation has a simple form, but in the mathematical term the formulation implies that the Bingham fluid is rigid and will yield when the stress the material reaches the yield stress. However, since the strain in a rigid body has no meaning and cannot be calculated, it becomes difficult to express the stress in terms of a kinematic parameter such as strain or strain rate using a linear form.

The vorticity on the left side of Eq. (3-6) is related to the stream function by Eq. (3-9). The volumetric flow rate (represented by ψ) of the flow is known because it is related to velocity of damper strut. Thus, the left side of Eq. (3-6) is a known variable. On the left side of Eq. (3-6), the shear stress, τ_{xy} depends on whether the fluid is in pre-yield or post-yield regime (Eq. 3-10) which could not be determined before solving Eq. (3-6). To address this problem, a

regularization procedure can be applied. It means that one may use a single smooth function that can fairly approximate the bilinear behaviour of Bingham function and eliminate the necessity of tracking the yield point in the flow field, and the constitutive relation could be applied anywhere in the flow field, pre-yield or post-yield region (Papanastasiou ,1987).

There are several choices for the regularization curve (Frigaarda and Nouar, 2005; Deana et al. 2007)) . In the present work, the generalizing function introduced by Papanastasiou (1987) has been used to approximate the Bingham model:

$$\tau_{yx} = \mu\dot{\gamma} + \text{sign}(\dot{\gamma})\tau_y(1 - e^{(-n|\dot{\gamma}|)}) \quad (3-11)$$

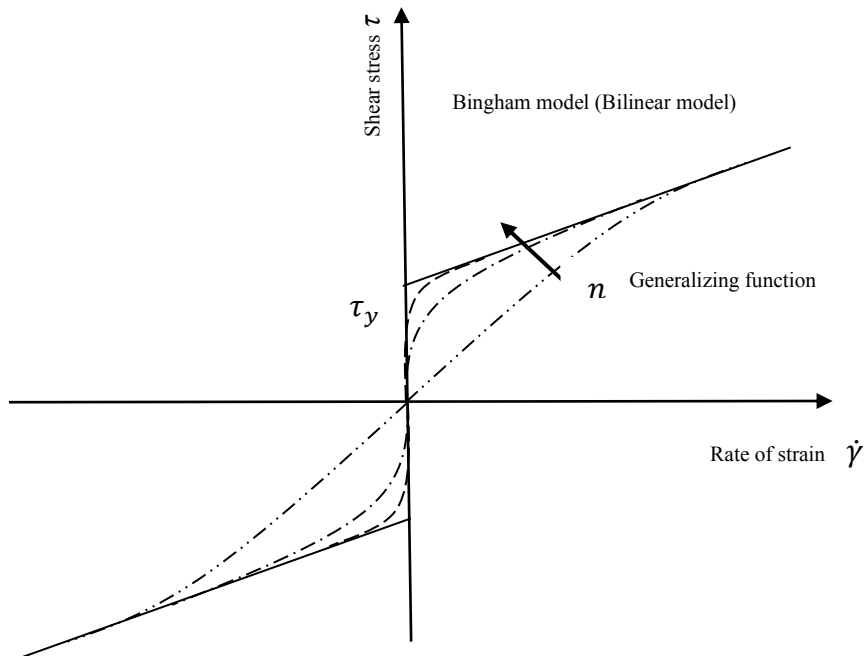


Figure 3-7: Approximation of generalizing function for Bingham model.

As it can be seen from Figure 3-7, by increasing parameter n in Eq. (3-11), the generalizing function becomes closer to the original Bingham model. For random loadings, Eq. (3-6) may not have closed-form solution, while it can be solved numerically using finite element or finite difference techniques. Finite difference technique is easier to implement for Computational Fluid Dynamics (CFD) problems concerning a differential equation for a section of fluid as needed in the present problem. Substituting Eq. (3-11) into Eq. (3-6) and applying the central finite difference method yields:

$$\omega_i(t + \Delta t) = \omega_i(t) + \alpha \times [\omega_{i+1}(t) - 2\omega_i(t) + \omega_{i-1}(t)] + \frac{\tau_y}{\mu} \times \alpha \times [\text{sign}(\omega_{i+1}(t))(1 - e^{-n|\omega_{i+1}(t)|}) - 2\text{sign}(\omega_i(t))(1 - e^{-n|\omega_i(t)|}) + \text{sign}(\omega_{i-1}(t))(1 - e^{-n|\omega_{i-1}(t)|})] \quad (3-12a)$$

$$\alpha = \frac{\mu}{\rho} \times \frac{dt}{dy^2} = \nu \times \frac{dt}{dy^2} \quad (3-12b)$$

Vorticity in time $[t+\Delta t, \omega_i(t + \Delta t)]$ is calculated using its value in time t . The numerical method involves computing the evolution of the vorticity from the initial value using the vorticity transport in Eq. (3-12), while simultaneously recovering the evolution of the stream function using Eq. (3-9). Since, Eq (3-9) and Eq. (3-12) are second order differential equations with respect to y , two boundary conditions for the vorticity and two boundary conditions for the stream function are required at each end of the solution domain; $y=0$ and $y=h$ as shown in Figure (3-8). The base level of the stream function can remain unspecified as adding an arbitrary constant to the stream function does not alter the velocity, and it can be assumed that, $\psi(y=0)=0$, and $\psi(y=h)=Q(t)$ (Pozrikidis, 2009). To illustrates the implementation of boundary condition in

flow and mix mode of MR/ER damper, the flow domain ($0 < y < h$) is divided into N intervals as shown in Figure (3-8). Substituting the y derivative on the right-hand side of Eq. (3-9) and using the finite difference method, the following terms can be obtained:

$$\omega_1 = \frac{\left(\frac{\partial \psi}{\partial y}\right)_{\frac{1}{2}(y_1+y_2)} - \left(\frac{\partial \psi}{\partial y}\right)_{y_1}}{\frac{1}{2}\Delta y} = -2 \frac{\psi_2 - \psi_1 - U_1}{\Delta y} = 2 \frac{\psi_1 - \psi_2}{\Delta y^2} + 2 \frac{U_1}{\Delta y} \quad (3-13)$$

$$\omega_{N+1} = \frac{\left(\frac{\partial \psi}{\partial y}\right)_{y_{N+1}} - \left(\frac{\partial \psi}{\partial y}\right)_{\frac{1}{2}(y_N+y_{N+1})}}{\frac{1}{2}\Delta y} = -2 \frac{U_2 - \psi_{N+1} - \psi_N}{\Delta y} = 2 \frac{\psi_{N+1} - \psi_N}{\Delta y^2} - 2 \frac{U_2}{\Delta y} \quad (3-14)$$

$$\psi_{N+1} = Q, \psi_1 = 0 \quad (3-15)$$

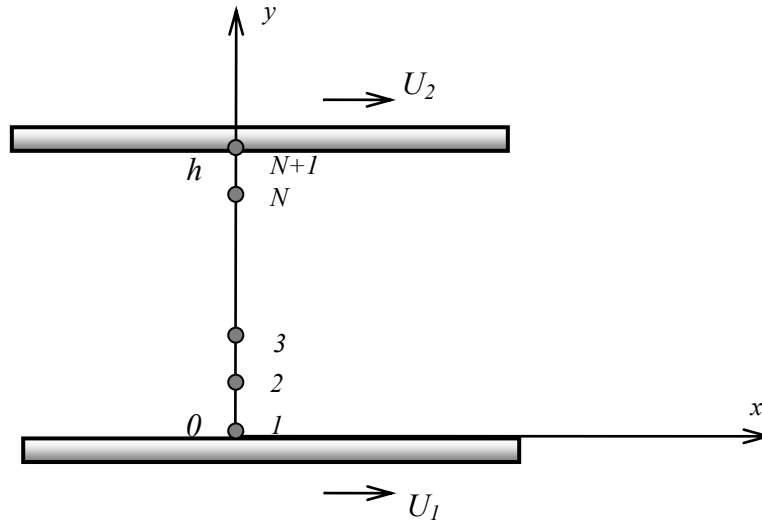


Figure 3-8: One-dimensional finite-difference grid used to compute the velocity profile in unidirectional channel flow (Pozrikidis, 2009).

By applying Eq. (3-9) for each node of a one dimensional finite difference mesh along with boundary conditions in Eqs. (3-16, 3-17 and 3-18) will provide the results for ω and ψ at each node (Pozrikidis, 2009). It should be mentioned that MR/ER damper in the flow mode has two

stationary walls such that, $U_1=U_2=0$, and for the mixed mode, there is one stationary wall with $U_1=0$, and one moving wall with $U_2 \neq 0$. Both the cases can be solved using the present method.

The velocity can also be retrieved using Equation (3-7), and to determine the pressure, one may use Cauchy's equation of motion as below:

$$\rho \left(\frac{\partial u_x}{\partial t} + u_x \frac{\partial u_x}{\partial x} + u_y \frac{\partial u_x}{\partial y} + u_z \frac{\partial u_x}{\partial z} \right) = \frac{\partial \sigma_{xx}}{\partial x} + \frac{\partial \sigma_{yx}}{\partial y} + \frac{\partial \sigma_{zx}}{\partial z} + \rho \times g_x \quad (3-16)$$

For unidirectional flow in which $\sigma_{yx} \equiv \tau_{yx}$, Eq. (3-16) can be rewritten as:

$$\rho \left(\frac{\partial u_x}{\partial t} \right) = -\frac{\partial p}{\partial x} + \frac{\partial \tau_{yx}}{\partial y} \quad (3-17)$$

Substituting τ_{yx} of Eq. (3-10) into Eq. (3-16), the finite difference equation is obtained as:

$$\Delta p(t) = -l \times \left[\frac{\rho}{\Delta t} \times (u_x(t + \Delta t) - u_x(t)) + \frac{\mu}{2\Delta y} \times (\omega_{i+1}(t + \Delta t) - \omega_{i-1}(t + \Delta t)) + \frac{\tau_y}{2\Delta y} \times \right. \\ \left. (\text{sign}(\omega_{i+1}(t + \Delta t)) \times (1 - e^{-n|\omega_{i+1}(t+\Delta t)|}) + \text{sign}(\omega_{i-1}(t + \Delta t)) \times (1 - e^{-n|\omega_{i-1}(t+\Delta t)|})) \right] \quad (3-18)$$

where, L is the length of duct.

The proposed method has advantages over the method presented in Section 3.2.2. The method covers mixed mode ER/MR damper as well as flow mode damper. Besides, it is not confined to harmonic motion only, and can be used when the motion is random.

For practical applications, the proposed mechanistic model could be used by manufactures and engineers to design new MR dampers and investigate the behavior of MR dampers to evaluate the key parameters. Furthermore, it is possible to develop a phenomenological model based on the results of the mechanistic model, and the resulting phenomenological model can be

integrated to the structural model to assess the influence of the number and locations of dampers on the performance of a structure. In that case, the phenomenological model should be simple enough such that the combined structure-damper system can be solved efficiently and required design iterations can be performed quickly.

3.5. A new phenomenological model for random loading in ER/MR damper

The proposed phenomenological model has been developed through investigation of the variation of the damping force with respect to the yield stress of ER/MR fluid and also its dependence on the ER/MR damper strut velocity. To achieve this, a small size damper studied by Choi and Nguyen (2009) and shown in Figure 3-9 has been chosen. The closed-form dynamic analytical model developed by Chen et al. (2004) and validated against experimented data by Choi and Nguyen (2009) has been considered as a benchmark for the proposed phenomenological model. ER/MR damper damping force is the function of both the yield stress τ_y and strut velocity v .

This can generally be stated as:

$$F_d = f(v, \tau_y) \quad (3-19)$$

where, F_d is the damping force in ER/MR damper, τ_y is yield stress in MR/ER fluid and v is the velocity of strut. To study how the damping force is related to the yield stress of ER fluid, one could study the variation of the damping force in ER damper versus different applied electrical

current (which alters the yield stress of ER fluid) at low frequency. The study has been done in 0.2Hz (Figure 3-10) to largely eliminate the effect of the strut velocity in damping force of ER damper. The variation of the damping force versus yield stress in ER fluid in very low velocity has been shown in Figure 3-11. As it can be seen the damping force varies linearly with respect to τ_y .

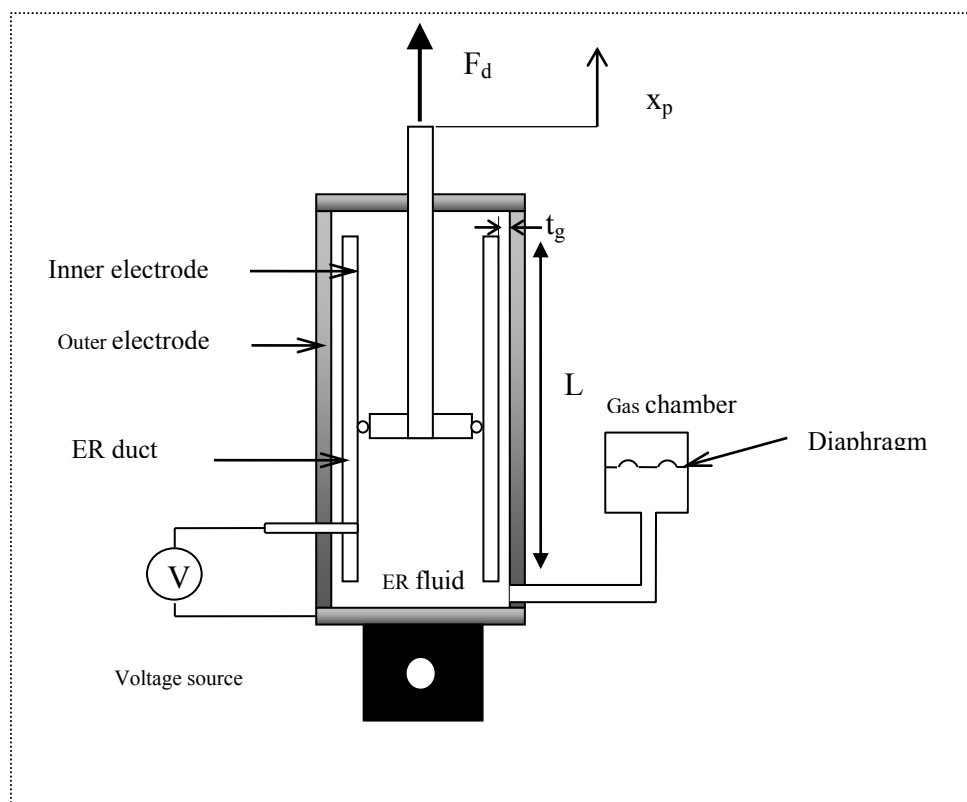


Figure 3-9: Schematic configuration of the ER damper (adapted from Choi 2009).

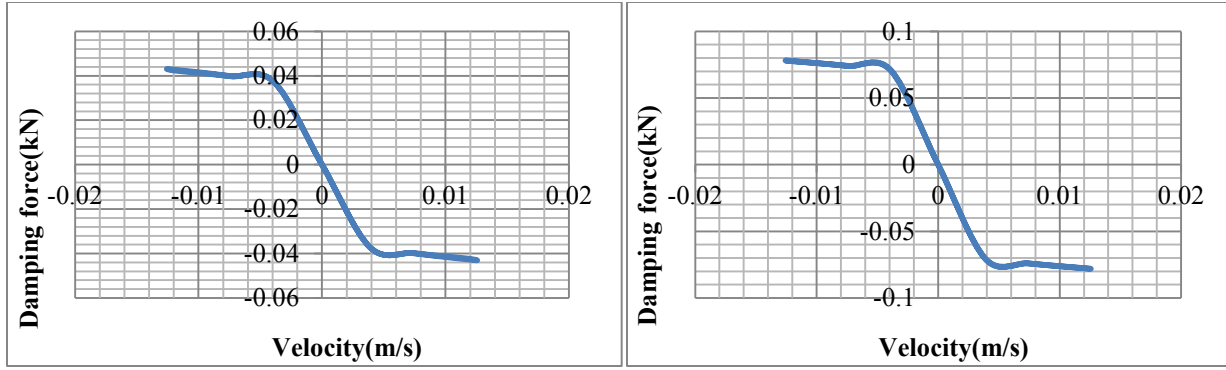


Figure 3-10: The variation of the damping force versus yield stress in ER fluid in very low velocity. Left (frequency = 0.2 HZ, $\tau_y = 100 \text{ kg/cm}^2$), Right (frequency = 0.2 HZ, $\tau_y = 200 \text{ kg/cm}^2$).

The relation between applied electric current and yield stress in ER fluid can be state as (Choi, 2009) :

$$\tau_y = \alpha E^\beta \quad (3-20)$$

where E is the applied electric current whose unit is KVmm^{-1} , α and β are 591 and 1.42, respectively.

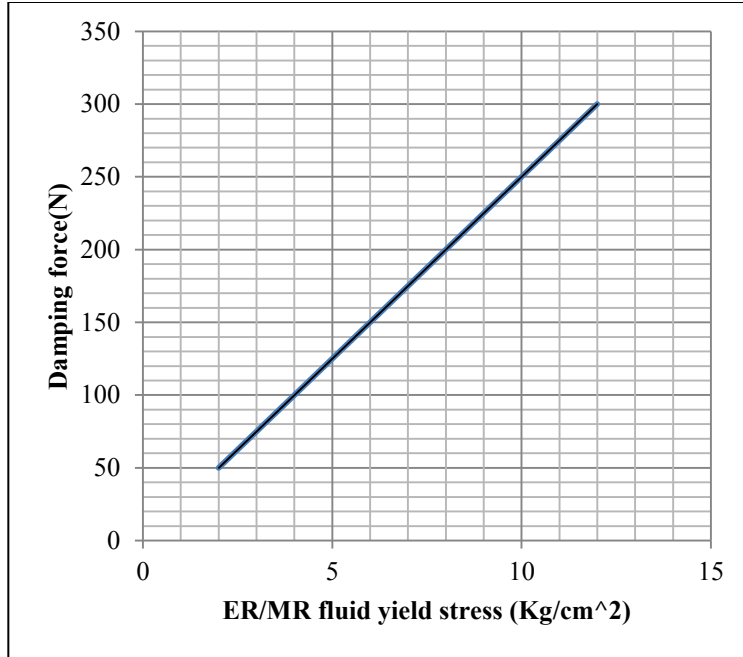


Figure 3-11: The damping force versus yield stress in ER fluid in frequency of 0.2 Hz.

Extensive parametric studies have been conducted to evaluate the dependency of the damping force to strut velocity. Considerable dependency of the ER/MR damper force to the velocity of strut is observed at high velocity which is the case in seismic loading. The following damping model has been proposed:

$$F_d = C_1 \times \tau_y \times \text{sign}(v) + C_2 \times \text{sign}(v) \times v + C_3 \times \text{sign}(v) \times v^\alpha \quad (3-21)$$

It has been found that the linear velocity term in Eq.(3-21) does not have a significant effect on the damping force ($C_2 = 0$). Moreover, by fine tuning of the simulation results with the results of the benchmark problem, the parameter α was found to be 2. Figure 3-11 shows the effect of the value of α on the damping force (Eq.(3-21)).

In this formulation F_d should be limited to maximum MR damper capacity. It can be done by implementing a saturation function to the maximum capacity of the MR damper.

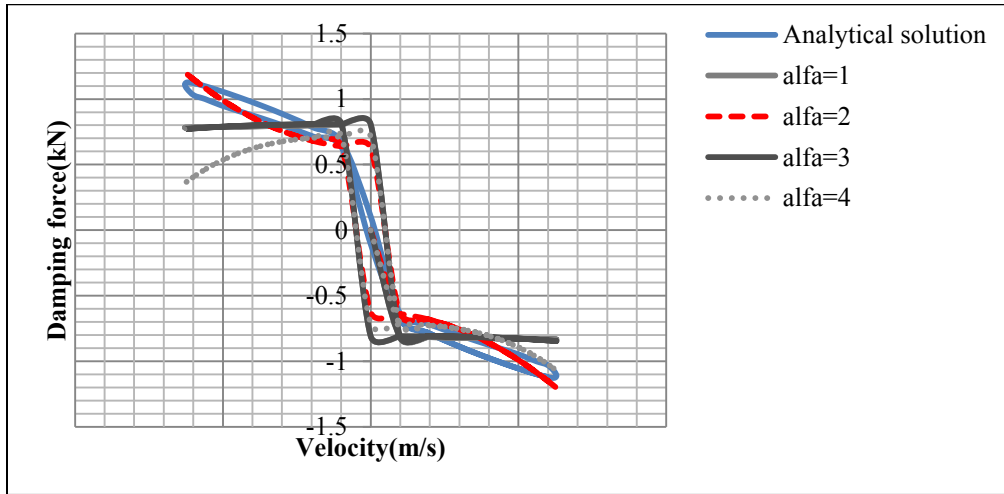


Figure 3-12: Damping force versus strut velocity for different value of α (frequency = 20 Hz, $\tau_y = 1500kg/cm^2$).

There are three disadvantages of a TMD application. First, TMDs are effective only for one mode which makes them less convenient for ground excitations which generally contain multiple frequencies. Second, they are responsive to de-tuning. Third, they occupy large space and TMD mass in heavy building becomes certainly big and heavy.

A simple arrangement of TMD is shown in Figure 3-13. The amount of mass is typically limited to the maximum value that can be installed. TMD mass ratio (TMD mass divided by the main structural mass) has a positive direct effect on the structural response and it is recommended that for all practical purposes the mass ratio be mainly limited to about 10 percent. For a tall building with a height of forty-storey such as the one considered in this study, the mass ratio can be between 1.5 to 2 percent (Watakabe et al. 2001). Watakabe et al. (2001) installed

TMD with a mass ratio of 1.73% in a 39-storey building. On the other hand, considering the assigned TMD mass ratio, the spring and damping coefficients of TMD system should be optimally designed to provide optimal structural vibration suppression. The optimum parameters of tuned mass dampers (TMD) that result in significant reduction in the response of structures to seismic loading were the subject of several researches (Warburton, 1982; Sadek et al ,1997; Rana and Soong,1998; Hoange et al. 2008; Yang et al. 2010). Most such research is limited to single degree of freedom systems, while only a few of them considered a wide range of mass ratio. In the current research, the response of the structure with passive TMD with a fixed mass ratio has been investigated. Here, the stiffness and damping of the TMD system are altered from 20% to 200% of the values corresponding to the perfect tuning condition and the response of the structure during ground motion has been determined accordingly. Although this approach provides a pair of values for the stiffness and damping of an optimal TMD system (based on minimum displacement), it is observed that different ground motion needs different pair of optimal stiffness and damping ratio for the TMD system. The response of the pilot (e.g. case study) structure is investigated with different ground motions. Thus, perfect tuning technique has been used in these works. In perfect tuning, the natural frequency of a TMD should be equal to the fundamental frequency of the main structure. For the mass ratio of 1.5%, perfect tuning states that:

$$\begin{aligned} m_{TMD} &= 0.015 \times M_{structure} \\ \omega_{TMD} &= \omega_{structure} \end{aligned} \quad (3-22)$$

Thus;

$$\frac{k_{TMD}}{m_{TMD}} = \omega_{structure}^2 \quad ; \quad c_{TMD} = 2 \times \xi_{structure} \times m_{TMD} \times \omega_{structure} \quad (3-23)$$

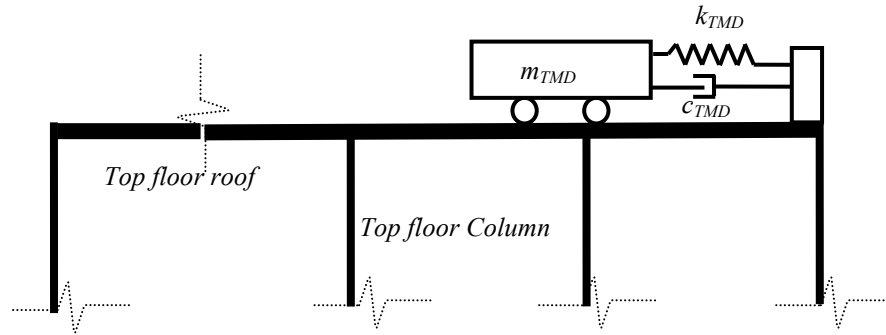


Figure 3-13: Typical arrangement of TMD system

3.6. Modeling of MR-based TMD and MR damper braces in building structure

To investigate application of MR damper in building structures two different types of usage of have been considered. In the first application, MR damper has been implemented into tuned mass damper. In the second application, MR damper has been employed in bracing system. For both cases, building structures has been designed and studied using a number of different seismic ground motion records.

For studying the effect of semi active tuned mass damper, a 40-storey high steel moment-resisting frame building located in Vancouver has been considered. The building has nine bays of six meters in one direction and five bays of six meters in another direction as shown in Figure (3-14). The dead and live loads are estimated to be 6 kPa and 2.4 kPa, respectively. The seismic and wind load provisions of the National Building Code of Canada, NBCC (2010) have been applied to estimate the lateral loads. The soil site class is assumed to be C. The lateral resisting system is considered to be ductile moment resisting frame. The base shear is estimated to be

2.2% of dead load of the building. The structural damping is considered to be 2.5% as it is the damping in steel structures is considered low. The NBCC (2010) does not allow the use of the equivalent static base shear for the design of a building higher than 60 m. The equivalent static forces are used here only for the preliminary design. The response spectral analysis has been used to evaluate the design forces in the structural members due to earthquake load. The steel structural design has been done using CSA-S16 standard (2009), and the CISC handbook (2010). The ETABS software (2012) has been used for the analysis and design of the Structure. The columns and beams section used in the building are listed in Table (3-1).

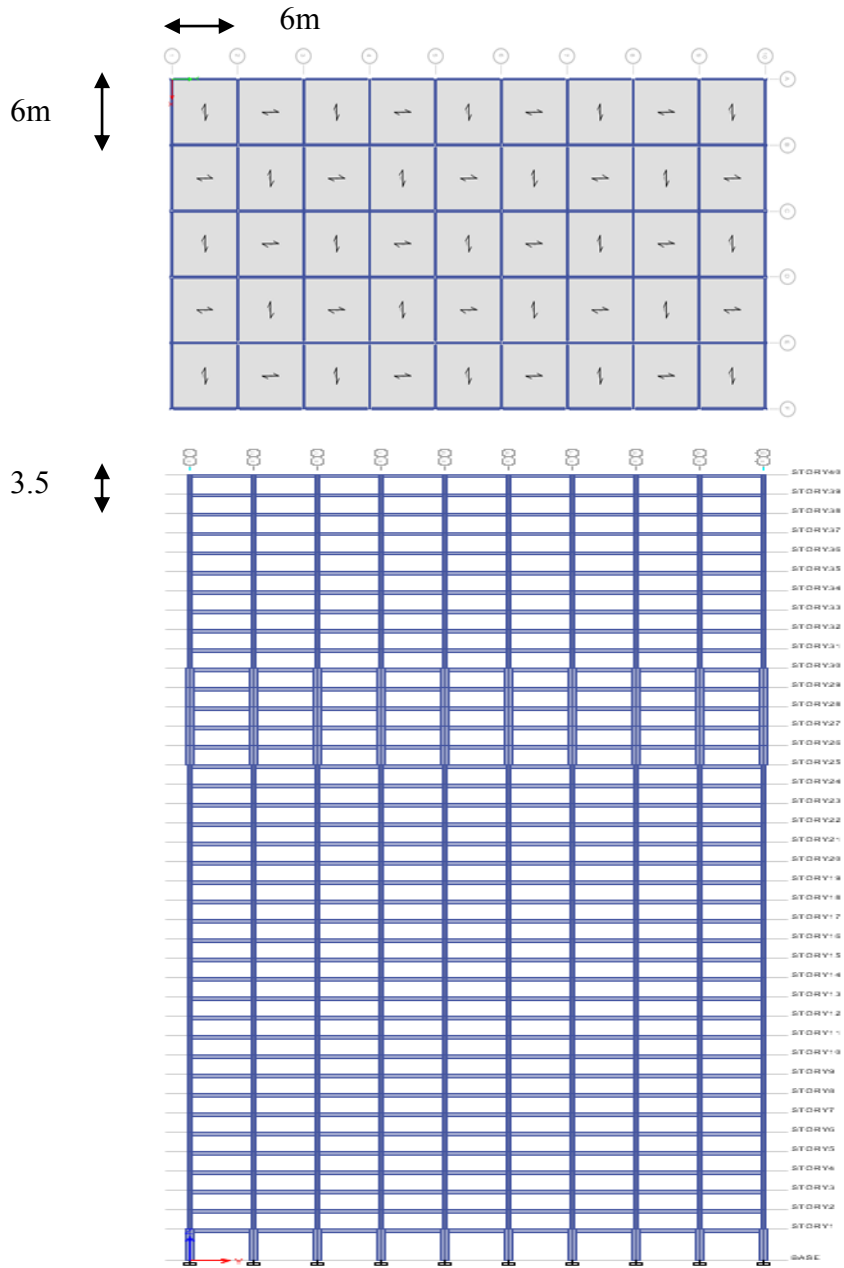


Figure.3-14: Beam frame plan and elevation of 40 storey building

Table3-1: Summary of tall building columns and beams sections.

Floor number	Column size	Beam size
1	WWF600x551	W610x101
2-5	WWF500x456	W610x101
6-10	WWF450x409	W610x101
11-15	WWF450x342	W610x101
16-20	WWF400x303	W510x101
21-25	WWF400x243	W610x91
26-30	w610x195	W610x91
31-35	W460x144	W530x82
36-39	W410x114	W460x67
40	Depends on position of mass (W410x114 mostly)	Depends on position of mass (W460x67 mostly)

A three dimensional finite element (FE) model of has been developed in the ETABS software for the purpose of analysis and design. The FE model has about 7000 degrees of freedom (DOFs) which makes it computationally very expensive with respect to analysis and also development of a control system. Thus, the 3D model has been simplified into to an equivalent 2D FE model (shear storey building). It should be noted that the simplification has been done without compromising the main DOFs (main floor displacements and velocities) and thus the modal and dynamics characteristics of the 3D FE model are matched in the 2D model. Among the key parameters of the structure affecting its dynamic characteristics, the mass and damping in the 2D model are kept the same as those in the 3D model. However the stiffness of the 2D model has been manipulated to realize the appropriate dynamic responses according to the 3D FE model. While the floor mass and damping are kept the same in both the models, structural stiffness matrix in the 2D model has been modified to provide the best agreement

between the first vibration mode of the 3D and 2D FE models. Then, the dynamics response of the 3D and 2D FE models due to random or seismic loading are compared to justify modification of the stiffness matrix.

The first four vibration modes of the building are shown in Figure 3-15. The initial estimate of the fundamental period using the empirical formula provided in NBCC (2010) is 3.3 seconds which is quite conservative. The code allows up to twice that period (i.e., 5.7 seconds) for base shear calculation, if the period calculated by the modal analysis is higher. The frequency of the vibration mode shapes and their modal participation factors are given in Table 3-2. As it can be seen from Figure 3-15, the torsional vibration modes are excluded from the first four vibration modes. The first four mode shapes include 94% of modal participation (Table 3-2). As the building is symmetric, the modal participation of torsional vibration mode is zero (Table 3-3). Thus, eliminating the torsional vibration modes will introduce no error in calculation and will simplify the computation very much. Torsional vibration mode shapes are shown in Figure 3-16.

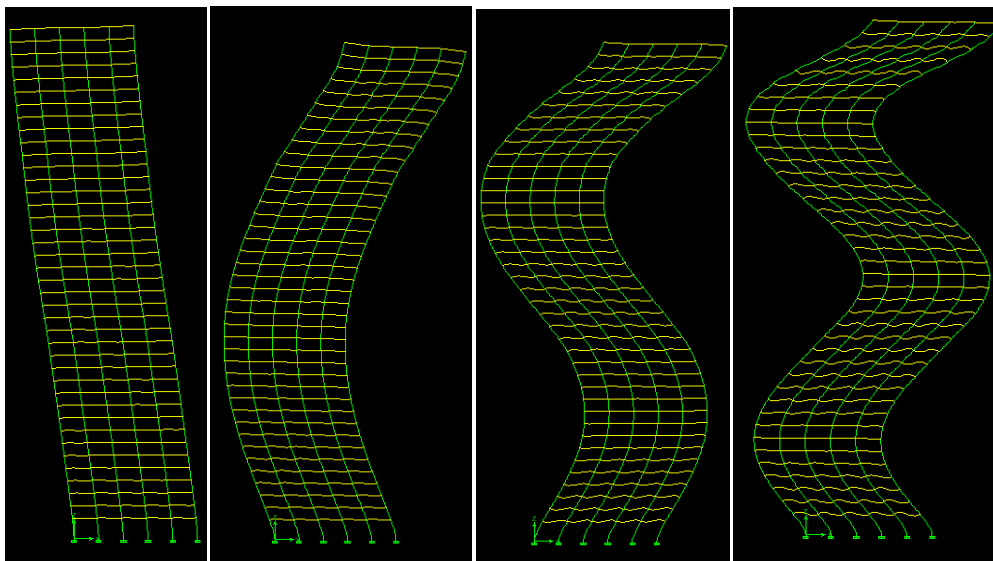


Figure.3-15: 40 Storey building mode shapes

Table 3-2: 40 storey building vibration frequency and modal participation.

	First mode ETABS	First mode NBCC	Second mode	Third mode	Forth mode
Period(second)	5.76	3.3	2.02	1.22	0.80
Frequency(Hz)	0.18		0.50	0.82	1.24
Modal Participation	75.7		12.8	4.3	2.1
Modal participation summation	94.8 %				

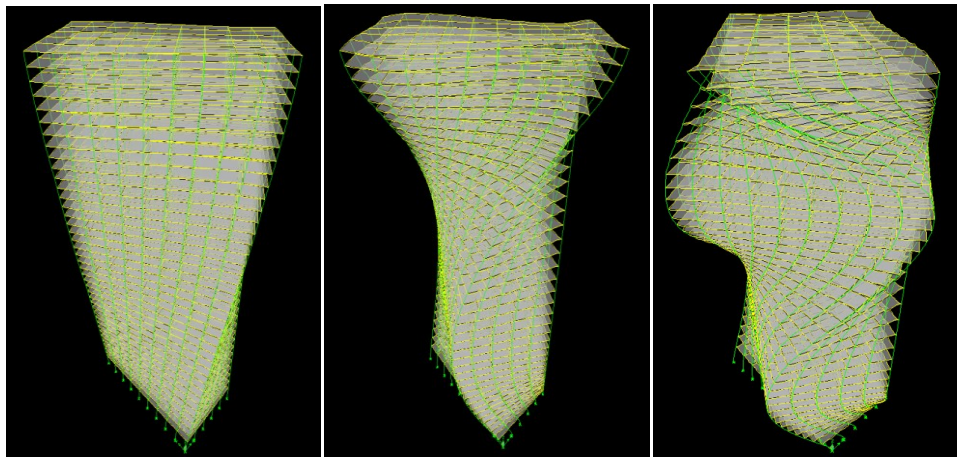


Figure 3-16: 40 storey building torsional vibration mode shape

Table3-3: 40 storey building torsional vibration frequency and modal participation.

	First torsional vibration mode	Second torsional vibration mode	Third torsional vibration mode
Period(second)	4.9	1.8	1.12
Frequency(Hz)	0.2	0.55	0.89
Modal Participation	0	0	0

A set of typical a five and a twenty storey steel moment resisting frame buildings have been designed according to the National Building Code of Canada and relevant standards. These buildings will be used as case study structures to do comparison between LQR-clip optimal semi active control system and passive-on mode control system under different seismic excitations. The buildings have nine bays of six meters in one direction and five bays of six meters in another direction as shown in Figure (3-15). The lateral load resisting system of building consists of ductile moment resisting frames. The soil site class is assumed to be C. The dead and live loads are assumed to be 6 kPa and 2.4 kPa, respectively. The seismic and wind load provisions of the National Building Code of Canada, NBCC (2010) have been applied to estimate the lateral loads. The base shear is estimated as 2.2% and 7% of total dead load of the 20 and 5 story building, respectively. The structural damping consider to be 2.5%. The steel structural design has been done using CSA-S16 standard (2009), and the CISC handbook (2009). The lateral load resisting system of building consists of moment resistant steel frames.

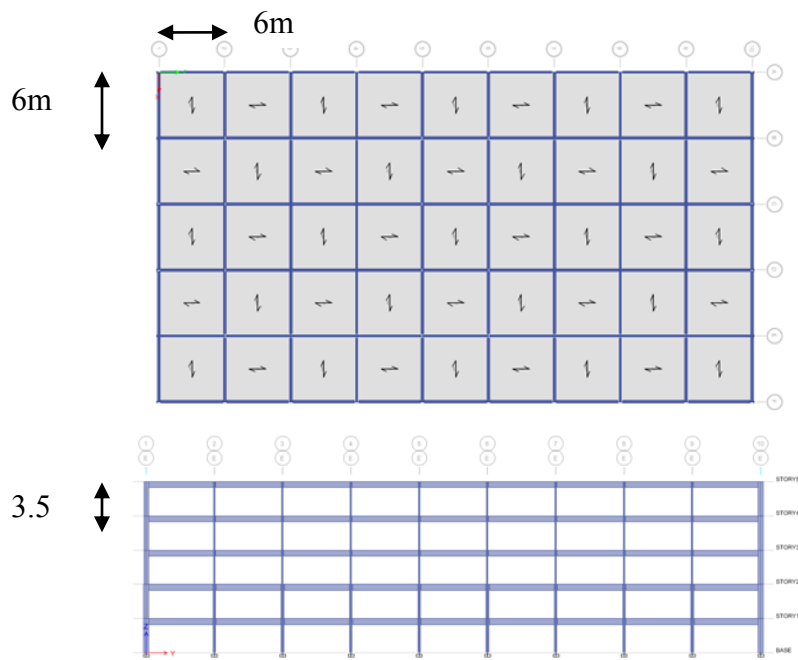


Figure.3-17: Beam frame plan and elevation of 5 storey building

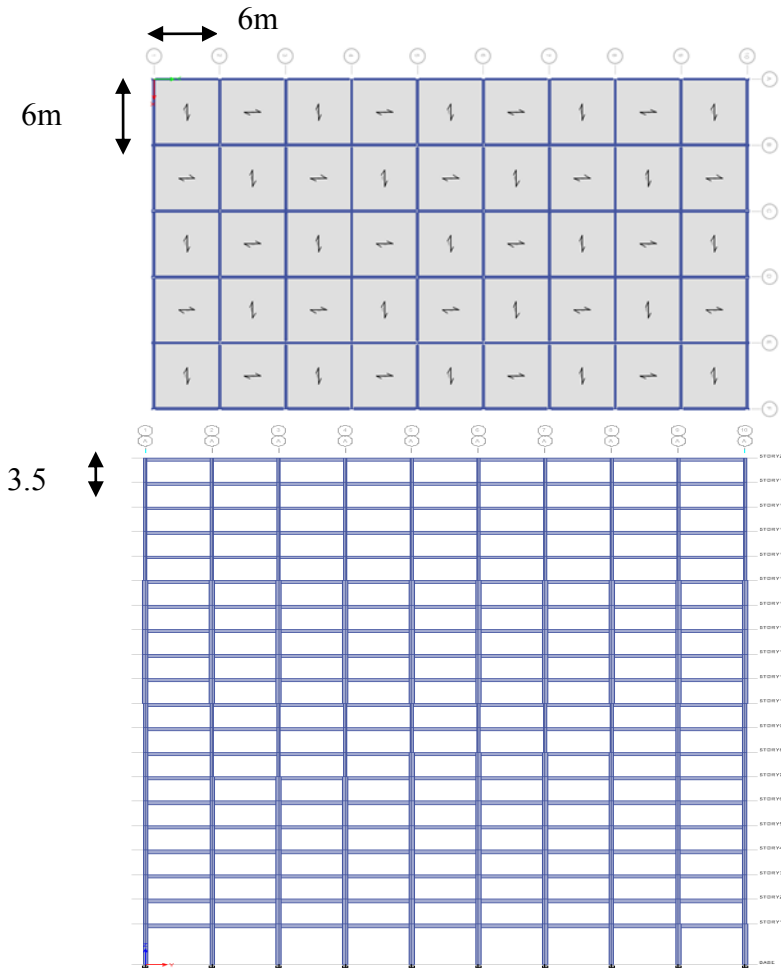


Figure.3-18: Beam frame plan and elevation of 20 storey building

Table 3-4: Summary of twenty storey building columns and beams sections.

Floor number	Column size	Beam size
1	WWF450x274	W460x61
2-5	WWF400x202	W460x67
6-10	WWF350x176	W410x67
11-15	W460x128	W410x61
16-20	W250x89	W360x51

Table 3-5: Summary of 5 storey building columns and beams sections.

Floor number	Column size	Beam size
1-2	W460x128	W530x72
3-5	W460x85	W530x72

The ETABS software (2012) has been used for the analysis and design of the structures. The columns and beams section used in the building are listed in Table (3-4 & 3-5). Dynamic response of a structure under seismic loading is closely related to dynamics characteristics of that building like natural frequencies, modal shapes and modal participation of that structure. Dynamic characteristics of five and twenty storey building are summarized in Tables (3-6 & 7). A three dimensional finite element (FE) model of the forty-storey building has been developed in the ETABS software for the purpose of analysis and design. The FE model has about thousands of degrees of freedom (DOFs) which make it computationally very expensive with respect to analysis and also development of control system. In order to reduce the number of degrees of freedom, the system can be reduced or condensed by available methods such as dynamic reduction (Guyan 1965) or Ritz vectors (e.g., Chopra 2012) which are mathematically complex. Here, the three-dimensional (3D) model has been simplified into an equivalent two-dimensional (2D) FE model (i.e., shear storey building). It should be noted that the simplification has been done without compromising the main DOFs (main floor displacements and velocities) and thus the modal and dynamics characteristics of the 3D FE model. Among three main dynamic characteristics of structure, the mass and damping are kept constant in 3D and 2D models; however the stiffness of the 2D model has been manipulated to realize appropriate dynamic

responses according to the 3D FE model. In the current study, the 3D model of structure is converted into 2D shear building with the same floor mass and structural damping and structural stiffness matrix has been modified to provide the best agreement between the first vibration mode of 3D and 2D FE models. Then, the dynamics response of 3D and 2D FE models due to random or seismic loading are compared to justify modification of the stiffness matrix.

Table (3-6) lists period, frequency and modal participation factors for the four modes of twenty storey building. Modal mass participation factors indicate how much a specific mode contributes to the overall response of the structure. As it can be observed from Table 3-6, modal participation factor is largest for the first mode. The sum of the modal participation factors for a given number of modes indicates the overall contribution of these modes to the dynamic response of the structure. For example, in the twenty storey building, 96.8% of the total mass is contributed by the participation of the first four modes. The frequency and modal participation of first four modes of five storey building is illustrated and itemized in Table (3-7).

Table3-6: Twenty storey building vibration frequency and modal participation.

	First mode ETABS	First mode NBCC	Second mode	Third mode	Forth mode
Period(second)	4.5	2.5	1.70	1.1	0.68
Frequency(Hz)	0.22		0.56	0.90	1.47
Modal Participation	79.2		11.0	4.5	2.0
Modal participation summation	96.8%				

Table 3-7: Five storey building vibration frequency and modal participation.

	First mode ETABS	First mode NBCC	Second mode	Third mode	Forth mode
Period(second)	1.1	0.72	0.35	0.2	0.137
Frequency(Hz)	0.9		2.85	5	7.2
Modal Participation	78%		12%	6%	2%
Modal participation summation	98				

3.7. Control algorithms for semi-active system

Equations of motion of a seismically excited structure in finite element form may be stated as:

$$M_s \ddot{Z} + C_s \dot{Z} + K_s Z = \Lambda U - M_s \Gamma \ddot{x}_g \quad (3-24)$$

where, M_s , C_s and K_s are the mass, damping and stiffness matrices of the system. U is the control force vector, Λ is the control force location matrix, and Γ is the direction matrix related to the base acceleration, \ddot{x}_g .

The equations of the motion as given by Eq. (3-24) are transformed into a state space representation (also known as the "time-domain approach") to provide a convenient way to model and control a system with multiple inputs and outputs. To accomplish this, one may write:

$$\begin{cases} x_1 = z \\ x_2 = \dot{z} \end{cases} \quad (3-25)$$

Where, the first state x_1 is the displacement and second state x_2 is the velocity.

Using the above change of variables, the state space presentation of Eq. (3-24) can be written as:

$$\dot{X} = AX + BU + E\ddot{x}_g \quad (3-26)$$

where, A , B and E , are matrices defined as:

$$A = \begin{bmatrix} 0 & I \\ -M_s^{-1}K_s & -M_s^{-1}C_s \end{bmatrix}_{2n \times 2n} \quad (3-27)$$

$$B = \begin{bmatrix} 0 \\ -M_s^{-1}\Lambda \end{bmatrix}_{2n \times n} \quad (3-28)$$

$$E = \begin{bmatrix} 0 \\ \Gamma \end{bmatrix}_{2n \times 1} \quad (3-29)$$

$$\Gamma = \begin{bmatrix} 1 \\ \vdots \\ 1 \end{bmatrix}_{n \times 1} \quad (3-30)$$

In TMD system A is defined as

$$A = \begin{bmatrix} 0 & 0 & 0 & \cdots & 0 \\ 0 & 0 & 0 & \cdots & 0 \\ 0 & 0 & 0 & \ddots & \vdots \\ \vdots & \vdots & \vdots & \ddots & \vdots \\ 0 & 0 & \cdots & -1 & 1 \end{bmatrix}_{n \times n} \quad (3-32)$$

While in MR damper in bracing system A is defined as

$$A = \begin{bmatrix} 1 & -1 & \cdots & 0 & 0 \\ \cdots & 1 & -1 & \cdots & 0 \\ 0 & \cdots & 1 & -1 & \cdots \\ 0 & 0 & \cdots & 1 & -1 \\ 0 & 0 & 0 & \cdots & 1 \end{bmatrix}_{n \times n} \quad (3-33)$$

and $X = \begin{bmatrix} \vdots \\ \vdots \end{bmatrix}_{2n \times 1} = \begin{Bmatrix} x_1 \\ x_2 \end{Bmatrix}$ is the state vector

As it can be realized from Eq. (3-26), the state vector (X) is related to its derivative in time domain, control force (U) and ground excitation. State space model of a structure under seismic excitation and control forces can be solved using the relevant numerical tools such as those available in MATLAB/SIMULINK (2011). The theory of optimal control is concerned with operating a dynamic system at the minimum cost. If the system dynamics is represented in the form of linear differential equations and the cost function can be written as a quadratic function, the LQR control strategy can be used to minimize the cost function. For the structural system, cost function can be written as:

$$J = \int_0^t (X^T Q X + U^T R U) dt \quad (3-33)$$

Where, the first term in Eq. (33) represents the structural kinetic energy due to vibration and the second term represents the work done by the control force. Q and R are arbitrary positive semi-definite and positive definite matrices, respectively, which are used to tune the control system. For example, if the Q matrix has small components, it results in large displacements and velocity in the system. On the other hand, if the elements of Q matrix have large values, it results in small displacements and velocity, but large gain factor (control force) which may not be practical. Also large values in the R matrix would cause small gain (small control force) and large displacements, while small values would produce large gain (large control force) and small displacements. It should be noted that Q and R matrices should be chosen in the way that gain matrix satisfies the maximum allowable displacements and maximum applicable control forces.

The control gain matrix K can be written as:

$$K = R^{-1} B^T P = \begin{bmatrix} \cdots & \cdots & \cdots \\ \vdots & \ddots & \vdots \\ \cdots & \cdots & \cdots \end{bmatrix}_{n \times 2n} \quad (3-34)$$

Where, P is the Riccati matrix which is governed by the following equation called Riccati equation:

$$-\dot{P}(t) = A^T P(t) + P(t)A + R - P(t)BR^{-1}B^T P \quad (3-35)$$

The solution of the LQR problem (control force) can now expressed as Eq. 3-36 and 3-37 for Tuned mass damper and bracing system, respectively.

$$U = -KX = \begin{bmatrix} 0 \\ 0 \\ \vdots \\ 0 \end{bmatrix} \quad \begin{matrix} \\ \\ \\ U_{TMD} \end{matrix} \quad n \times 1 \quad (3-36)$$

$$U = -KX = \begin{bmatrix} \text{Control force for floor 1} \\ \vdots \\ \vdots \\ \vdots \\ \text{Control force for floor } n \end{bmatrix} \quad n \times 1 \quad (3-37)$$

Figure (3-17) shows a block diagram of the state space representation of equations of motion. The vector of states (X) is multiplied by matrix A to give kinematic forces of the structure. In addition, the vector of states (X) is used to compute the control forces by multiplication of the gain matrix (K) by the state vector ($U = -K * X$). Computationally speaking, this procedure considers the ground excitation as the input signal and tries to minimize the response of the

system by introducing the control forces into the system (structure). These control forces (in this research is TMD reaction) are limited to the capacity of the actuators (in this research is MR damper forces).

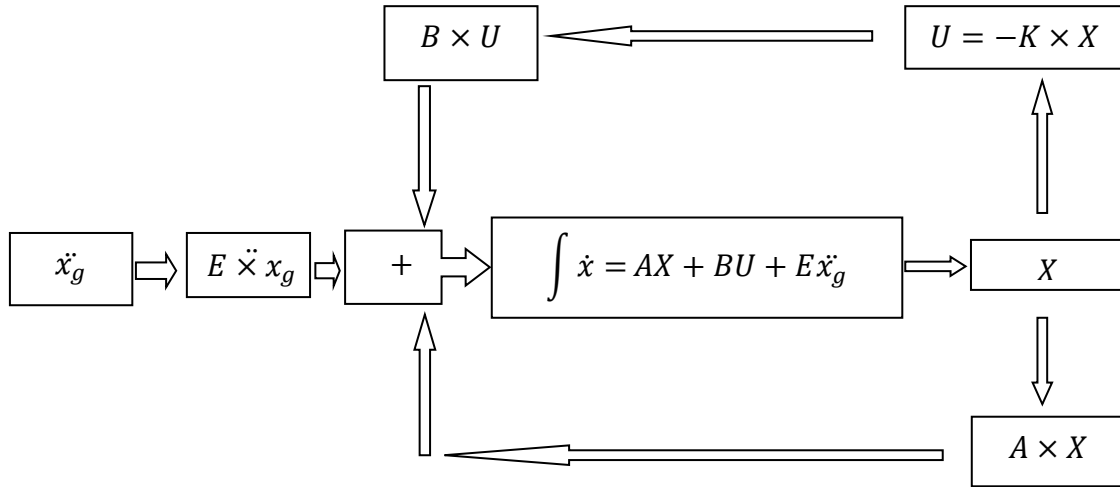


Figure 3-19: State space flow chart for SATMD and TMD analysis

Ground acceleration is input of the system. This acceleration will be multiplied by E matrix and will be added to $AX+BU$. Then, the result \dot{X} , will be integrated and will yield X which is state vector. State vector will be multiplied by gain factor (K) and results control force vector. Control force vector will be multiply by B matrix that determines the effect of control force in state equation Eq.(3-26) and will be added to $E\ddot{x}_g$ which is ground acceleration effects in state equation Eq.(3-26).Another term in state equation is multiplication of A matrix with state vector. The summation of these three terms ($AX, BU, E\ddot{x}_g$) will be integrated and will produce state vector X .As it can be seen, all operation is done by matrix multiplication, summation and signal integration.

In the other words, earthquake occurrence is a disturbance for the structural system; this disturbance causes the structural system to react. This reaction can be measured by state vectors. In the phase control system should be involved to calculate the control force to minimize the reaction of structure and in the case of LQR control system, the cost function. Now by combining effect of incoming disturbance ($E\ddot{x}_g$), structural reaction to disturbance (AX) and exerting of control force (BU) and integrating, new set of state vector (X) will be produced. This is a procedure continuous and should be noted that equation of equilibrium for structure is converted to equation of states (Eq. 3-26).

During the occurrence of a seismic event, sensors measure the ground motion and structural responses (in each floor). This data is processed by a central control system. According to control system strategy (which in this research is cost function), the central control system determines which damper should be kept “ON” or should be switched to “OFF” mode and vice versa. On the other words, when an earthquake hits the building, initially the damper is in the passive mode, but depending on the response of the structure (i.e., velocity, displacements) the control system may be triggered; and at that time an ON signal may be passed to a set of dampers to increase the viscosity of the MR fluid to control the motion; and when the response reduces, the controller sends an OFF signal to the corresponding dampers to put them back to passive mode.

The control force obtained from Eq. (3-34) should be augmented with a semi-active control strategy in order to be used with a semi-active control system. A semi active control system with an MR damper can only apply passive force (i.e., applicable MR damper force, F_{MR}) which is

opposite to direction of relative velocity of the two ends of the MR damper (V_{MR}). Thus, it can be written as:

$$F_{MR} \propto -\text{sign}(v_{MR}) \quad (3-38)$$

This applicable passive force is only useful when it has the same direction as the calculated active control force given by Eq. (3-34). If applicable MR damper force, F_{MR} has the opposite direction as compared to the calculated control force, then it should not be applied.

Thus, the semi-active control strategy can be described as:

$$\begin{cases} \text{if } U_A \times F_{MR} \geq 0 & \text{Apply } I_{\max} \\ \text{if } U_A \times F_{MR} \leq 0 & \text{Apply } I = 0 \end{cases} \quad (3-39)$$

where, U_A is the force from active control.

Therefore, when MR damper measured force and the commanded force do not have the same sign, the MR damper voltage is also set to zero. If MR damper measured force and the commanded force have the same sign and control force is bigger than measured MR damper force then maximum voltage should be applied. The clip optimal law can be state as:

$$v_i = V_{\max} \times H\{(F_{ci} - f_i)f_i\} \quad (3-40)$$

Where $H(\cdot)$ = Heaviside step function, v is the MR damper voltage, F_c is control force and f_i is MR damper measured force.

3.8. **Summary**

Two MR damper models have been developed here. The first one is a Mechanistic model which is capable of predicting the dynamic behaviour of an MR damper only based on its physical and material properties like geometric parameters and MR fluid characteristics. The developed Physical/Mechanistic model can represent the flow mode MR damper as well as the mixed mode MR damper. In addition, the model can be used for any type of dynamic motion (e.g., harmonic or random) of an MR damper and is not limited to harmonic only. The second model of an MR damper is a simplified model which can be easily implemented into a structural analysis software. Furthermore, the application of MR damper in building structures is studied using MR damper in two forms, which are semi-active tuned mass damper and semi-active bracing in a building. To complement the available researches which are done based on Laboratory size buildings structure and unreal dynamic excitation, this research aims to study real size buildings structures designed based on Canadian code and properly actual seismic ground motion records. This approach will yield more realistic understanding of the application of MR damper in TMD system or bracing system in building structures.

Chapter 4: MR Damper Modeling

4.1. Introduction

The purpose of this chapter is to investigate two MR damper models which are proposed in current research in chapter three. The first model is Mechanistic model of MR damper which implements geometry of MR damper and physical properties of MR fluid to predict MR damper dynamics behaviour. The second proposed model is phenomenological model which is very simple and is developed to be easily incorporated in structural analysis subroutine. The results of Mechanistic model are presented in section 4.2. The proposed Mechanistic model has been verified using an analytical model with experimental validation in harmonic motion. The results of phenomenological model are presented in section 4.3. The performance of the proposed phenomenological model has been compared to that of the modified Bouc-Wen (1971) model which was validated with test results.

4.2. Results of the Duct-Flow model

The proposed Mechanistic model for MR damper which is presented in chapter three is validated using analytical model which is proposed by Choi and Nguayen (2009) and explained in chapter three. It should be noted that analytical model presented by Choi and Nguayen (2009) has experimental validation.

4.2.1. Case study and numerical analysis

In this research, ER damper for vehicle suspensions proposed by Choi and Nguyen (2009) is considered. A schematic diagram of the damper is depicted in Figure 4-1. The ER damper is divided into upper and lower chambers by the piston. As the piston moves, the ER fluid flows from one chamber to the other through the annular duct between the inner and outer cylinder. The inner cylinder is connected to the positive voltage, acting as the positive (+) electrode. On the other hand, outer cylinder is acting as the negative (-) electrode. Besides, the gas chamber operates as an accumulator of the ER fluid. If electric field is interrupted, the ER damper produces the damping force like a hydraulic damper. However, in presence of electric field, the ER damper produces additional damping force due to the yield stress of the ER fluid. This damping force of the ER damper can be managed by controlling the electric field intensity.

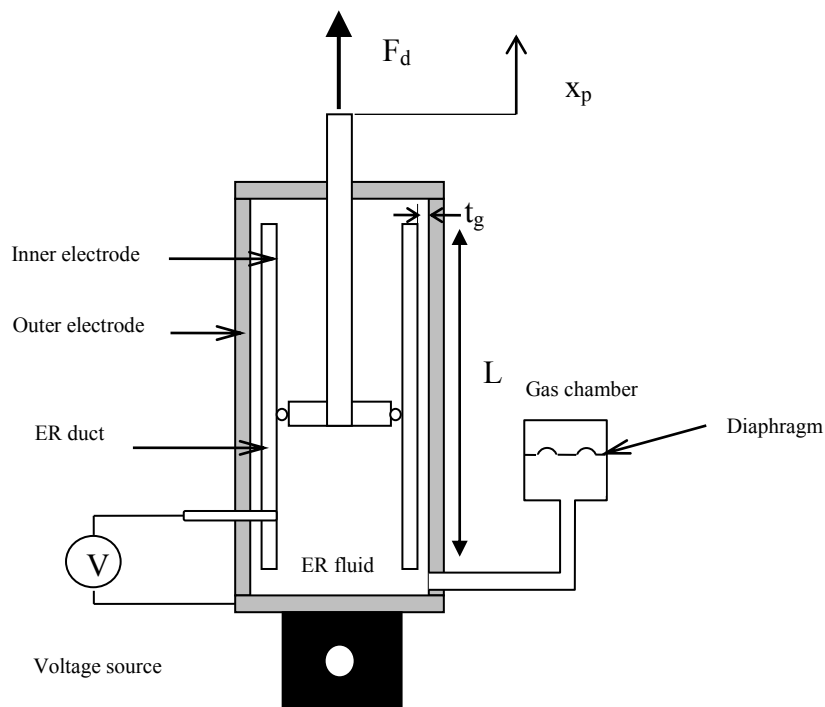


Figure 4-1: Schematic diagram of the ER damper

By neglecting the compressibility of the ER fluid, and the frictional force, the damping force in the ER damper can be calculated as:

$$F_d = P_a A_s + \Delta p (A_p - A_s) \quad (4-1)$$

Where ΔP_a is the pressure drops of the ER fluid flow from the lower chamber to the accumulator and ΔP is the difference between pressure in upper chamber and lower chamber. A_p and A_s are the piston and the piston-shaft effective cross-sectional areas, respectively.

P_a can be stated as (Choi and Nguyen 2009):

$$P_a = P_0 \left(\frac{V_0}{V_0 + A_s x_p} \right)^\gamma \quad (4-2)$$

where, P_0 and V_0 are the initial pressure and volume of the accumulator. The gas chamber of ER damper is filled up with nitrogen gas whose thermal expansion coefficient is $\gamma = 1.4$. Therefore, according to Eq (4-1) in order to calculate the damping force in ER damper two pressure drop should be calculated. Pressure drop in accumulator which can be estimated in by Eq (4-2) and the pressure drops of the ER fluid flow through the annular duct between the outer and inner cylinder which will be calculated using two methods described in Chapter three (Mechanistic model of MR damper) and (Analytical dynamics model of ER/MR damper).

To calculate the pressure drop of ER fluid flow through the annular duct by methods described in chapter three (Mechanistic model of MR damper and Analytical dynamics model of ER/MR damper) ER/MR fluid properties and ER/MR damper geometry properties is needed.

The induced yield stress of the ER fluid can be estimated by:

$$\tau_y = \alpha E^\beta \quad (4-3)$$

where, E is the applied electric field (kV/mm), α and β are intrinsic values of the ER fluid. The values of α and β are 591 and 1.42, respectively. On the other hand, the post-yield viscosity of the ER fluid is 30 cSt. The relation between τ_y and E is a characteristics of MR fluid which depends on the density and the size of the suspended particles, the depth of the fluid etc. The above relationship could be specified by the manufacturer or determined experimentally.

The above information will conclude the ER/MR fluid propertied before and after yielding. In addition, ER damper geometries properties have been measured as listed in Table 4-1.

Table 4-1: Configuration parameters of the prototype ER damper.

Parameter	Value
Piston radius R_p	16mm
Piston-shaft radius R_s	10mm
Annular duct radius R	19.4mm
Annular duct length L	280mm
Annular duct gap t_g	0.8mm
Initial volume of gas chamber V_0	$0.1 \times 10^{-3} \text{ m}^3$
Initial pressure in gas chamber P_0	$5 \times 10^5 \text{ N m}^{-2}$

The above information will complete what is need as physical information of ER/MR damper in Mechanistic model.

As no experimental test is done to validate proposed method in current research, the proposed model will be evaluated versus the method presented in chapter three by Choi and Nguyen (2009). The analytical model for dynamics behaviour of ER/MR damper has experimental validation and proposed method in current research will be examined against that model. Figures 4-2 to 4-5 show the ER damping force as function of strut velocity and displacement under

harmonic excitations. The analysis is done under different electric field or ER fluid yield stress. As it can be realized from Figures, good agreement exists between the analytical closed form solution (Choi and Nguayen 2009) and the present results. It should be mentioned that present approach is also capable of predicting the damping force under the random motion.

The same damper configuration depicted in Figure 4-1 is used to investigate proposed method versus analytical method for MR fluid. MRF-122EG and MRF-140CG Magneto-Rheological fluid which are produced by LORD Company have been used as MR fluid in damper. Figures 4-6 to 4-9 show the damping force as function of strut velocity and displacement under harmonic excitations for MR fluid. There is a good agreement between the analytical solution (Choi and Nguayen 2009) and current results. It should be noted that the damping force in MR damper is quite higher than in ER damper with the same damper configuration and the same yield point of 600kg/cm^2 (Figure 4-3 and 4-9), mainly because of the higher density of MR fluid than that of ER fluid. As the density of the fluid plays an important role in the damper force, dynamics analysis of ER/MR damper is preferable to quasi-static methods which ignore fluid density.

A pseudo random motion has been shown in Figure 4-10. This pseudo random motion is the results of addition of two sinusoidal motion of 10 Hz and 20 Hz with amplitude of 10 mm. The response of ER damper to this pseudo random motion has been shown in Figure 4-12. As it can be observed from Figure 4-12 the estimation of the damper forced by superposition of the solution of the two harmonic excitations using the analytical method, and the solution of the combined excitation using the proposed method are quite different. The response of the analytical method has been produced by summing up the estimation of the analytical method for each sinusoidal motion individually (superposition of waves or motion) which is not appropriate

as the solution is nonlinear. The difference in the estimated damper force in ER fluid damper confirms that nonlinearity of the ER damper problem. It means that superposition of motion to simulate the random motion is not valid for a nonlinear problem like ER/MR damper problem.

As it is mentioned earlier, present approach is also capable of predicting the damping force under the random motion. The random motion of MR/ER damper in literature review are studied using phenomenological models in which damper configuration does not matter and so are not specified in papers. On the other hand, no physical model can predict the random behavior of ER/MR damper. Because of these reasons, the results of proposed model for random motion cannot be verified. However, the damping force of ER damper (depicted in Figure 4-1) under random excitation is shown in Figure 4-11. Random excitation of Figure 4-11 is highly fluctuating. Thus, the estimated response of ER damper for the same random vibration in different time duration have been depicted in Figure 4-12 and 4-13. Figure 4-13 demonstrates the response of ER damper in the same random vibration for time duration between 1.5 to 3 second. As it can be seen from Figure 4-13, there is very good correlation between strut velocity of the damper and damping force. This correlation is true for most of dampers and it is true for this configuration of ER damper. The correlation has been clearly demonstrated in Figure 4-14. This correlation may or may not be exist in other ER/MR dampers but it can be deduced how useful the proposed method can be in analyzing, estimating and interpreting dynamics behavior of ER/MR damper during design process of ER/MR damper,

Updating the vorticity based on Eq. (3-73) is free of oscillations only when the time step is small enough so that the dimensionless numerical diffusion number (α) is less than 0.5 for Newtonian fluid (Pozrikidis, 2009). For larger time steps, the velocity profile is distorted due to numerical instability unrelated to the physics of the motion. This behavior is shown in Figure (4-14). In the

present study for non-Newtonian (MR/ER fluid), it is observed that dimensionless numerical diffusion number α should be less than 0.005 to yield a stable finite difference solution (Figure 4-15). On the other hand, results show no sensitivity to stress growth exponent number n in Eq (3-66).

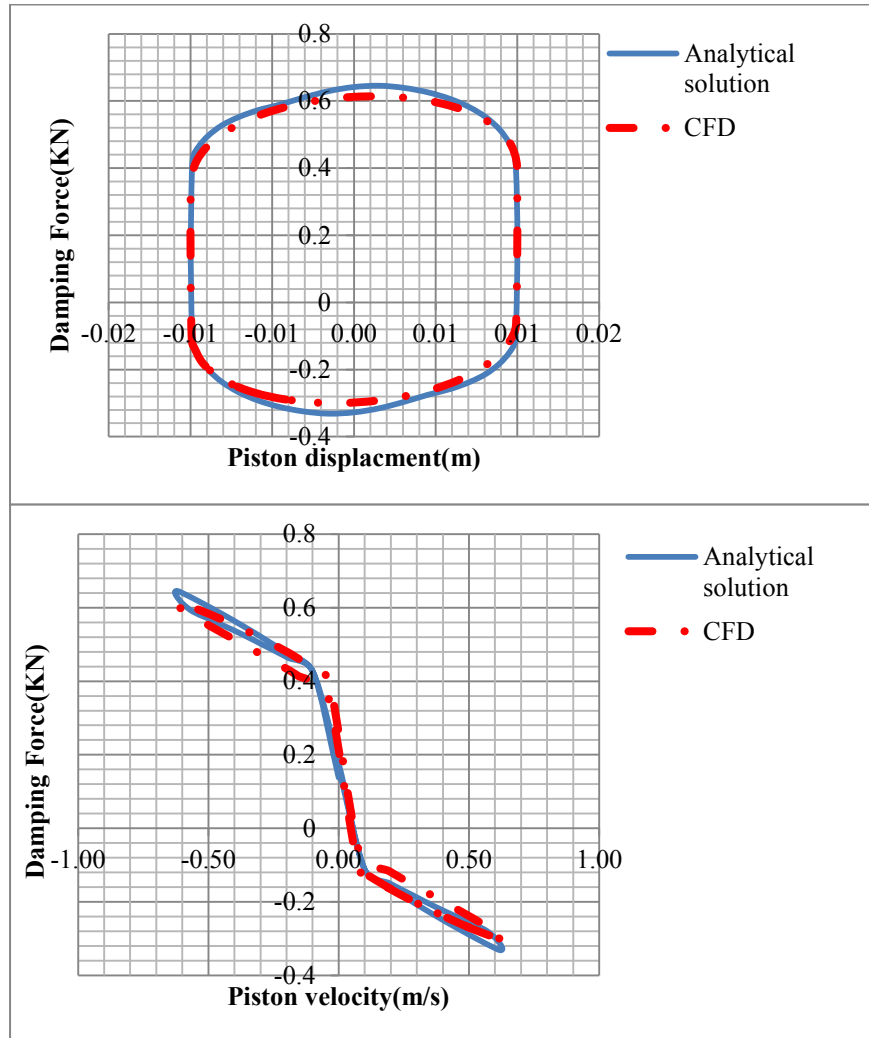


Figure 4-2: Damping force versus piston velocity and displacement of ER damper due to sinusoidal motion of the piston at medium frequency (frequency: 10 Hz, amplitude: 10 mm, $\tau_y = 600 \text{ Kg/cm}^2$).

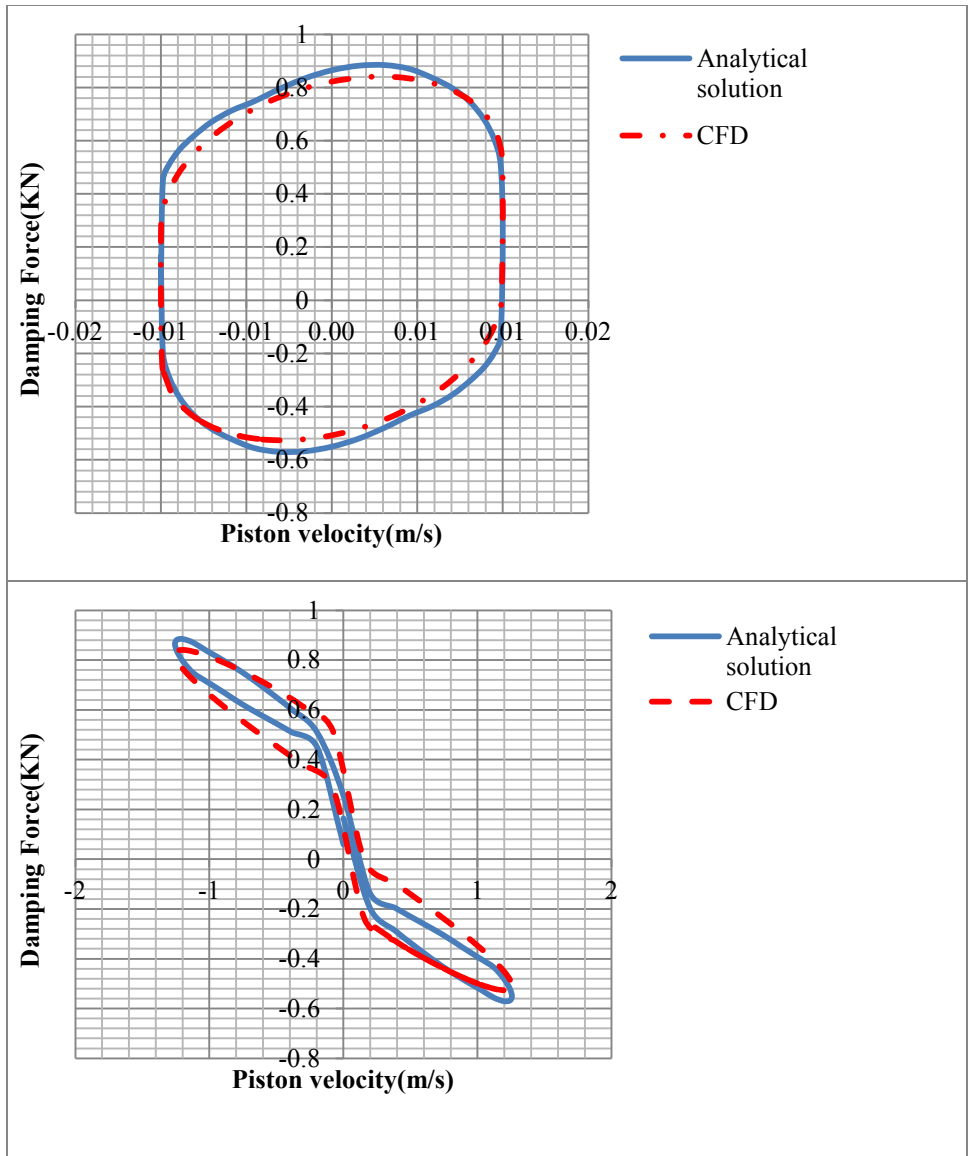


Figure 4-3: Damping force versus piston velocity and displacement of ER damper due to sinusoidal motion of the piston at medium frequency (frequency: 20 Hz, amplitude: 10 mm, $\tau_y = 600 \text{ Kg/cm}^2$).

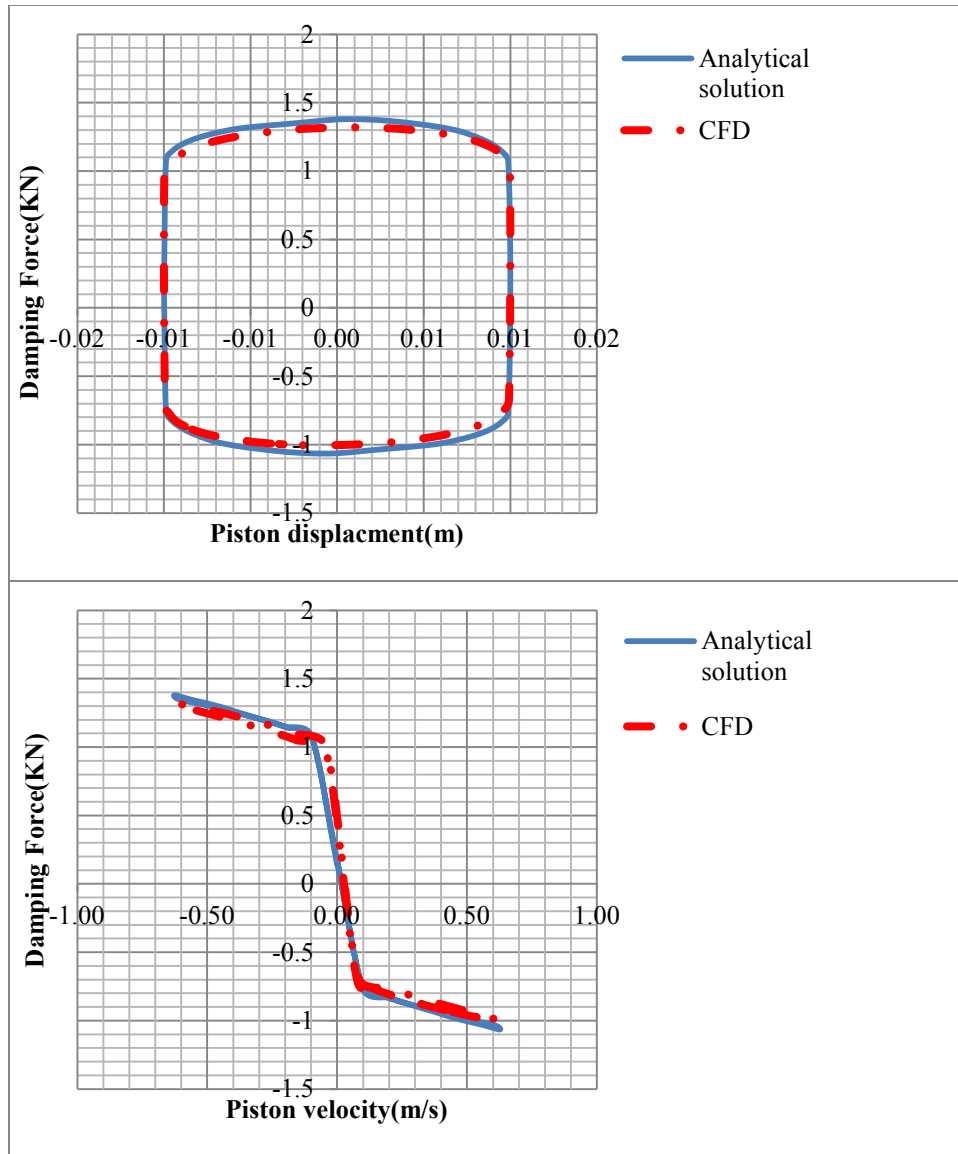


Figure 4-4: Damping force versus piston velocity and displacement of ER damper due to sinusoidal motion of the piston at medium frequency (frequency: 10 Hz, amplitude: 10 mm, $\tau_y = 2500 \text{ Kg/cm}^2$).

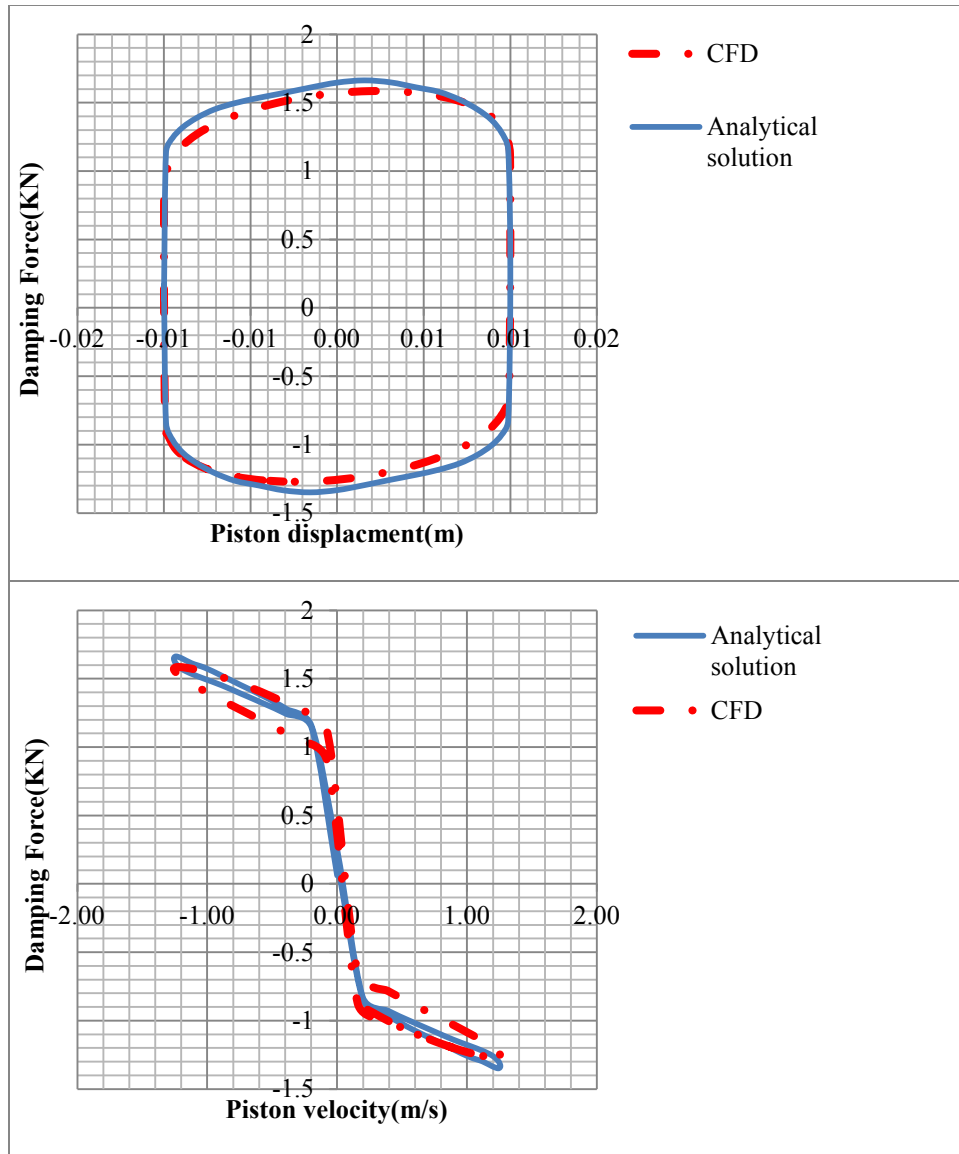


Figure 4-5: Damping force versus piston velocity and displacement of ER damper due to sinusoidal motion of the piston at medium frequency (frequency: 20 Hz, amplitude: 10 mm, $\tau_y = 2500 \text{ Kg/cm}^2$).

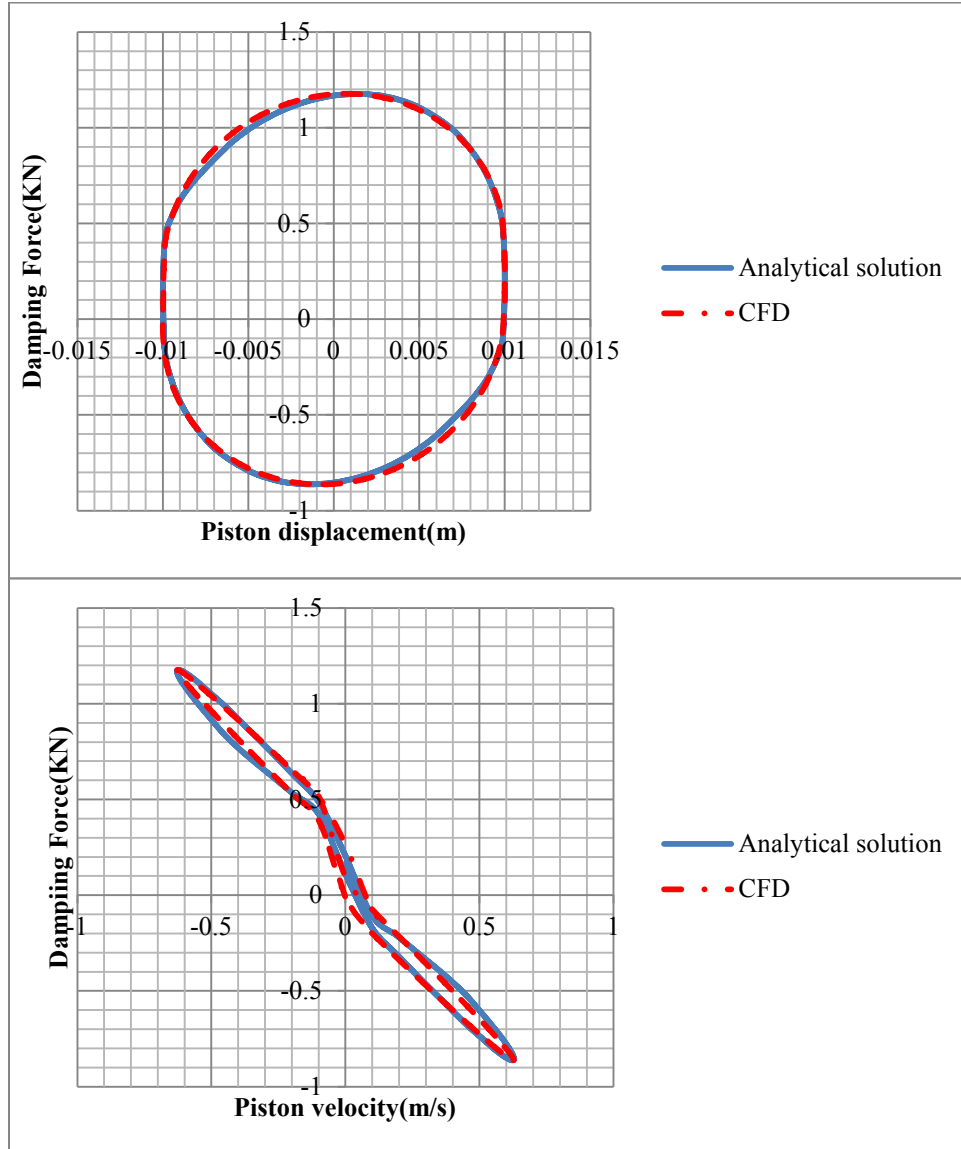


Figure 4-6: Damping force versus piston velocity and displacement of MR damper due to sinusoidal motion of the piston at medium frequency in MR damper (frequency: 10 Hz, amplitude: 10 mm, $\tau_y = 350 \text{ Kg/cm}^2$, MR fluid type; MRF-122EG).

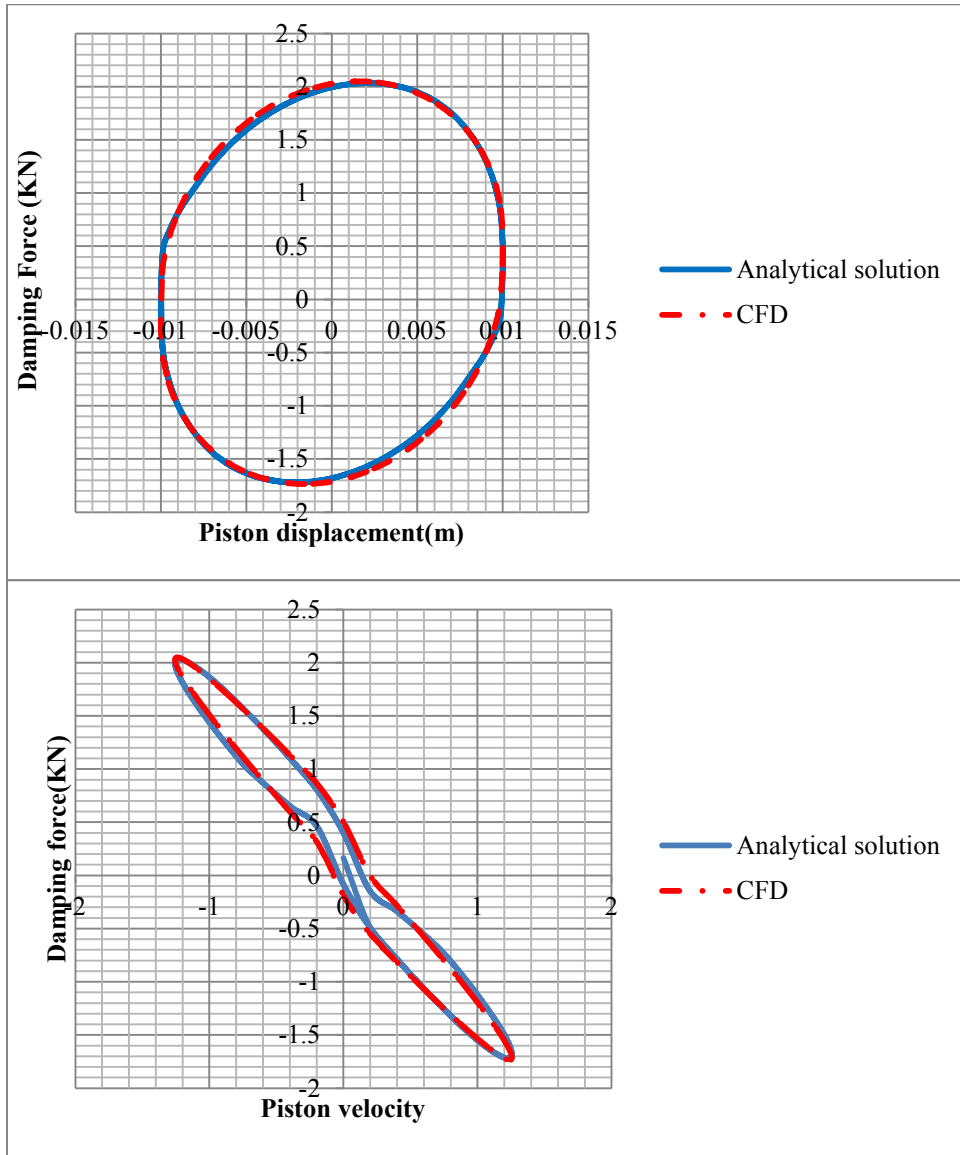


Figure 4-7: Damping force versus piston velocity and displacement of MR damper due to sinusoidal motion of the piston at medium frequency in MR damper (frequency: 20 Hz, amplitude: 10 mm, $\tau_y = 350 \text{ Kg/cm}^2$, MR fluid type; MRF-122EG).

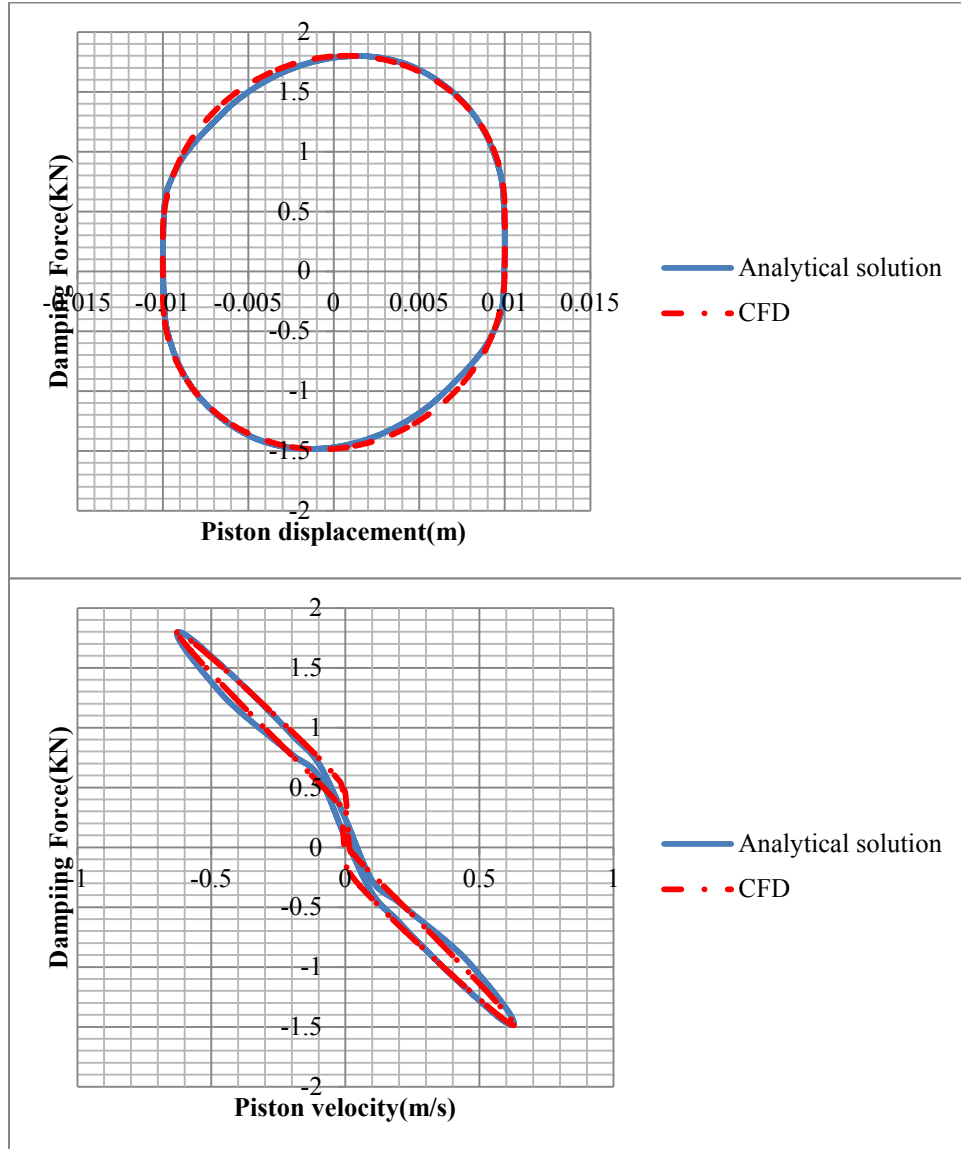


Figure 4-8: Damping force versus piston velocity and displacement of MR damper due to sinusoidal motion of the piston at medium frequency in MR damper (frequency: 10 Hz, amplitude: 10 mm, $\tau_y = 600 \text{ Kg/cm}^2$, MR fluid type; MRF-140CG).

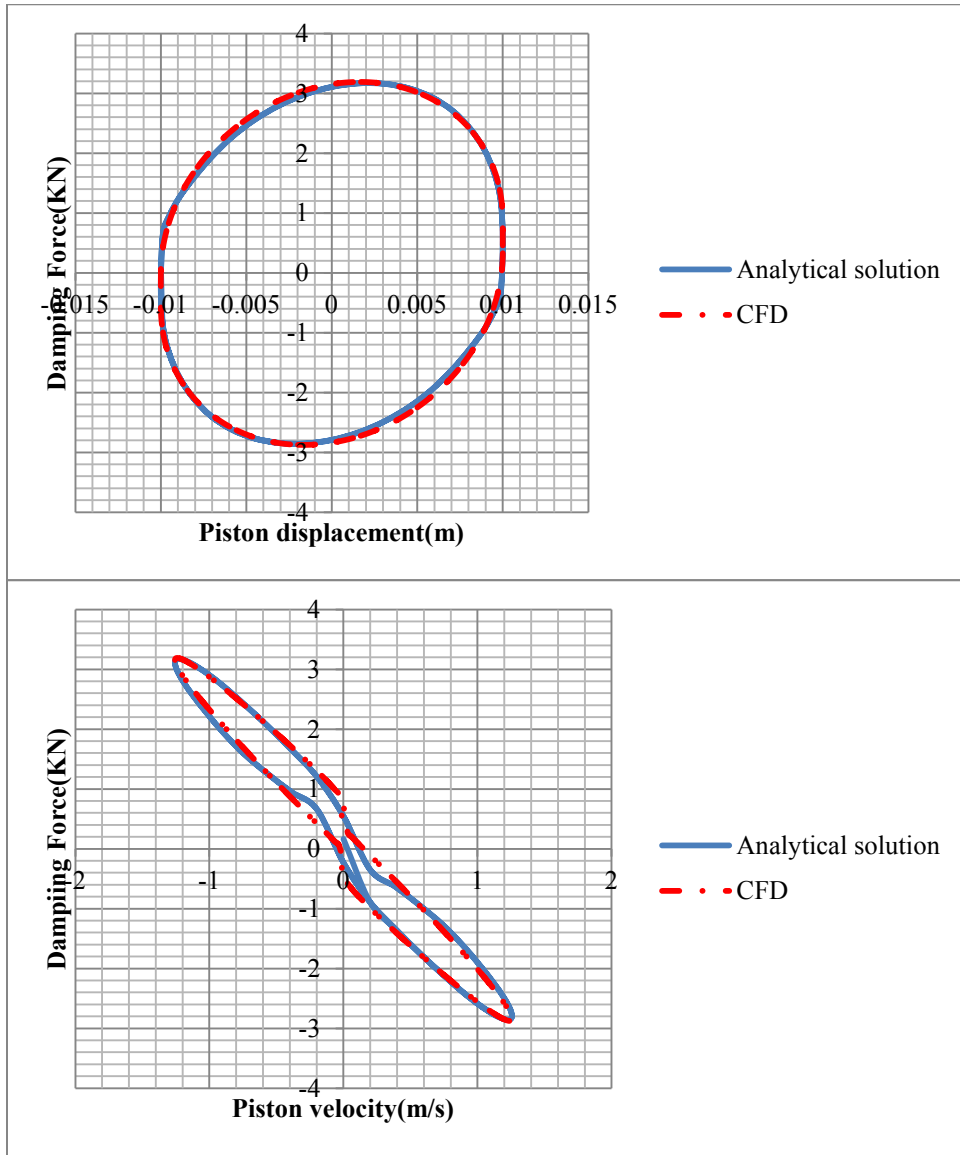


Figure 4-9: Damping force versus piston velocity and displacement of MR damper due to sinusoidal motion of the piston at medium frequency in MR damper (frequency: 20 Hz, amplitude: 10 mm, $\tau_y = 600 \text{ Kg/cm}^2$, MR fluid type; MRF-140CG).

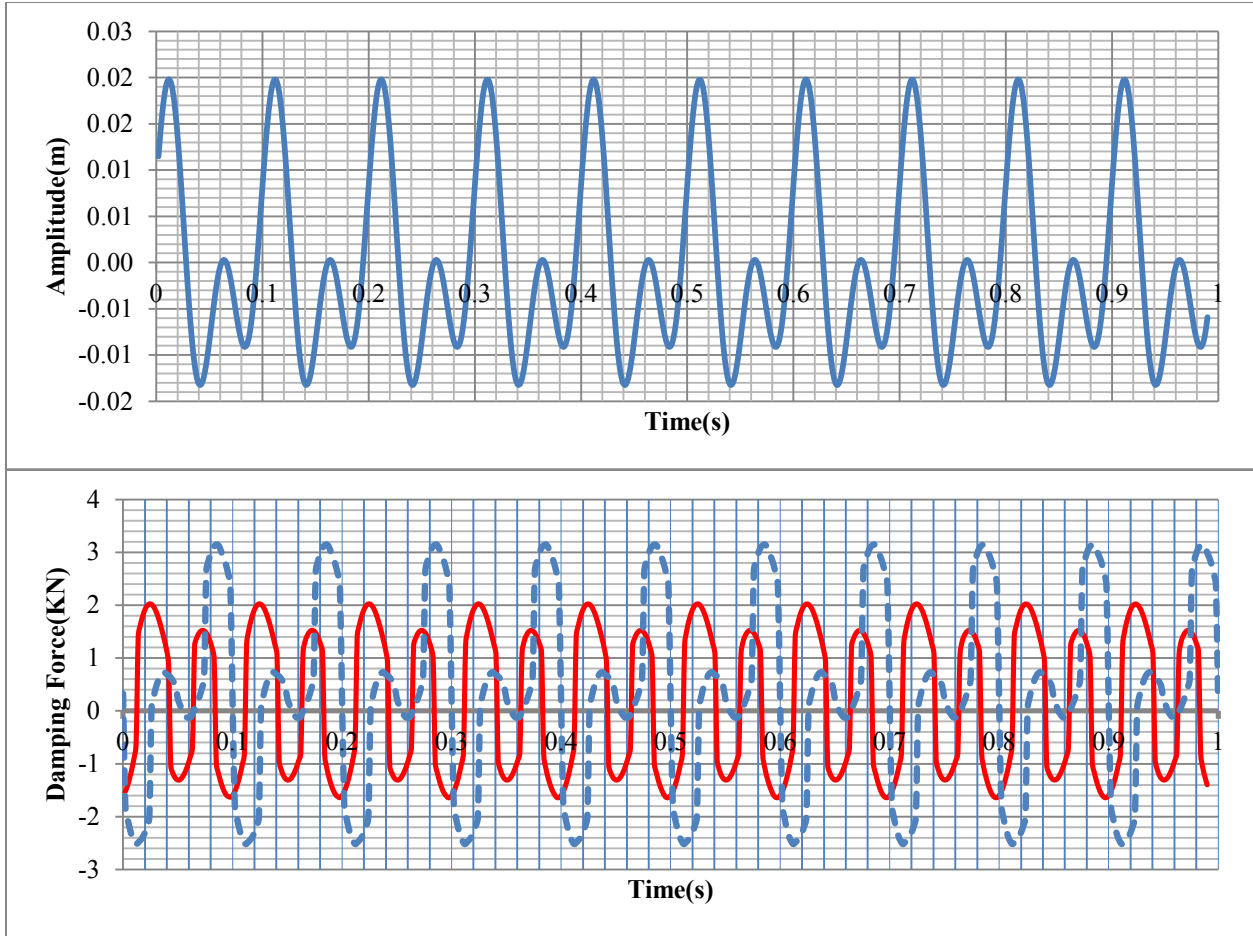


Figure 4-10: Pseudo-random excitation(combination of 10 and 20 Hz sinusoidal motion) (Top) and damping force (Bottom) in ER damper with $\tau_y = 2500 \text{ Kg/cm}^2$; Red solid line is ER damper estimated damping force with proposed method, Blue dash line estimated damping force in ER damper using sum up the solution which is calculated by analytical method for two harmonic motions.

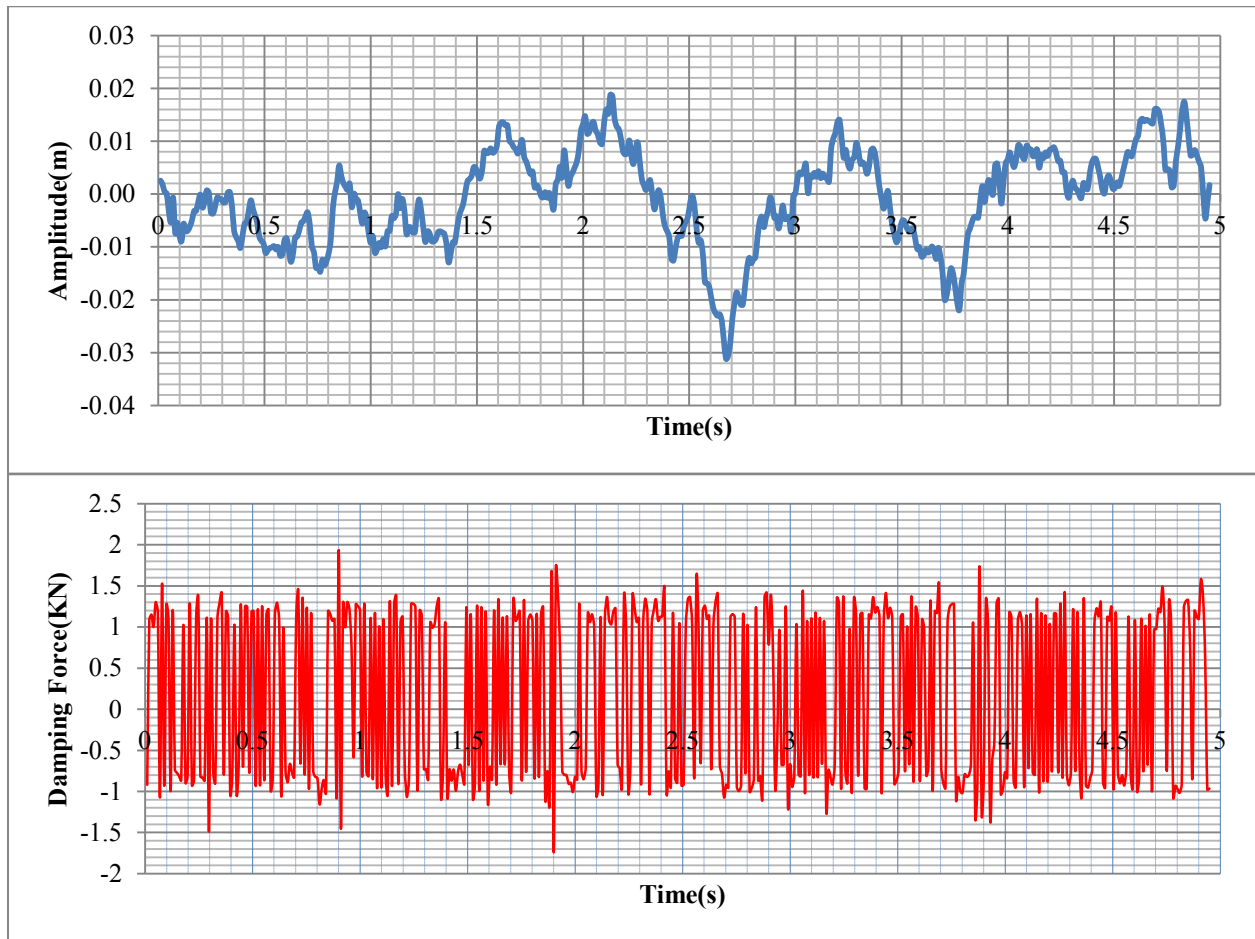


Figure 4-11: Random excitation (Top) and damping force (Bottom) in ER damper with $\tau_y = 2500 \text{ Kg/cm}^2$.

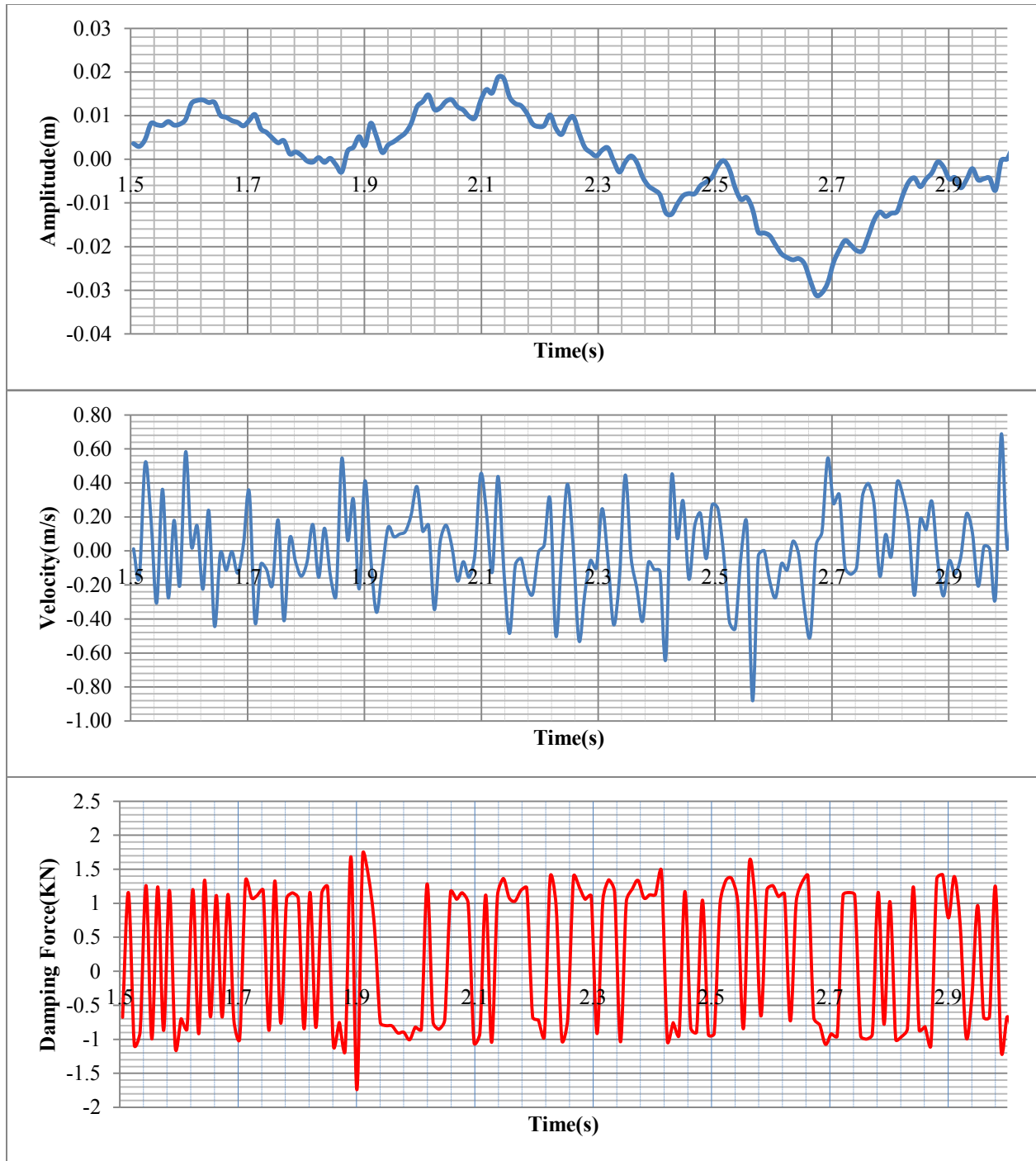


Figure 4-12: Random excitation (Top), velocity of random motion (Middle) and damping force (Bottom) in ER damper with $\tau_y = 2500 \text{ Kg/cm}^2$ between 1.5 and 3 second.

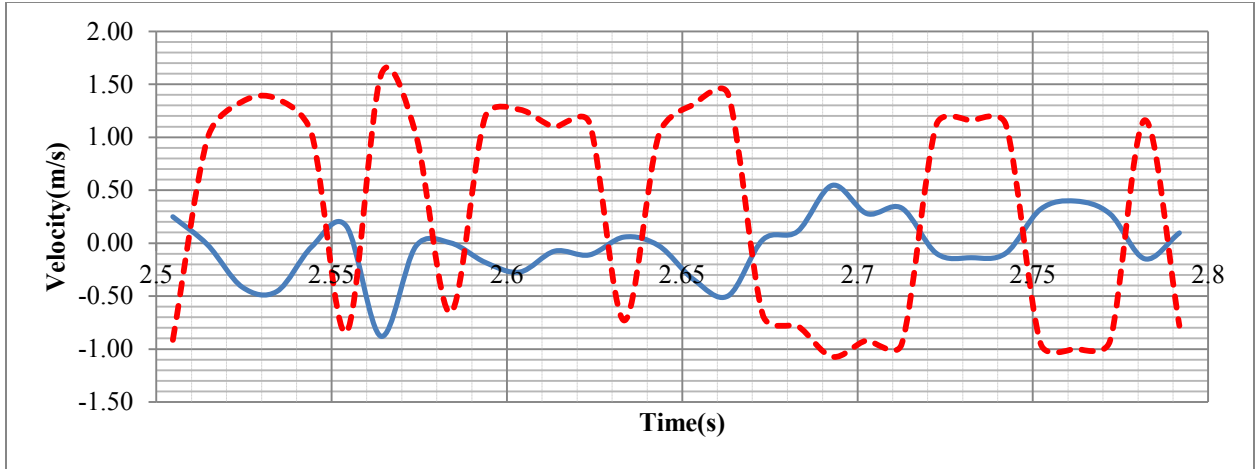


Figure 4-13: Velocity of random motion of ER damper strut (Blue solid line) and ER damper force (Red dash line) with $\tau_y = 2500 \text{ Kg/cm}^2$ between 2.5 to 2.8 second.

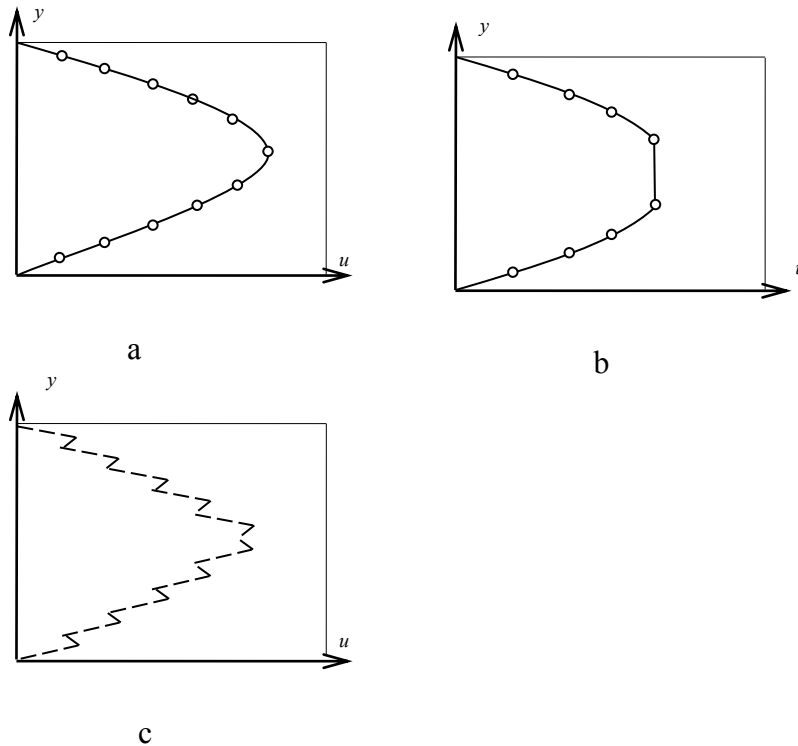


Figure 4-14: a) Velocity profile of Newtonian fluid b) Velocity profile of Bingham fluid c) Velocity profile of Bingham fluid in unstable solution (large diffusion number).

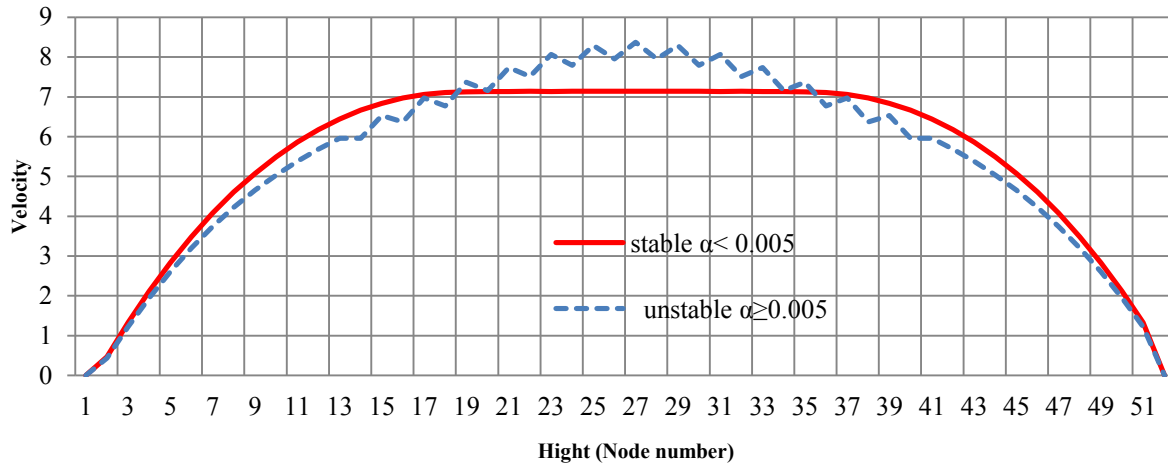


Figure 4-15: Snapshots of velocity profile for unidirectional flow; the blue Figure is a manifestation of numerical instability $\alpha \geq 0.005$, while the red curve shows stability in velocity profile.

Once the Mechanistic mode of ER/MR damper has been established, it is feasible to do parametric study on ER/MR damper. The variation of maximum damping force generated in ER/MR damper versus change in duct length in ER/MR damper has been depicted in Figure 4-16. Maximum damping force in ER/MR damper increases linearly with increase in duct length.

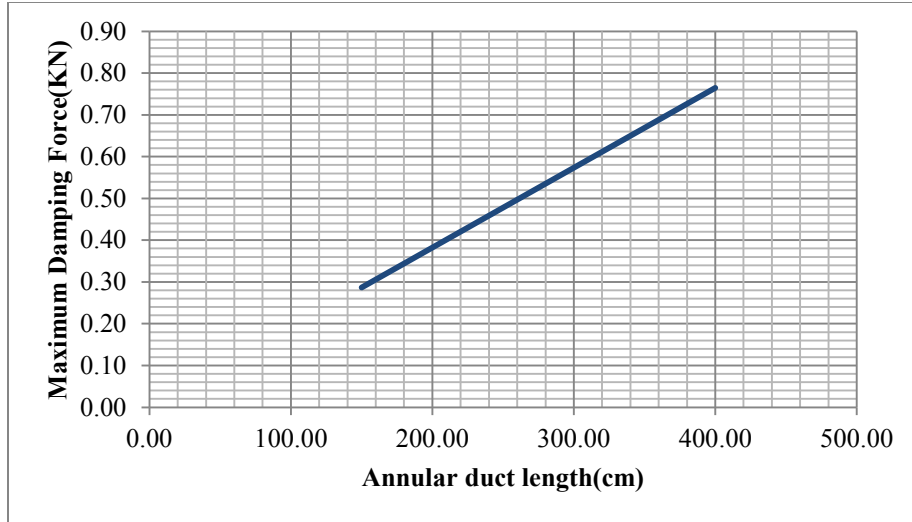


Figure 4-16: Maximum damping force in ER/MR damper versus ER/MR damper duct length

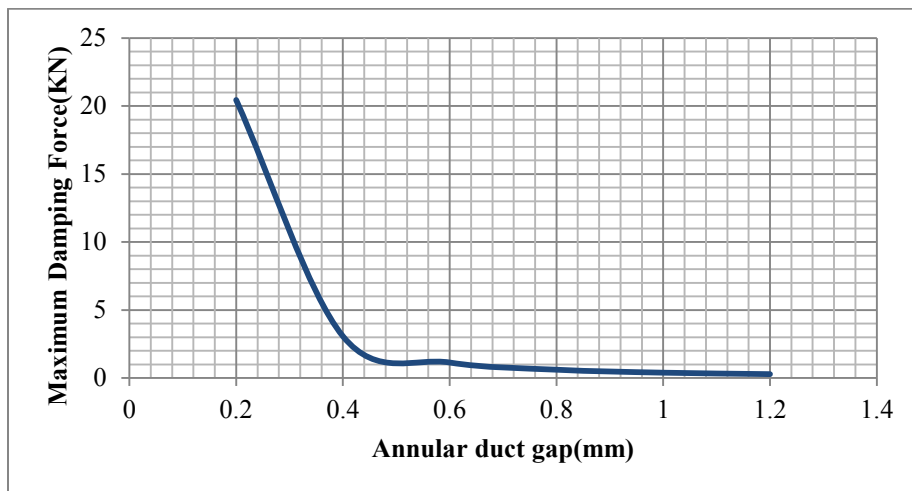


Figure 4-17: Maximum damping force in ER/MR damper versus ER/MR damper duct gap

The change in maximum damping force in ER/MR damper against duct gap has been illustrated in Figure 4-17. Reduction of the duct gap from 1.2mm to 0.45, increases the maximum damping force moderately. While more reduction in duct gap from 0.45, boosts maximum damping force generated in ER/MR damper.

4.3. Results of the Simple Phenomenological model

The proposed simple phenomenological model is presented in section 4.3. As explained earlier, the proposed model is developed to be easily incorporated in structural analysis programs. This model is validated against modified Bouc-Wen model in harmonic and random excitation.

4.3.1. Case study 1

As the first case study to verify the credibility of the proposed model, the ER damper form Choi and Nguyen (2009) is selected. In the current research three harmonic motions are used to identify parameter C_1 and

1. Frequency=5HZ, $\tau_y = 500kg/cm^2$
2. Frequency=10HZ, $\tau_y = 1000kg/cm^2$
3. Frequency=20HZ, $\tau_y = 2000kg/cm^2$

It is found that: $C_1 = -0.0004$ and $C_2 = -0.3660$

So damping force in the ER damper can be stated as:

$$F_d = -0.0004 \times \tau_y \times \text{sign}(v) - 0.3660 \times \text{sign}(v) \times v^2 \quad (4-4)$$

Where v is in (m/s) and F_d in (KN)

The force-velocity behaviours of the ER damper based on the developed model and its comparison with the closed form analytical model by Choi and Nguyen(2009) for different ER fluid yield stresses and different harmonic loading are shown in Figure 4-18.

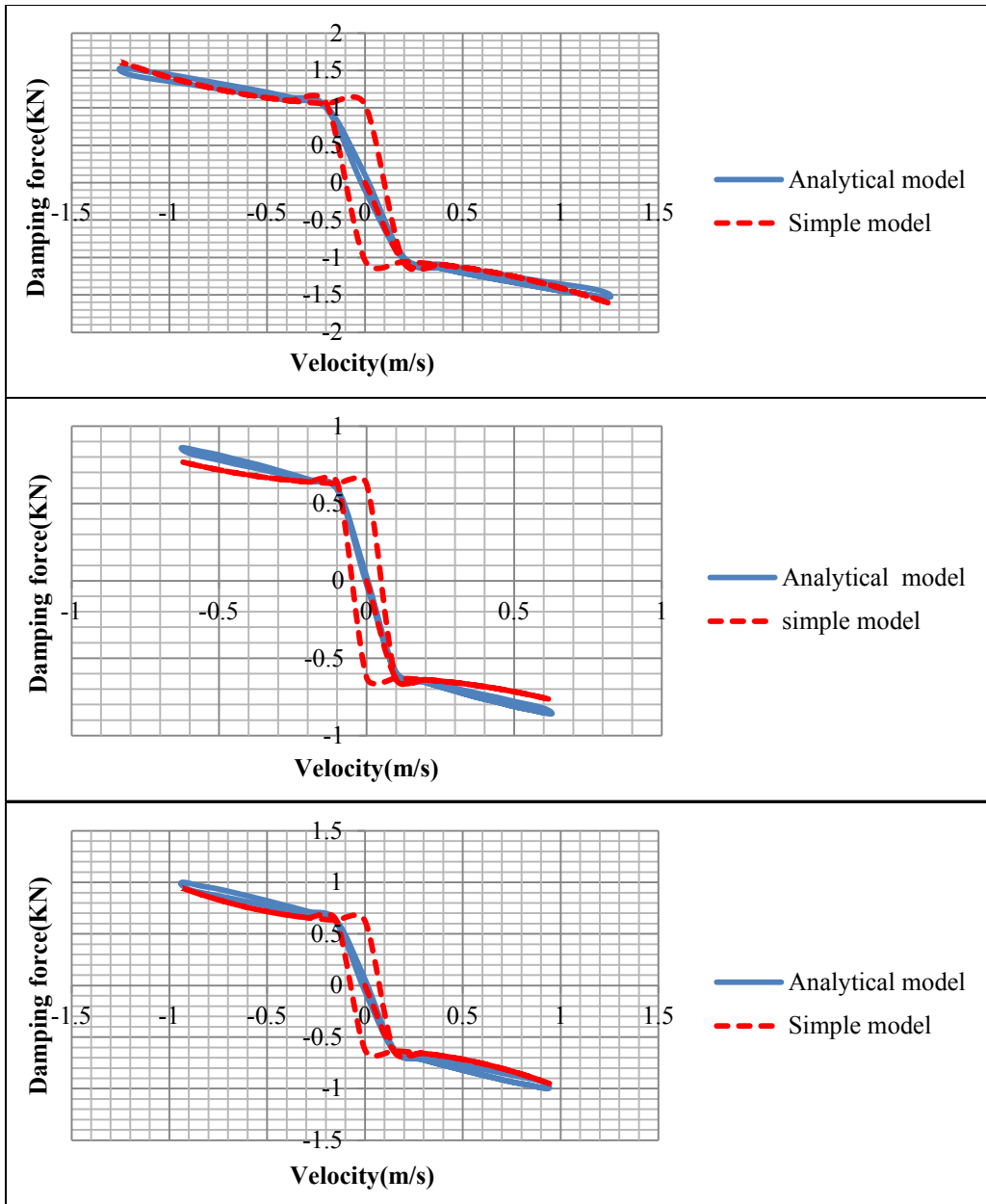


Figure 4-18: Comparing analytical model (blue) with the proposed model (red); Right-up (frequency=10HZ, $\tau_y = 1500 \text{ kg/cm}^2$). Left-down (frequency=15HZ, $\tau_y = 1500 \text{ kg/cm}^2$). Left-up (frequency=20HZ, $\tau_y = 2500 \text{ kg/cm}^2$).

4.3.2. Case study 2

To verify the application of the proposed model to simulate the Hysteresis behaviour of the large MR damper, the 20 ton MR damper modeled by Yang et al (2002) as shown in Figure 4-19 has been chosen. This damper is a 20 ton MR damper which its Bouc-Wen model coefficient are calculated for both harmonic and random motion. The damping force based on the Bouc-Wen model (Figure 4-20) has been formulated as (Yang et al ,2002)

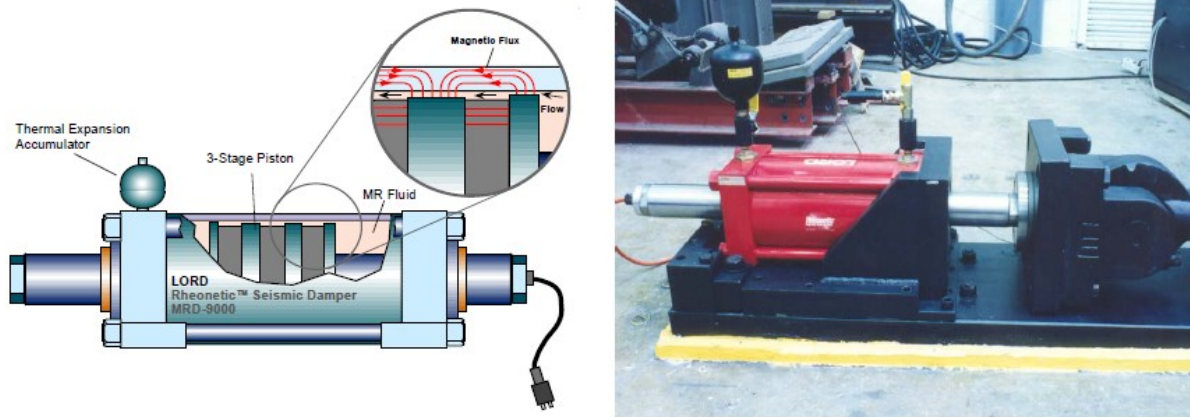


Figure 4-19: Schematic of the full-scale 20-ton MR fluid damper (Yang et al, 2002).

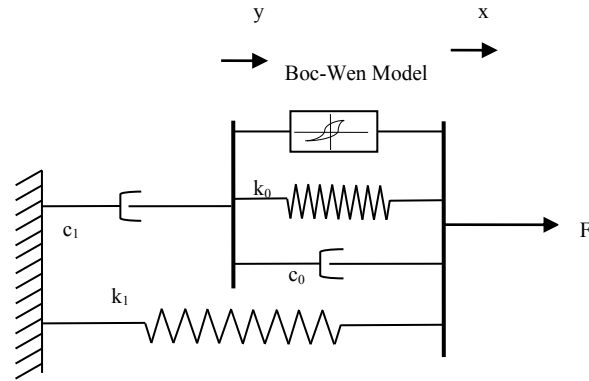


Figure 4-20: Mechanical model of MR damper

$$F_d = \alpha z + c_0(\dot{x} - \dot{y}) + k_0(x - y) + k_1(x - x_0) = c_1\dot{y} + k_1(x - x_0) \quad (4-5)$$

$$\dot{z} = -\gamma|\dot{x} - \dot{y}|z|z|^{n-1} - \beta(\dot{x} - \dot{y})|z|^n + A(\dot{x} - \dot{y}) \quad (4-6)$$

$$\dot{y} = \frac{1}{c_0 + c_1} \langle \alpha z + c_0(\dot{x} - \dot{y}) + k_0(x - y) \rangle \quad (4-7)$$

k_1 =accumulator stiffness; c_0 =viscous damping at large velocities; c_1 =viscous damping for force rolloff at low velocities; k_0 =stiffness at large velocities; and x_0 =initial displacement of spring k_1 .

The parameters values are given in Table4-2:

Table 4-2: Model parameters identified for the large-scale 20-ton MR damper (Yanng et al. 2002).

Parameter	Value
Piston radius R_p	16 mm
Piston-shaft radius R_s	10 mm
Annular duct radius R	19.4 mm
Annular duct length L	280 mm
Annular duct gap t_g	0.8mm
Initial volume of gas chamber V_0	$0.1 \times 10^{-3} \text{ m}^3$
Initial pressure in gas chamber P_o	$5 \times 10^5 \text{ N m}^{-2}$

Where α, c_0 and c_1 are functioning of current I:

$$\alpha(i) = 16566i^3 - 8707i^2 + 168326i + 15114 \quad (4-8)$$

$$c_0(i) = 437097i^3 - 1545407i^2 + 1641376i + 457741 \quad (4-9)$$

$$c_1(i) = 437097i^3 - 1545407i^2 + 1641376i + 457741 \quad (4-10)$$

By tuning the proposed damping model with Bouc-Wen model of MR damper in harmonic motion, the constant parameters C_1 and C_3 were identified to be:

$$C_1 = 1.95 \text{ and } C_2 = 13.15 \quad \text{for } I = 1 \text{ amp}$$

To estimate C_1 and C_2 , nonlinear least squares technique in MATLAB has been used.

And thus the damping force can be simply state as (under constant current of 1Am):

$$F_d = 1.95 \times 62 \times 10^3 \times \text{sign}(v) + 13.15 \times \text{sign}(v) \times v^2 \quad (4-11)$$

Where v is in (mm/s) and F_d in (Newton).

The constant parameters C_1 and C_3 were identified to be:

$$C_1=0.4526 \text{ and } C_2 = 5.7904 \text{ For } I=0 \text{ amp}$$

As it can be realized the proposed damping force equation stated in Eq.(4-11) is much simpler than the Bouc-Wen model and yet can accurately predict the MR damper force specifically at high velocity region which is of concern for seismic loading. The response of the MR damper under the random excitations has also been evaluated. The results are shown in Figure 4-22 to 4-25 under constant current of one or zero Ampere. As it can be realized, there is a very good agreement between the result based on the developed model and that of the Bouc-Wen model.

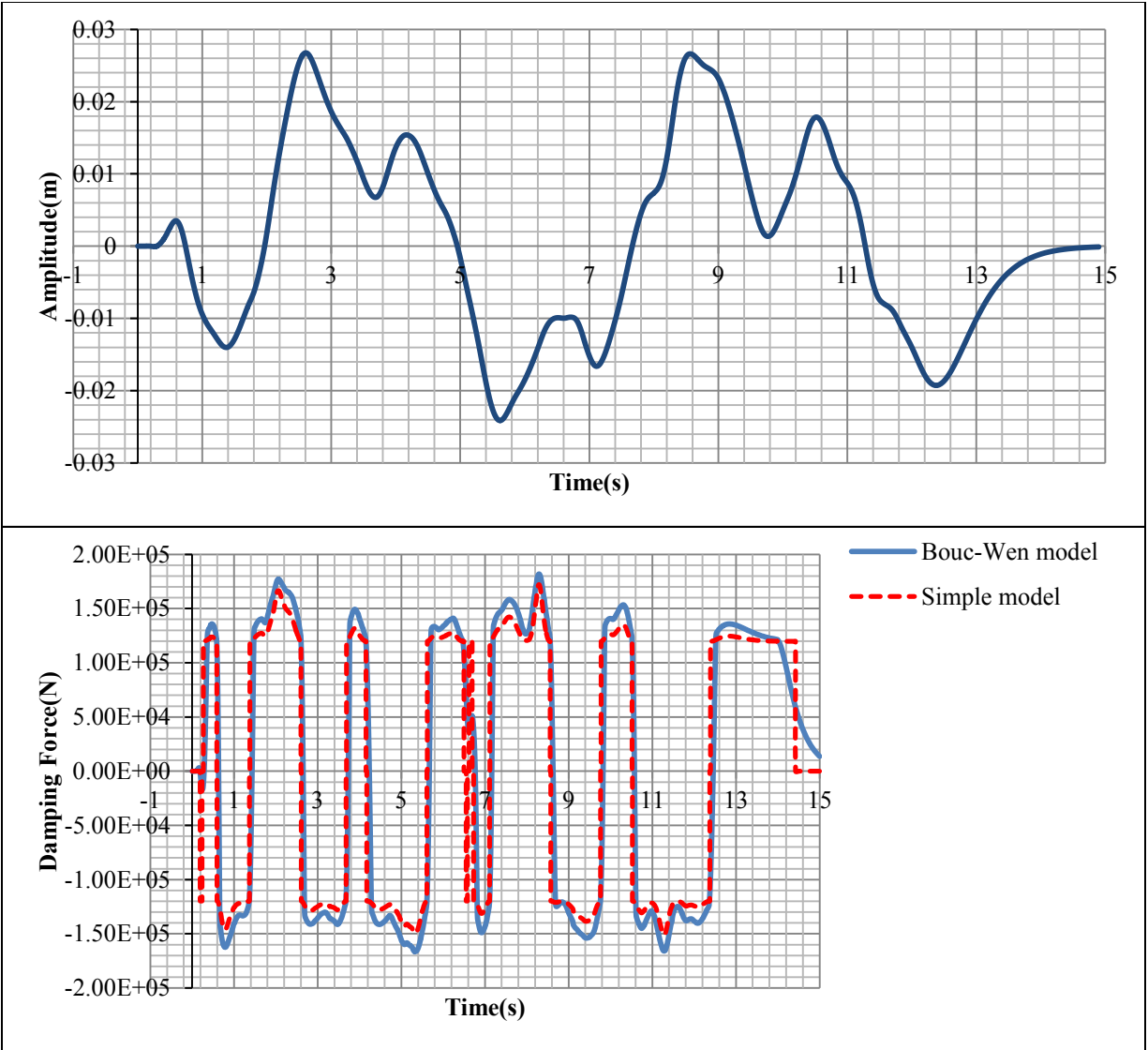
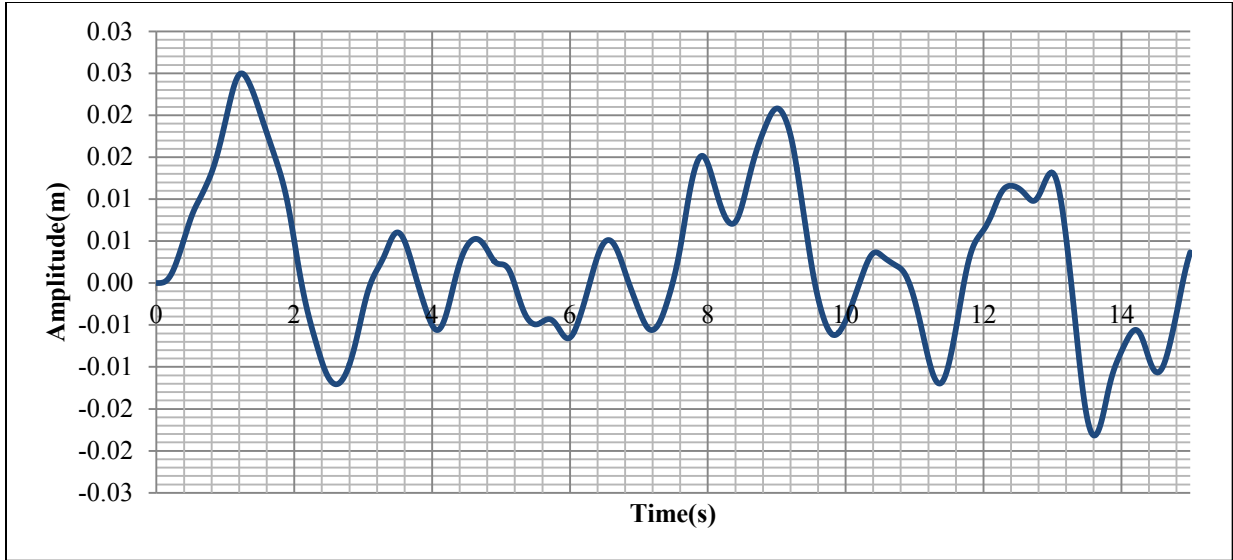


Figure 4-21: Random excitation (Top) and MR damper models predictions (Bottom) at constant current of $I=1$ amp.



0

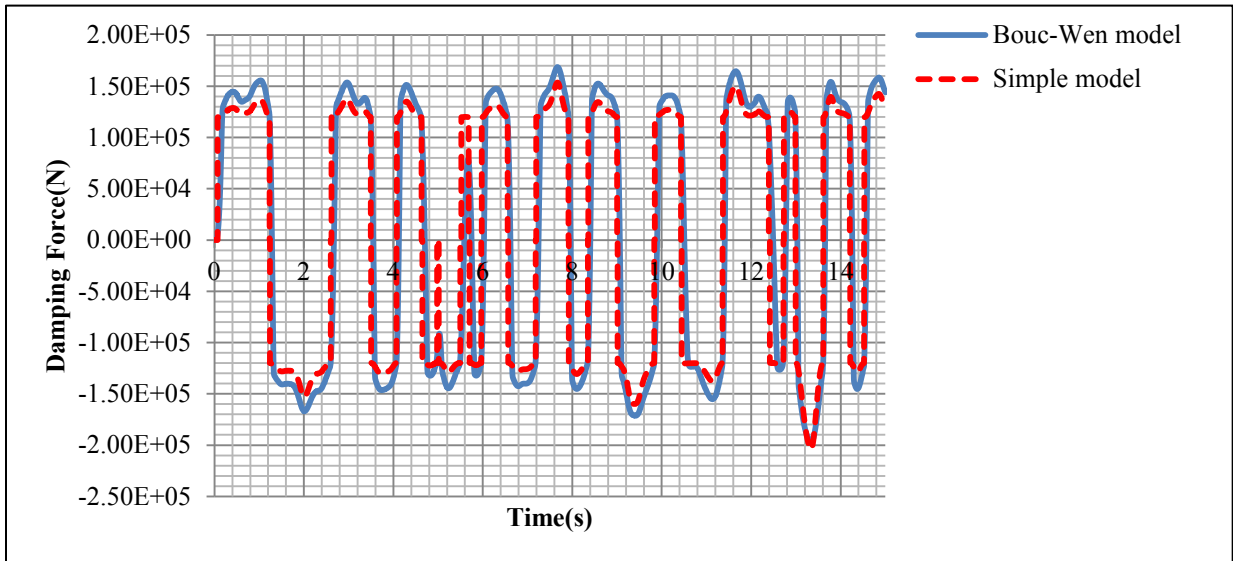


Figure 4-22: Random excitation (Top) and MR damper models predictions (Bottom) at constant current of $I=1$ amp.

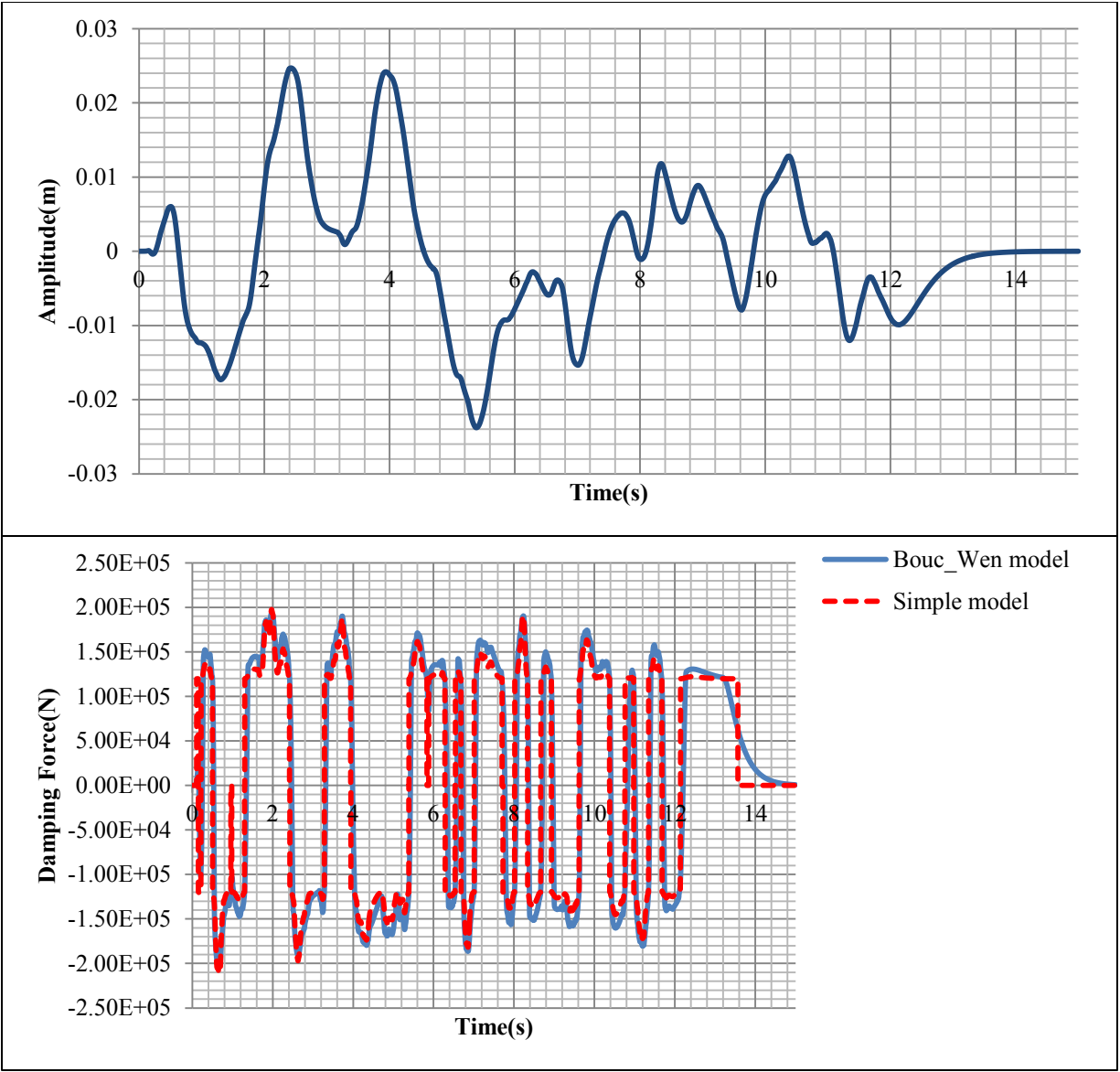


Figure 4-23: Random excitation (Top) and MR damper models predictions (Bottom) at constant current of $I=1$ amp.

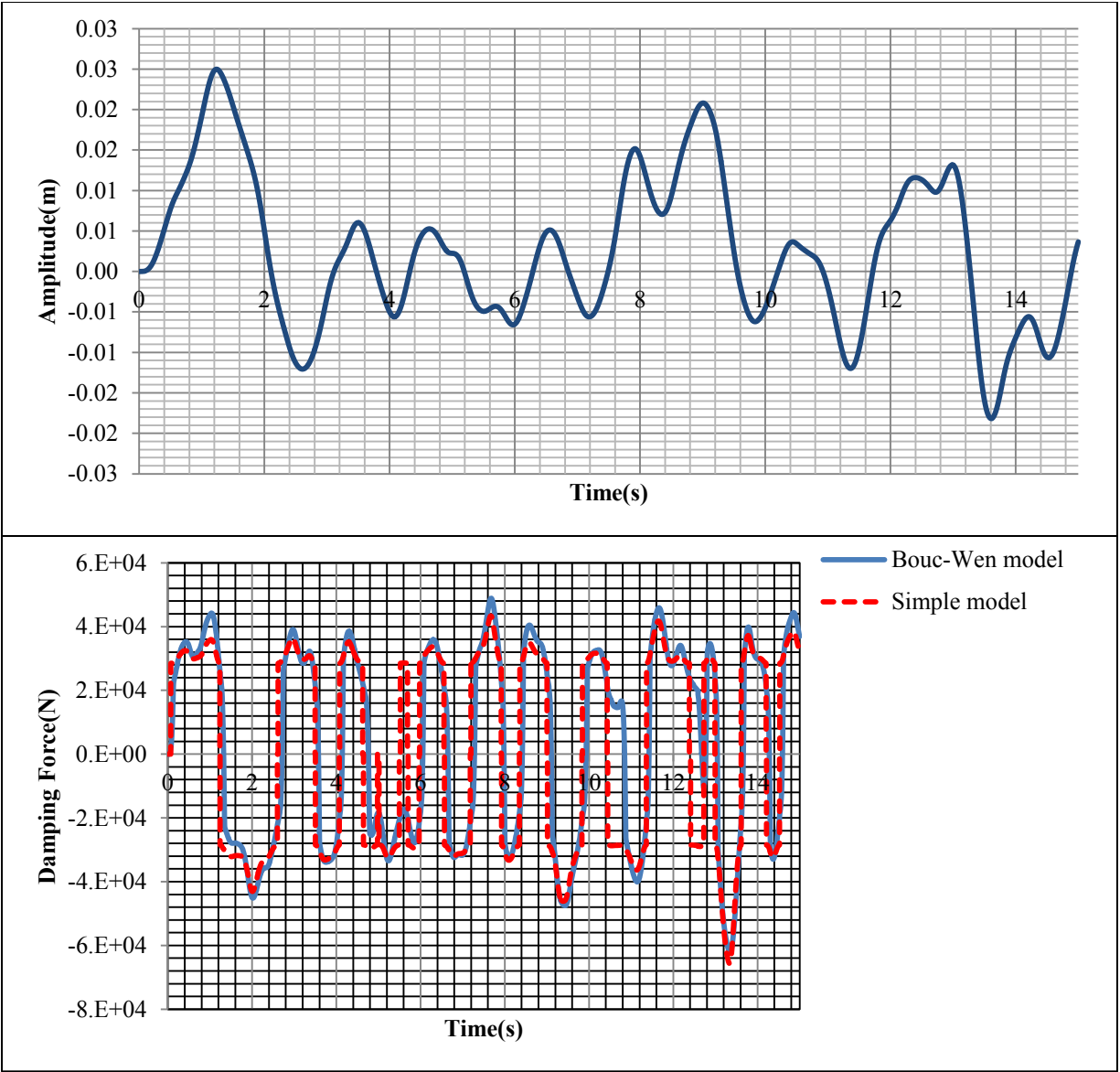


Figure 4-24: Random excitation (Top) and MR damper models predictions (Bottom) at constant current of $I=0$ amp.

4.4. Summary

A CFD-based numerical method for dynamic analysis of MR/ER damper for mixed and flow modes under arbitrary excitation, has been presented here. The procedure employs the vorticity transport equation and the regularization function to tackle the unsteady flow and nonlinear behavior of ER/MR fluid in general motion. The finite difference method is used to solve the governing equations. The method is compared with a recent study with experimental validation. The results from the present method agree very well with the closed form solution for harmonic excitations at all level of frequencies. The finite difference model is sensitive to factor α . For numerical stability of the finite difference model it is strongly advisable to keep $\alpha \leq 0.005$. The model is not so sensitive to n in Eq (3-66). It is reasonable to keep $5 < n < 20$. The present study shows that Δp in Eq.(3-73) is only function of velocity and yield stress of ER/MR fluid although damping force (Eq.(3-73)) contains displacement and pressure terms. There are no benchmark-results available for random excitation to the ER damper used in the case study that could be used for comparison with the results from the present study.

The presented model although uses only physical properties of the ER/MR damper, can estimate the response of the ER/MR damper under general loading. Furthermore, it can be easily adapted for analysis of mixed mode or bypass ER/MR damper. One of the interesting aspects of using physical or mechanistic model of ER/MR damper is that researchers and engineers could alter the main parameters in ER/MR damper and study the impact of the variation of those factors in behavior of ER/MR damper in order to aid in the design of a damper and the systems using it. Although the current research uses generalizing function to deal with non-linearity of ER/MR fluid (which makes it faster comparing to alternative method), the developed CFD based numerical model is rather computationally time-consuming as compared with phenomenological

models. Thus, this method cannot be directly used in implementing a semi-active control system for a structure under random loading (e.g., seismic).

The proposed algebraic model relates the damping force in MR damper to MR fluid yield stress and motion velocity. In high velocity the damping force in MR damper is mainly due to these factors (yielding stress of MR fluid and motion velocity). In the low velocity a portion of the force is due to the accumulator. The force due to accumulator is the function of initial pressure in accumulator and displacement that it is ignored in the present research for the sake of simplicities. So in the low velocity the developed model cannot predict the damping force correctly. Furthermore, the main goal to develop such a simple model is to calculate the damping force in random and seismic motion. The proposed model generates very good results for random excitation. It is useful to add that parameters for the proposed model have been only for two constant currents: one and zero Ampere. As it will be seen later, the proposed control system is off-on control system, such that the MR damper operates only using the maximum current (which is one ampere of 200kN MR damper) or zero current (i.e., passive mode).

Chapter 5: Seismic Response of a Building with Semi-active TMD

5.1. Introduction

This chapter focuses on controlling the seismic performance of a tall building using a semi-active TMD system. The lateral load-resisting system of a forty-storey building considered here consists of typical steel moment frames (MRF) designed based on the current versions of the relevant codes and standards in Canada. The details of the design of the building frame have been presented in Chapter two. A magneto-rheological fluid based semi-active tuned mass damper has been optimally designed to suppress the vibration of the structure against seismic excitation, and an appropriate control procedure has been implemented to optimize the building's semi-active tuned mass system to reduce the seismic response. Furthermore, the control system parameters have been adjusted to yield the maximum reduction in the structural displacements at different floor levels. The response of the structure subjected to a set of seismic ground motions with low, medium and high frequency contents has been calculated to investigate the performance of the building with semi-active tuned mass damper in comparison to that of the corresponding structures with passive and active TMD systems. The response of the structure to these seismic loadings has been studied in time and frequency domain. Furthermore, control system tuning, and the effect of the mass ratio on the response of SATMD have been investigated. At the end of chapter, a comparative study has been done between passive, active and semi active TMD systems. It has been shown that the semi-active control system modifies

structural response more effectively than the classic passive tuned mass damper in both mitigation of maximum displacement and reduction of the settling time of the building.

5.2. Response of the forty-storey building equipped with SATMD

In current research the performance of a forty-storey tall, steel MRF structure equipped with SATMD has been studied. To better realize the characteristics and functionality of the designed semi-active tuned mass system, analysis of the structure has been carried out for six different earthquake records. The results are shown in time domain as well as frequency domain. All earthquake records are scaled to 0.2g (g is the acceleration due to gravity) to represent in the seismicity of Vancouver in long direction of the building.

Kobe ground acceleration record and its Fast Fourier Transform analysis are shown in Figure 5-1. Kobe ground acceleration record has duration of about 20 second and its FFT analysis shows frequency content to be in the range of 1 to 5 Hz. Time domain roof top response of structure due to the scaled Kobe ground acceleration is illustrated in Figure 5-2. As it can be seen from the figure, while both TMD and SATMD reduce the response of the structure for up to 20 seconds, SATMD performs better than passive TMD. After 20 seconds, SATMD shows its superior performance by suppressing the vibration completely, while passive TMD system does not damp out the vibration that effectively.

Table 5 -1: The name, location and occurrence name of seismic design used in analysis.

Ground motion name	Location	Year
Kobe	Japan	1995
Irpinia	Italy	1980
Kocaeli	Turkey	1980
Tabas	Iran	1978
Nahanni	Canada	1985
Upland	California	1990

The performance of TMD and SATMD can be better studied in the frequency domain. Figure 5-3 shows the comparison of the frequency response of the uncontrolled structure with those of controlled structures using passive TMD and SATMD systems. It can be observed that, TMD decreases the first vibration mode appreciably. However, it generates other two peaks in right and left side of fundamental frequency. SATMD generally performs better in the given frequency range and clearly suppress the vibration in the above mentioned two peaks generated by passive TMD. In addition, it can be seen from Figure 5-3 that SATMD not only reduces the first mode frequency response but also reduces the frequency responses at higher modes such as the second and third modes. This means that SATMD increases the effectiveness of TMD for the second and third modes of vibration; or in the other words, it expands the frequency band of a TMD system. The same conclusion can be deducted for Irpinia (Figures 5-4, 5-5, 5-6) and Kocaeli earthquake recode (Figures 5-7, 5-8, 5-9). The maximum displacement reduction in roof top and the settling time for three low frequency content seismic records is provided in Table 5-

2.

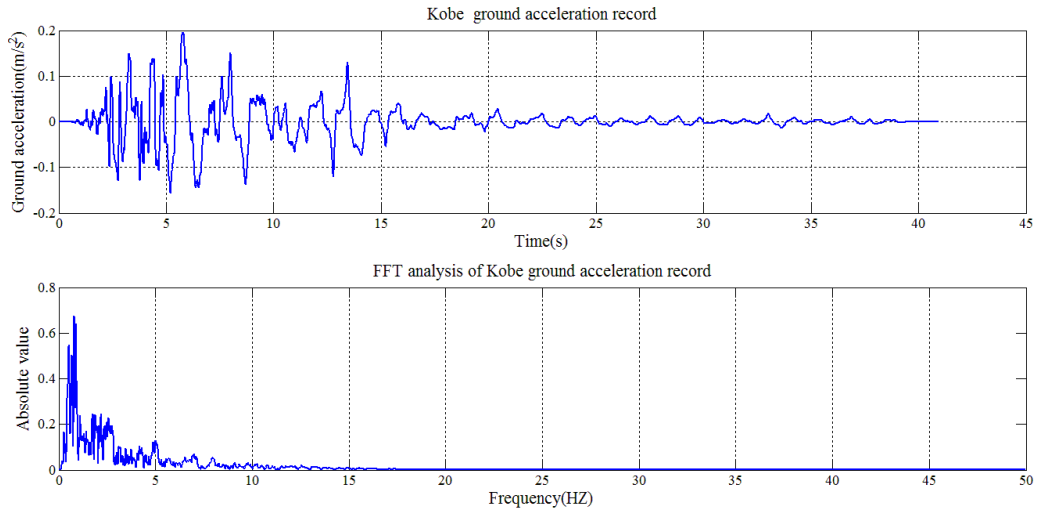


Figure 5-1: Kobe ground acceleration record and its FFT diagram.

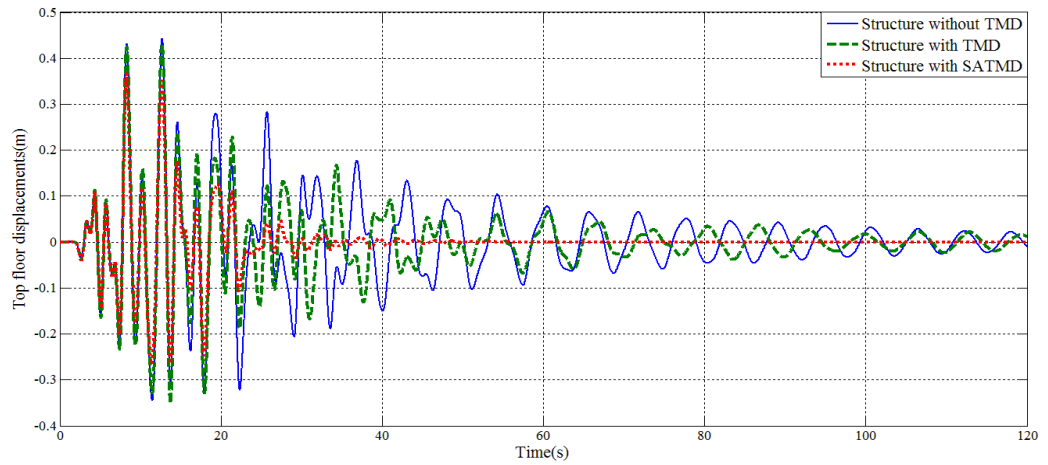


Figure 5-2: Roof top response of the structure due to Kobe ground motion in time domain.

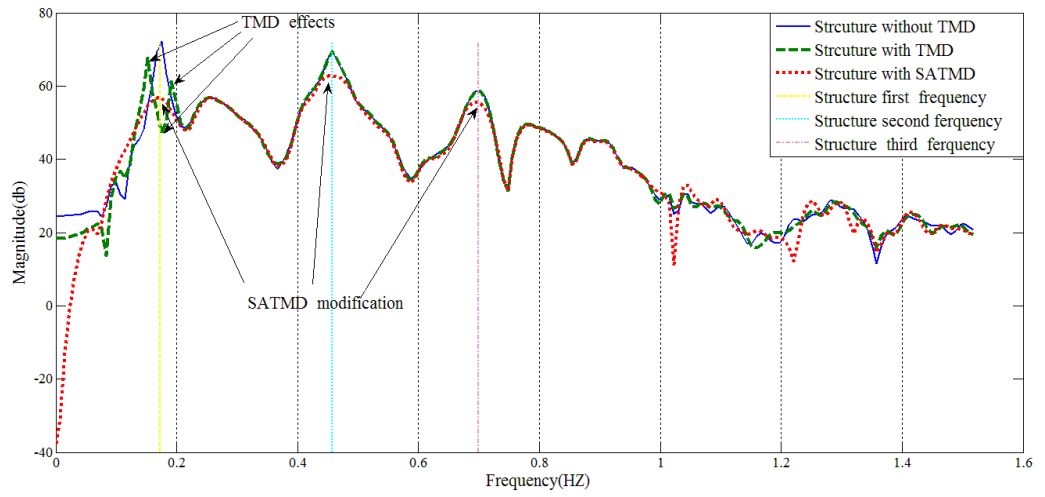


Figure 5-3: Roof top response of the structure due to Kobe ground motion in frequency domain.

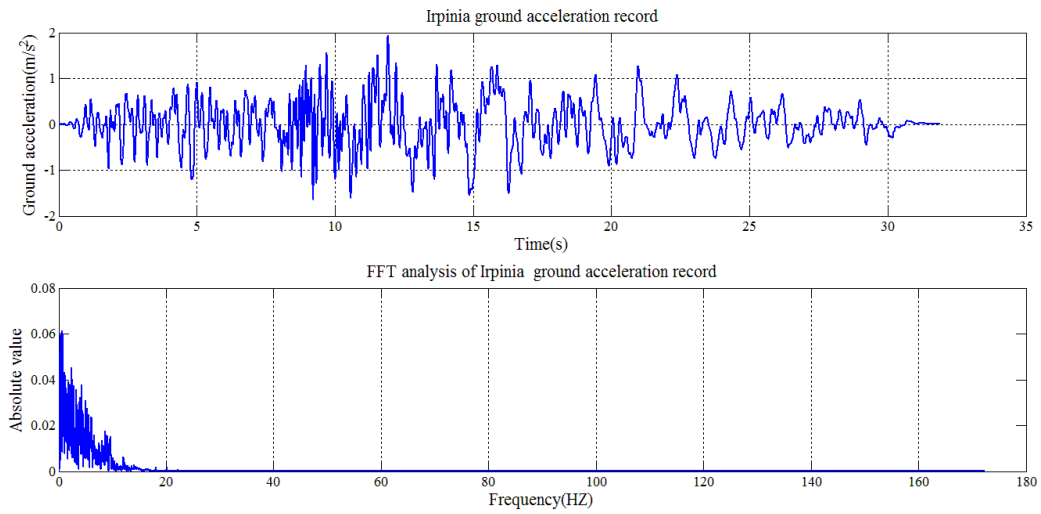


Figure 5-4: Irpinia ground acceleration record and its FFT diagram.

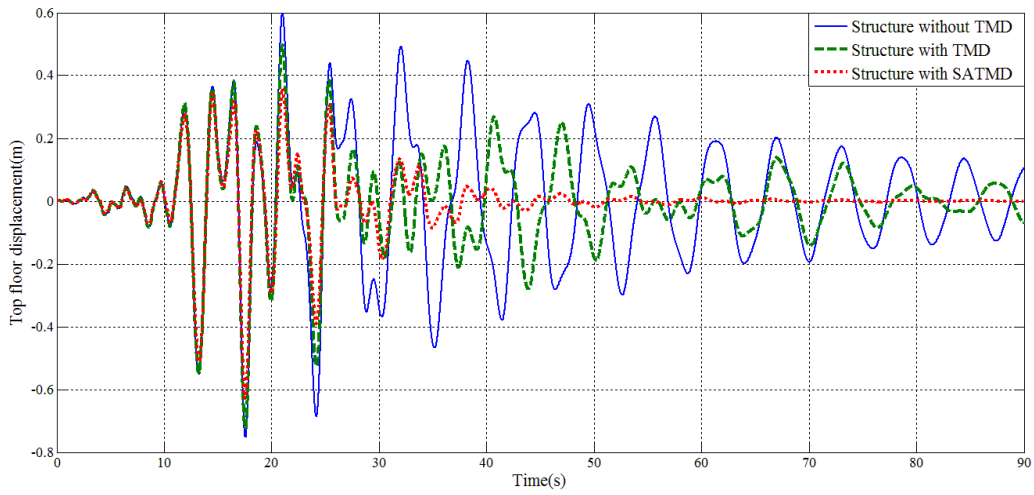


Figure 5-5: Roof top response of the structure due to Irpinia ground motion in time domain.

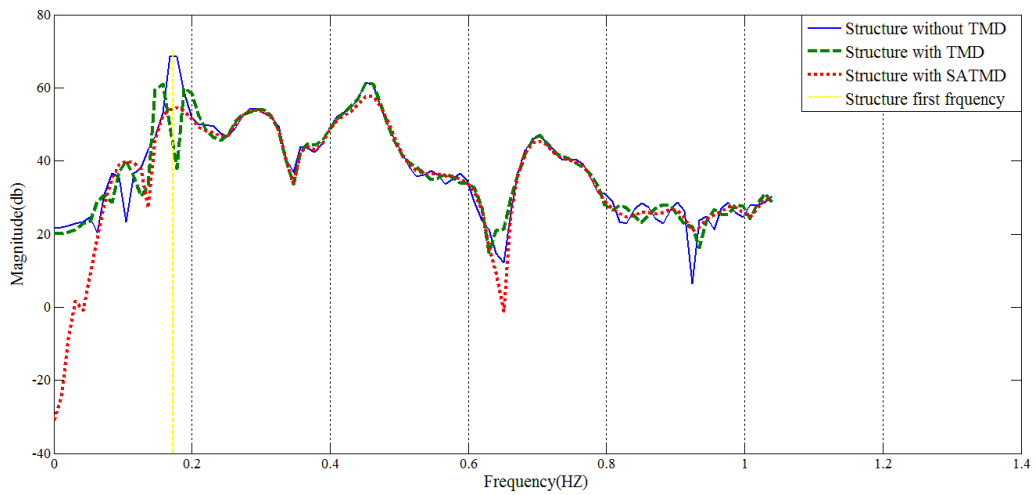


Figure 5-6: Roof top response of the structure due to Irpinia ground motion in frequency domain;
TMD effect.

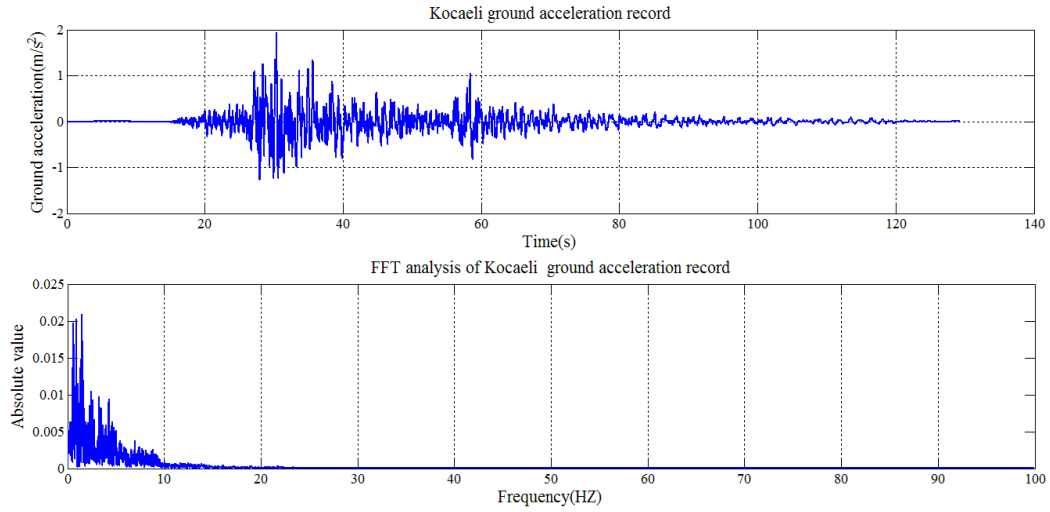


Figure 5-7: Kocaeli ground acceleration record and its FFT diagram.

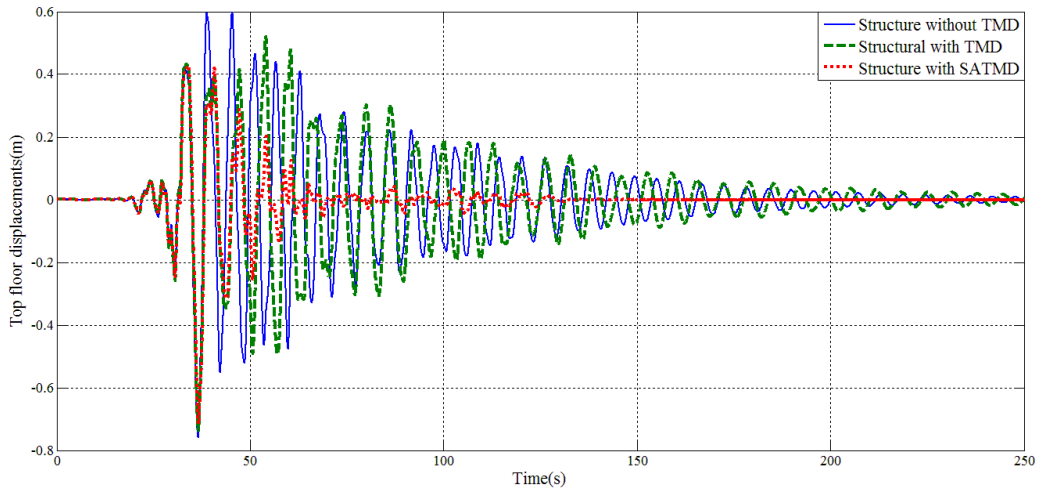


Figure 5-8: Roof top response of the structure due to Kocaeli ground motion in time domain.

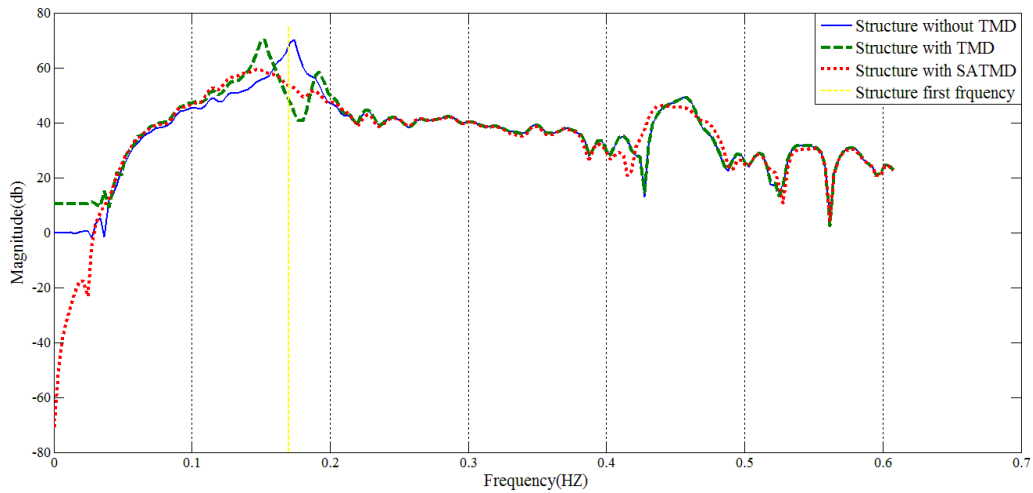


Figure 5-9: Roof top response of the structure due to Kocaeli ground motion in frequency domain; TMD effect.

Table5-2: Maximum displacements reduction and settling time.

Ground motion record	Maximum displacements reduction (percent)		Settling time (second)	
	TMD	SATMD	TMD	SATMD
Kobe	2.5	17	67	27
Irpinia	3.8	16.5	90	34
Kocaeli	2.9	6	159	64

Table 5-2 clearly shows the superior performance of SATMD system compared with conventional TMD system. As it can be seen from Table 5-2, the SATMD reduces maximum displacements more effectively than the TMD system, and the main advantage of the SATMD is observed in the reduction of the setting time which is almost less than half of that of TMD.

The time histories and the frequency contents of earthquake records (Tabas, Nahanni, Upland) are shown in Figures 5-10, 5-13 and 5-16. Since the distribution of frequency of these seismic records do not match with fundamental frequency of the structure considered here, they cause very small deformation in the structure. The roof top displacement is about 150 mm due to the Tabas ground motion record and 60 mm and 10 mm due to Nahanni and Upland records, respectively. These displacements for a tall building which is 120 m high are quite negligible. The same improvements in response of structure equipped with SATMD comparing to passive TMD can be seen in time domain (Figures 5-11, 5-14, 5-17) as well as frequency domain (Figures 5-12, 5-15, 5-18). Maximum displacements reduction and settling time for low frequency seismic records in 40 storey building with TMD and SATMD are shown in Table 5-3.

Table 5-3: Maximum displacements reduction and settling time.

Ground motion record	Maximum displacements reduction (percent)		Settling time (second)	
	TMD	SATMD	TMD	SATMD
Tabas	6	11	70	30
Nahanni	21	27	35	15

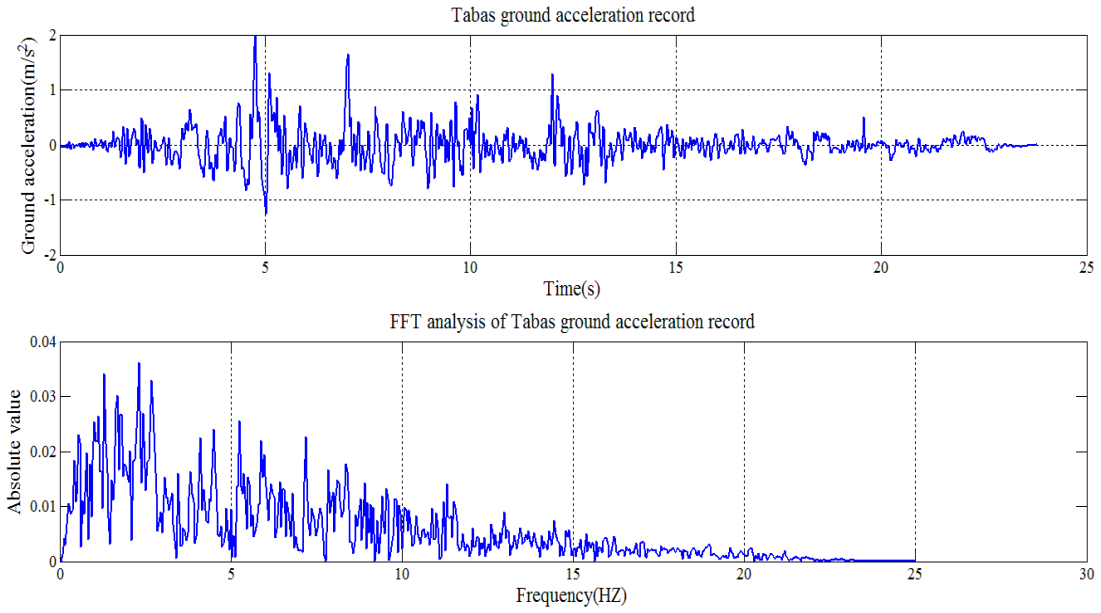


Figure 5-10: Tabas ground acceleration record and its FFT diagram.

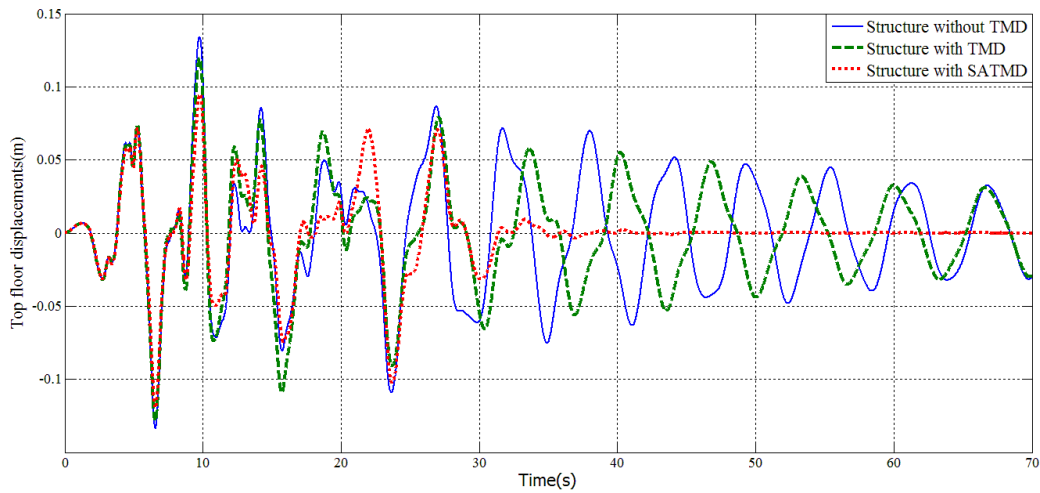


Figure 5-11: Roof top response of the structure due to Tabas ground motion in time domain.

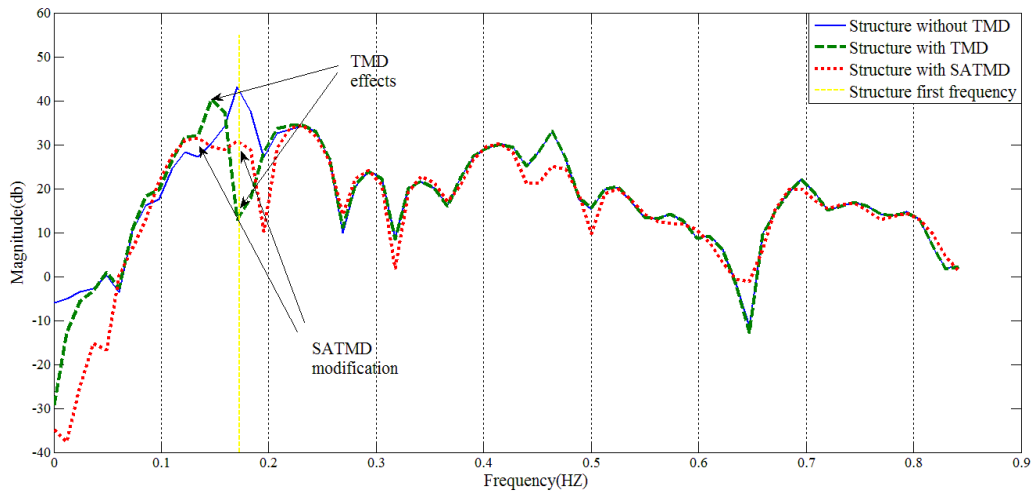


Figure 5-12: Roof top response of the structure due to Tabas ground motion in frequency domain

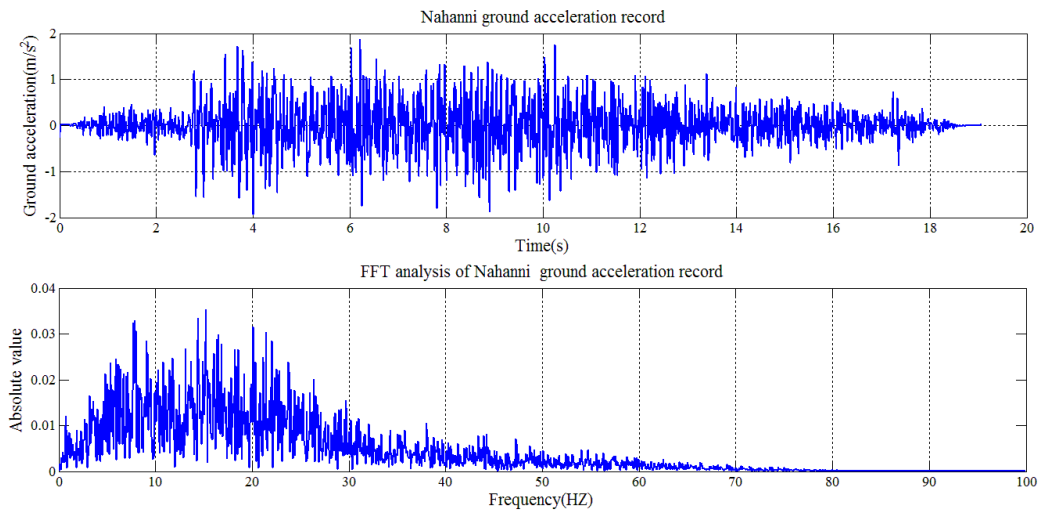


Figure 5-13: Nahanni ground acceleration record and its FFT diagram.

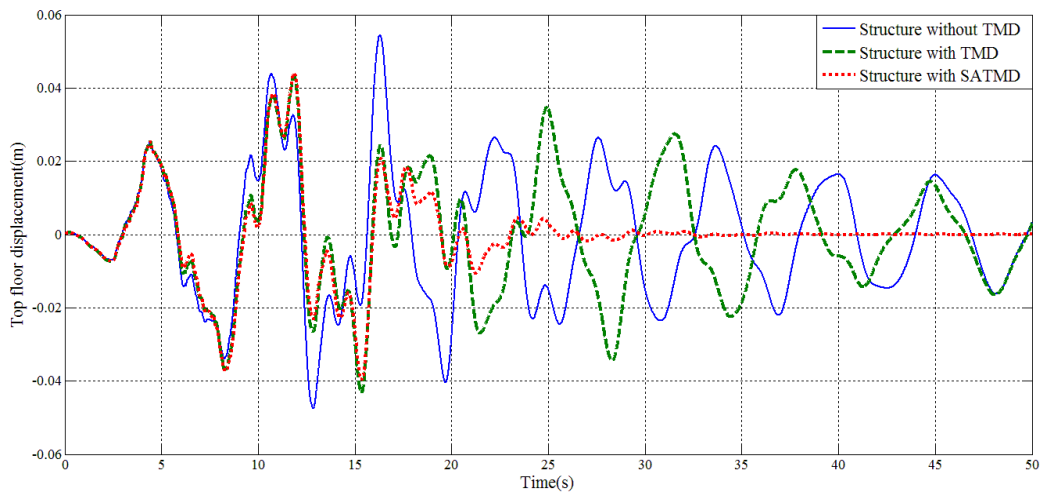


Figure 5-14: Roof top response of the structure due to Nahanni ground motion in time domain.

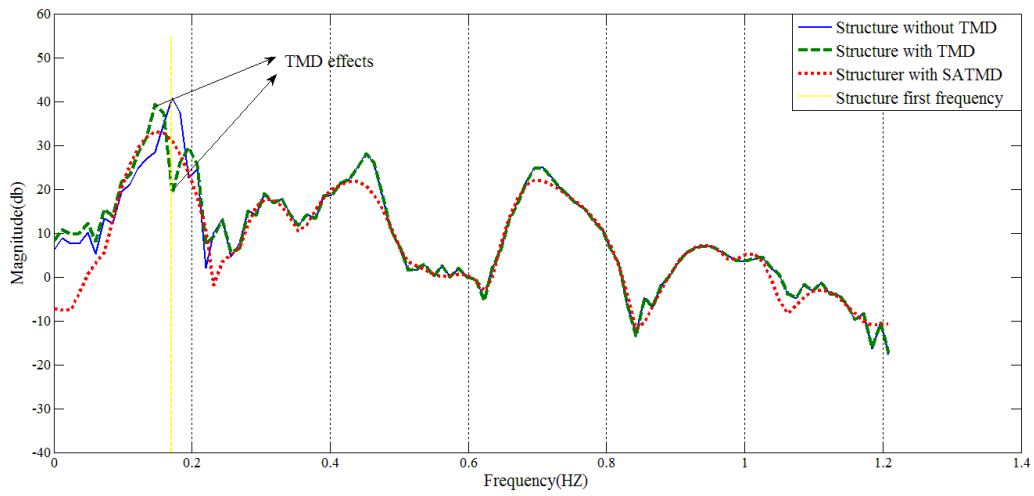


Figure 5-15: Roof top response of the structure due to Nahanni ground motion in frequency domain

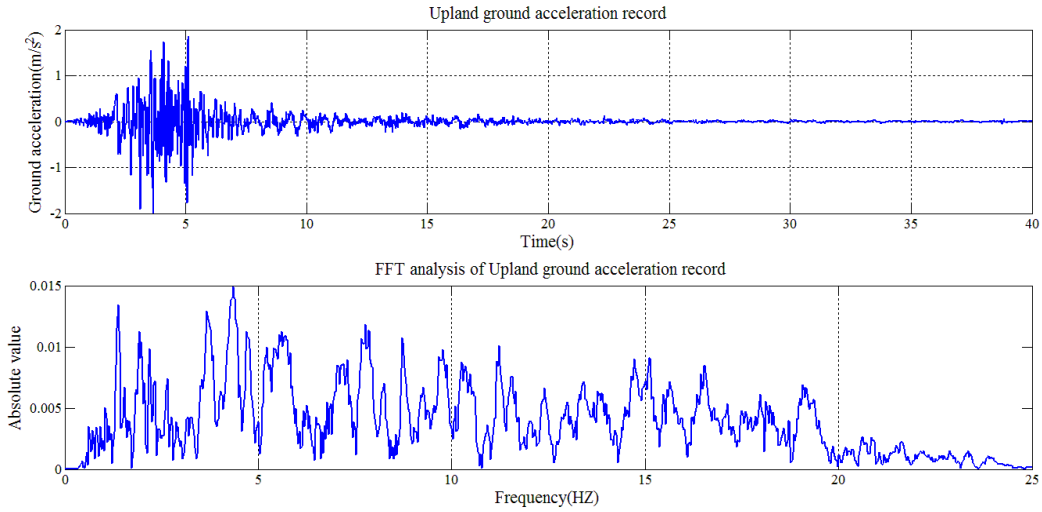


Figure 5-16: Upland ground acceleration record and its FFT diagram.

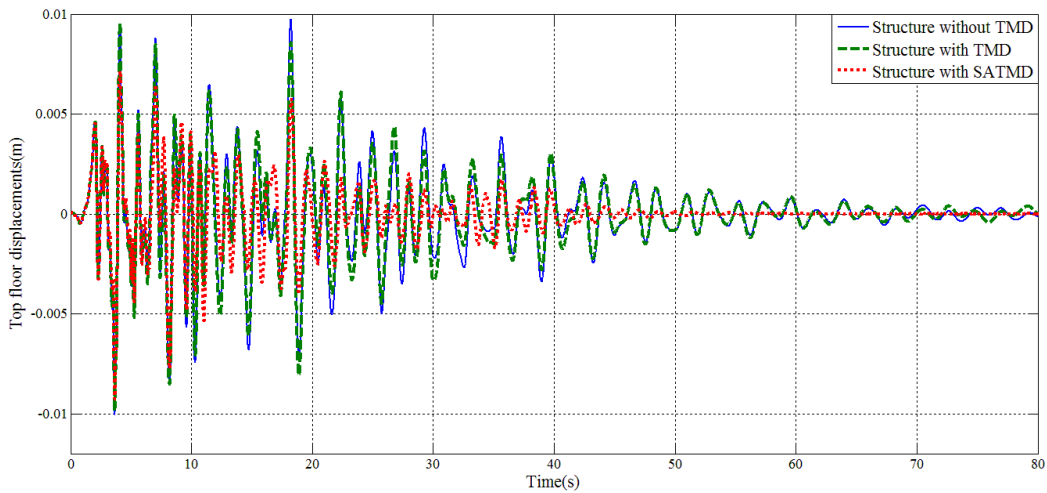


Figure 5-17: Roof top response of the structure due to Upland ground motion in time domain.

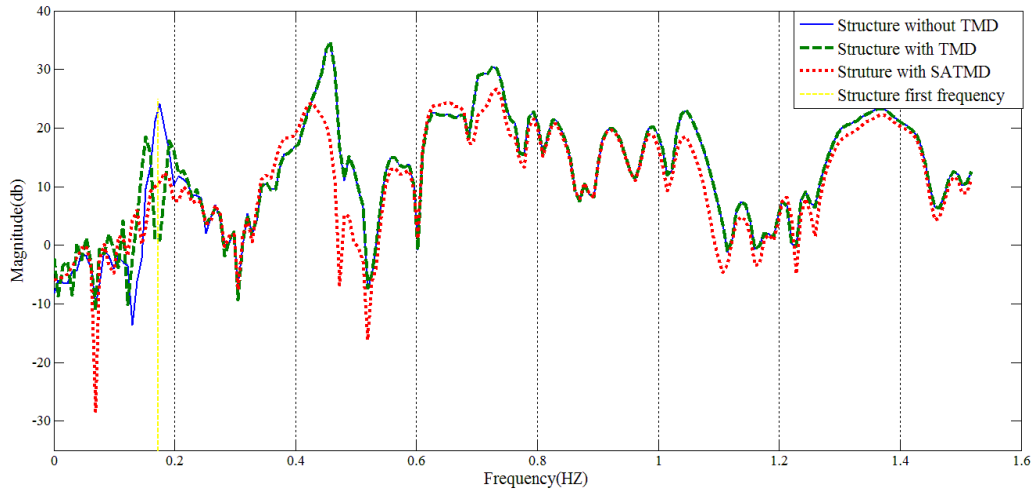


Figure 5-18: Roof top response of the structure due to Upland ground motion in frequency domain.

5.3. Control system tuning

The performance of control system directly affects the response of SATMD system. LQR control system uses optimization to determine gain matrix in order to optimize the cost function. Thus, defining various cost functions will results in different gain matrices and different control forces, and consequently different structural responses.

$$J = \int_0^t (X^T Q X + U^T R U) dt \quad (5-1)$$

The cost function, J as given in Equation (5-1) is a combination of state vector (displacements and velocities) and control force vector weighted by the coefficients defined by Q and R matrices, respectively. Therefore, Q and R matrices can change the cost function, gain matrix, control force and structural response, respectively. R matrix is a unit matrix multiplied by a constant coefficient which should be determined so that gain matrix can yield applicable control

forces. In the current research responses of the structure with SATMD system using three different Q matrices has been investigated. Q_1 (Eq. (5-2)) considers both displacement and velocity, Q_2 (Eq (5-3)) considers only velocity, and Q_3 (Eq. (5-4)) considers only displacement.

In using Q_3 in Eq. (5-1), the structural displacements will be included in the cost function and the object of the control system is to minimize the structural displacements (except TMD mass displacement). On the other hand, if matrix Q_1 and Q_2 are used, the control system will minimize both structural displacements and velocity. The response of the structure to using Q_1 , Q_2 and Q_3 are computed and illustrated in Figure 5-19.

$$Q_1 = \begin{bmatrix} 1_{4 \times 41} & 0_{4 \times 41} \\ 0_{4 \times 41} & 1_{4 \times 41} \end{bmatrix} \quad (5-2)$$

$$Q_2 = \begin{bmatrix} 0_{4 \times 41} & 0_{4 \times 41} \\ 0_{4 \times 41} & 1_{4 \times 41} \end{bmatrix} \quad (5-3)$$

$$Q_3 = \begin{bmatrix} 1_{4 \times 41} & 0_{4 \times 41} \\ 0_{4 \times 41} & 0_{4 \times 41} \end{bmatrix} \quad (5-4)$$

As it can be seen from Figure 5-19, the variation of Q matrix greatly alters the results of the SATMD system. The best results for minimizing the top floor displacement is reached by Q matrix defined in Eq. (5-4). Eq. (5- 4) results in a cost function contain structural displacements only.

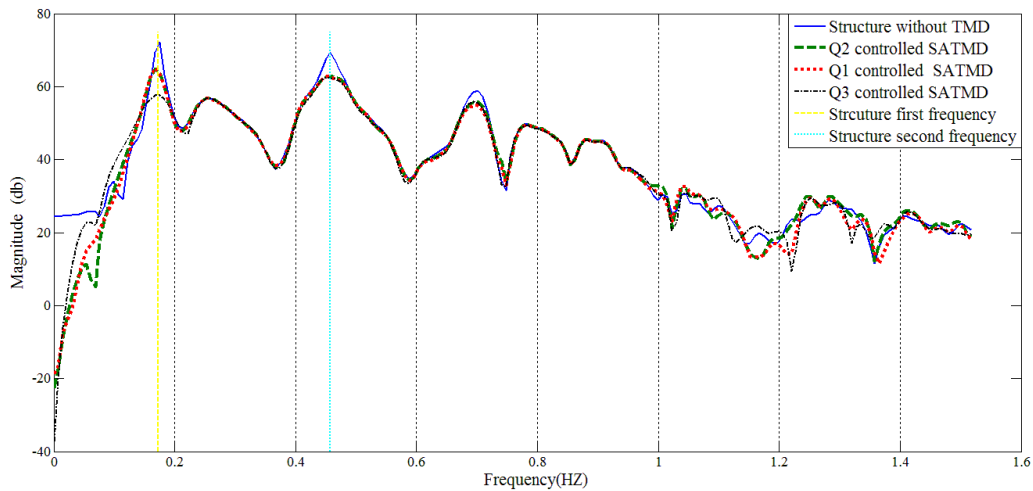


Figure 5-19: Roof top response of the structure with different Q weighting matrix due to Kobe ground motion in frequency domain.

5.4. Mass ratio effect on response of SATMD system

The influence of the mass ratio (i.e. the mass of the TMD divided by the mass of the structure) on the response of the tall building with SATMD system subjected to Kobe earthquake excitation is illustrated in Figure 5-20. In low rise building or light weight mechanical systems the mass ratio can be increased up to 10 percent. For high rise buildings and heavy mechanical systems mass ratio is kept low. In Figure 5-20, the mass ratio is increased from 1.5 percent to 2 percent which is within a practical range of mass ratio for a 40-storey tall building. As it can be realized, the increase of mass ratio from 1.5 percent to 2 percent has little to no effect on the response of the structure. It is noted that the difference in the response of the structure due to the change in the mass ratio is not visible in the time domain. For that reason, only frequency domain response

is reported in Fig.25. Thus the results suggest that increasing mass ratio in SATMD system in the practical range of 0.5% to 1% will not improve the efficiency of SATMD system.

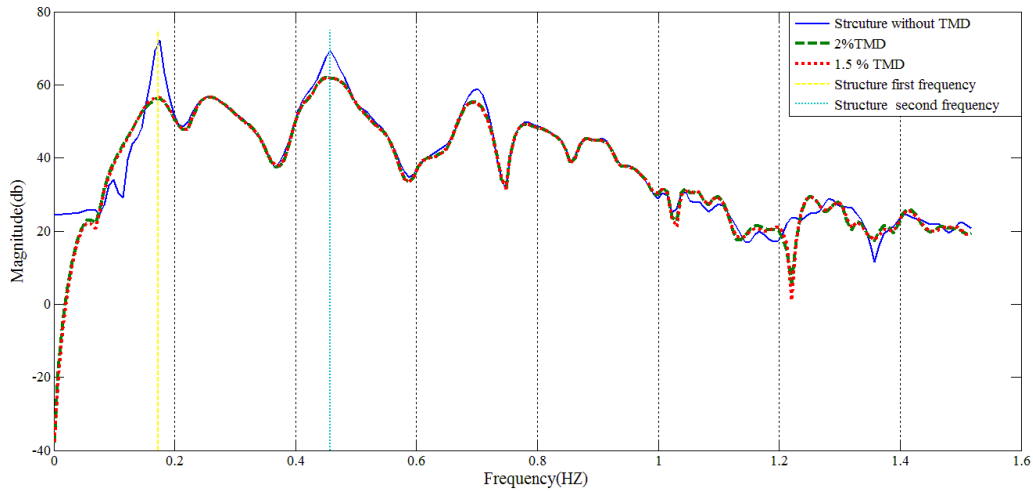


Figure 5-20: Roof top response of structure with different mass ratio for SATMD due to Kobe ground motion in frequency domain.

5.5. Summary

In this chapter a MR-based semi-active tuned mass damper system (SATMD) has been designed to control the vibration of a forty-storey tall steel building structure designed according to the National Building Code of Canada (NBCC 2010) and the relevant standard for steel design (CAN/CSA-S16-09). The LQR control algorithm has been used to find the optimal damping forces. The response of the uncontrolled structure and controlled structure equipped with traditional passive TMD system and SATMD system under different earthquake records with low, medium and high frequency contents have been determined and compared. It has been shown that SATMD system has superior performance as compared to the traditional TMD

system in reducing the displacement demand as well as the settling time of the structure. SATMD system can suppress the vibration in a wide range of frequencies in contrast to TMD system which is tuned at a particular frequency. To minimize the structural response due to a seismic excitation, an optimal Q matrix for LQR control system in TMD application has been proposed. Furthermore, it has been illustrated that in a practical range of the auxiliary mass in a tall building (1.5% to 2.5% of building mass), the response of structure does not change appreciably.

Chapter 6 : Seismic Response of Buildings with Semi-Active Bracing System

6.1. Introduction

The response of the structural building with MR damper in bracing system is investigated in this chapter. The behaviour of two buildings, one five and twenty storey high, which have been designed for the seismicity of Vancouver in western Canada, are investigated under different frequency content seismic records. The behaviour of building with MR damper in harmonic ground motion is also studied here. The details of the building are provided in Chapter 3. The response of the structures is illustrated in time and frequency domain for convenient in all cases. One of the main goals of the present study is to investigate the effectiveness of MR damper braces in building frames using LQR control strategy combined clip optimal semi active control system as compared to passive on mode control system. The twenty and a five storey buildings, representing a short and a tall structure have been equipped with MR damper braces in all floors. Number of the installed MR dampers is increased from top floor to first floor in proportion to the design storey shear due to seismic force. Then, structural response of these buildings is carefully studied for several earthquake records. MR damper used in this research is of capacity 200 kN,

developed by the Lord Corporation, which is the only large capacity MR damper for which the relevant parameters are available in the literature.

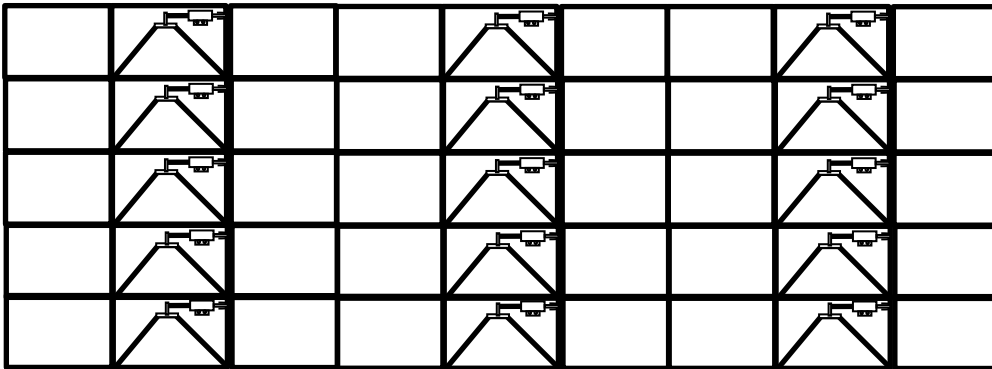


Figure 6-1: Schematic MR brace location in five storey building.

6.2. Response of the twenty and the five-storey buildings

In this study, the performance of MR dampers equipped with control systems has been compared to that under constant current (*passive ON* mode) during different types of ground acceleration (as discussed earlier). The details of the seismic ground motion records are summarized in Table (5-1) in the previous chapter.

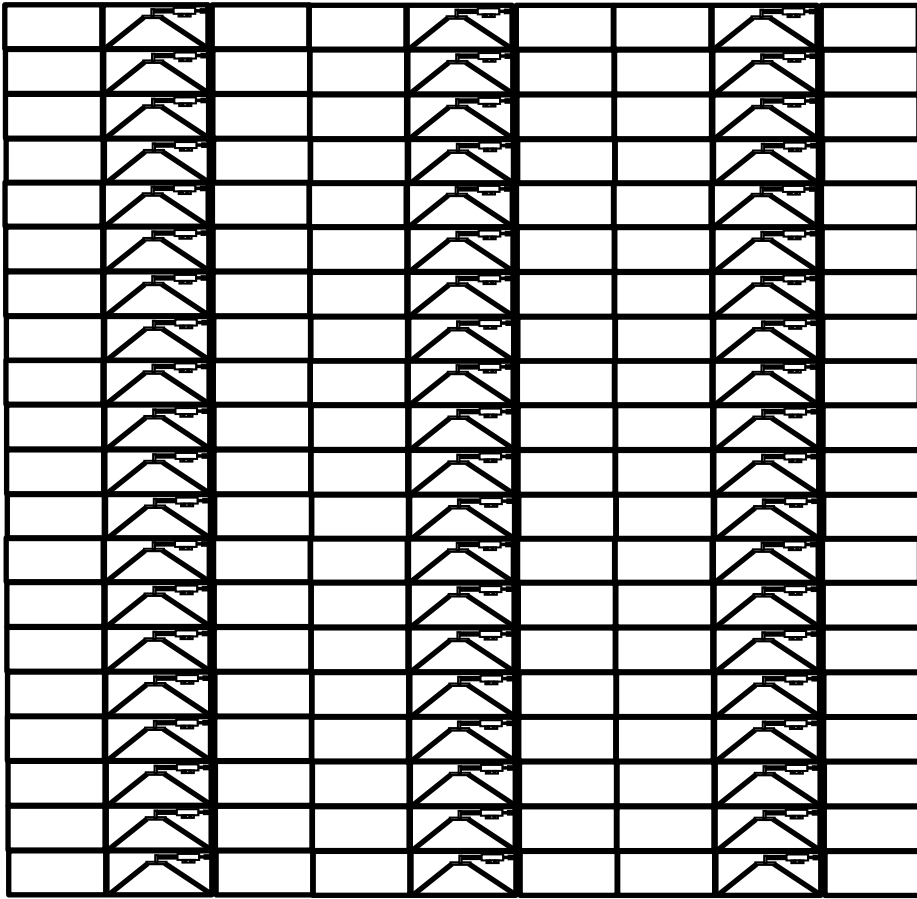


Figure 6-2 : Schematic MR brace location in twenty storey building.

The response of any structure to ground excitation is influenced by how closely the frequency contents of the ground excitation match the natural frequencies of the structure. The earthquake record for the ground-acceleration and corresponding fast Fourier transformation are shown earlier in Figures (5-1, 5.4, 5.7, 5.10, 5.13 and 5.16). As it can be realized from the FFT diagrams in the abovementioned figures, Kboe, Irpinia and Kocaeli records have a frequency range from 0

to 10 Hz with a higher frequency density around 5 Hz. On the other hand, Tabas, Nahanni and Upland records have frequency range from 0 to 30 Hz with higher frequency density around 15 Hz. The buildings considered here all have fundamental frequencies lower than the dominant frequencies of both low and frequency ground motion records. However, they are expected to excite the short and tall buildings differently. The ground acceleration is scaled to 0.3g for 20 story building and 0.6g for 5 story building based on design spectra and the maximum displacement and interstory drift are found to be below 2.5% of the height of building. Scaling remains constant for different ground excitation.

The numbers of MR dampers in different floors determined in such way that MR damper force remains less than maximum MR damper capacity (200kN).

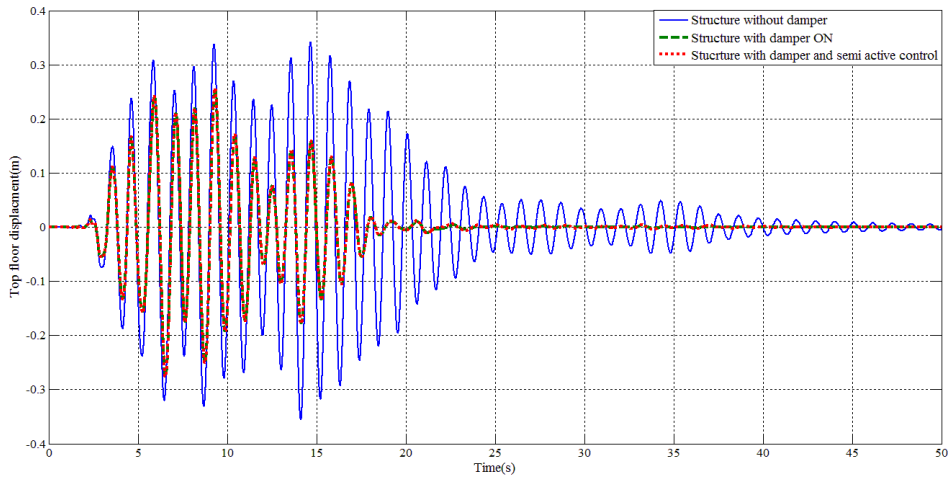
6.2.1. **Response to seismic records**

The time domain and frequency domain response of the five-storey building under Kobe and Irpinia records (scaled to 0.6g) are shown in Figures (6-3 and 6-4). Location and numbers of the MR damper braces for the five-storey building under Kobe and Irpinia ground excitations are shown in the accompanying table in these Figures (6-3 & 6-4). It can be observed from Figure (6-3), that the *passive ON* mode and LQR control system generate comparable responses of the building in both time and frequency domains. As mentioned earlier, the fundamental frequency of the five-storey building is 0.9 Hz. Seismic response of the structure due to each of these excitations clearly shows a peak at around 0.9 Hz as shown in Figure (6-3)

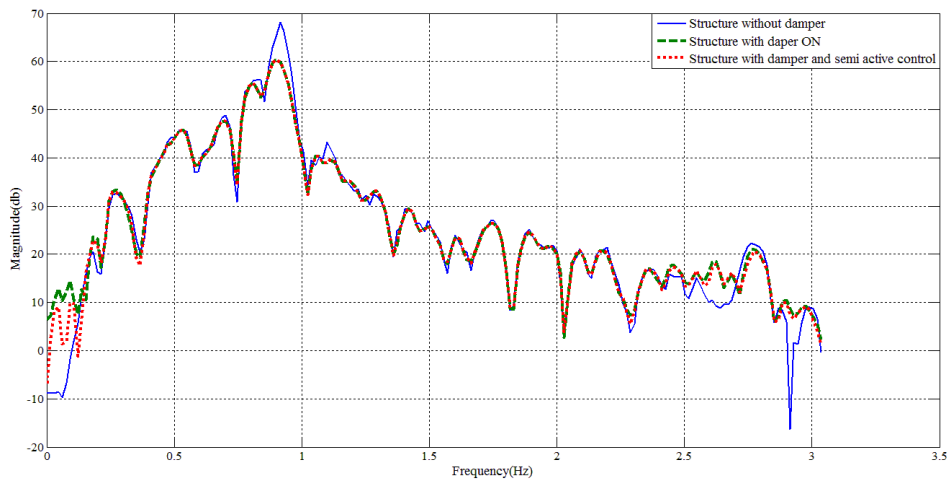
It is interesting to note that the MR dampers are capable of reducing the response significantly, especially the peak response at the fundamental frequency of the structure. Moreover, as

compared to the uncontrolled structure the controlled system was capable of dissipating the seismic vibratory energy faster.

It should be noted that although the five-storey building is a rather short building, its first natural frequency is around 0.9 Hz which can be excited by a seismic ground motion with low frequency contents like Kobe which has dominant frequencies around 2-3 Hz. The first mode period calculated using the empirical formula provided in NBCC (2010) is about 0.76 second and that obtained from modal analysis is 1.1 sec. Kobe ground excitation duration is about 15 second and it can be observed from Figure (6-3) that MR damper dissipates the seismic vibration very fast.



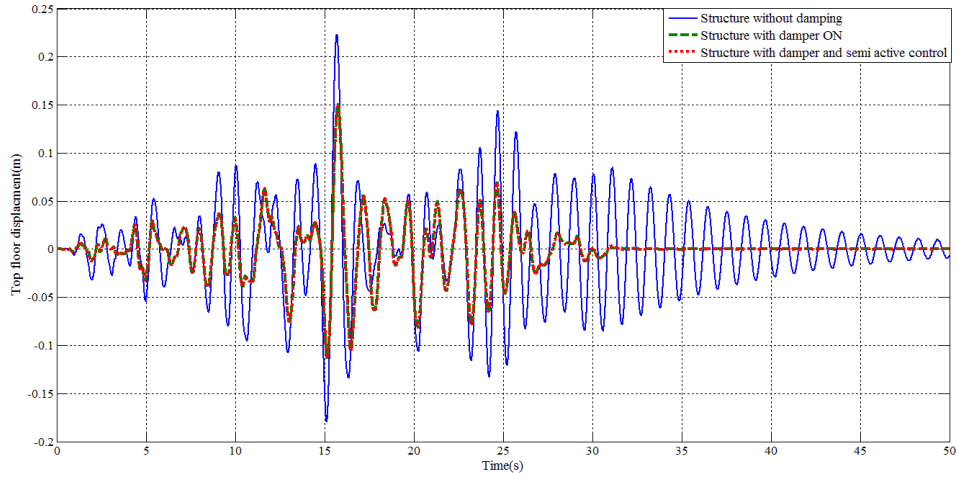
a)



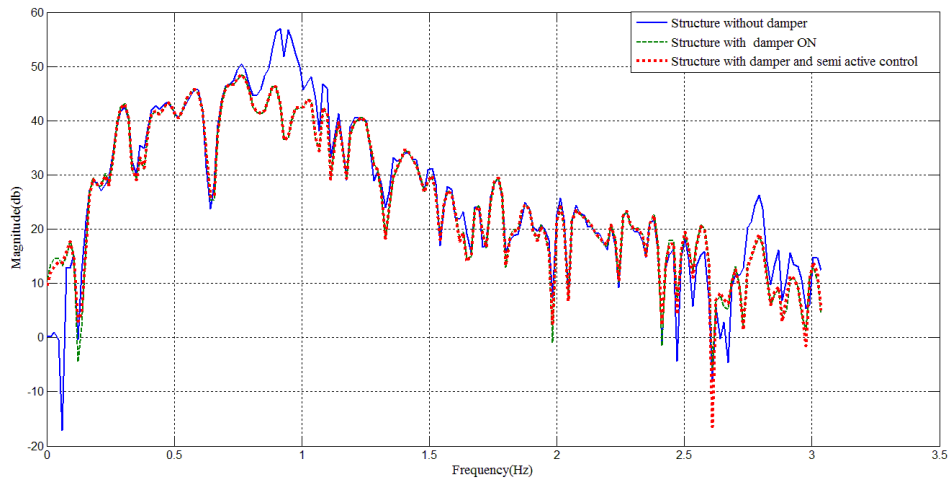
b)Floor number	Number of dampers
1-3	6
4	3
5	3

c)

Figure 6-3: Response of five storey building under KOBE record ground excitation: a) Response in time domain; b) Response in frequency domain; c) Allocation of dampers



a)



b)

Floor number	Number of dampers
1-3	6
4	3
5	3

c)

Figure 6-4: Response of five-storey building under Irpinia record ground excitation: a) Response in time domain b) Response in frequency domain c) Allocation of dampers

The control sequence using the semi-active “ON” and “OFF” commands according to combined LQR and the clip-optimal control strategy for the first floor MR dampers installed in the five-storey building under Kobe ground excitation are shown in Figure 6-5. It can be observed that the control command fluctuates between ON and OFF, where for up to about 40 seconds the control is ON and for about 40 seconds it remains OFF.

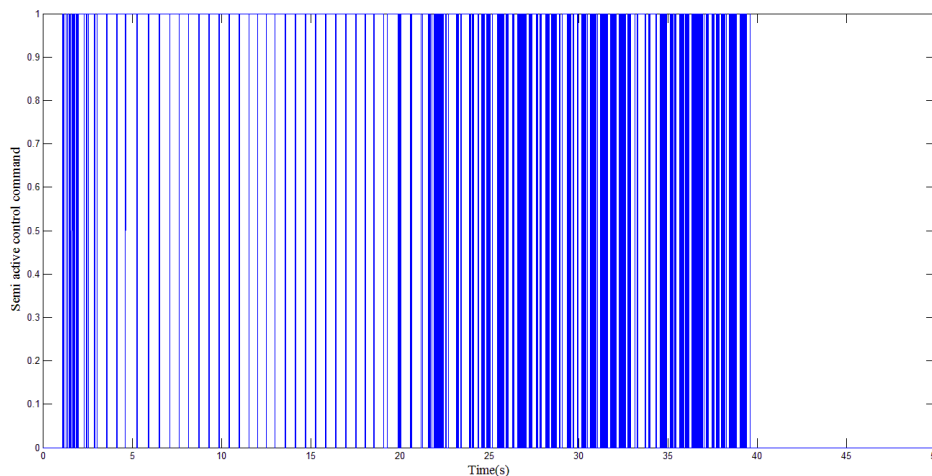


Figure 6-5: Semi active ON and OFF control command for first floor MR damper up to 50second.

To better realize this, a detailed breakdown of semi-active control ON command for first floor MR dampers under Kobe ground excitation for five storey building has been shown in Figure 6-6.

It seems that in the first 5 seconds of the earthquake (Kobe) occurrence, the structure does not experience much of the ground excitation and the structural response remains low. Thus, the semi-active control system only gives the ON command 42% of the time. As the ground excitation and consequently structural response build up, the semi-active control system shows

an increase in the ON command up to 95% between 5 and 15 seconds when the structure experiences the largest response. Between 20 to 25 seconds, the semi-active controlled structure does not indicate a large response, while the uncontrolled structure undergoes a rather large displacement. As the ground excitation fades out, the semi-active control ON command declines to 40%, and then 0% at 40 second and beyond.

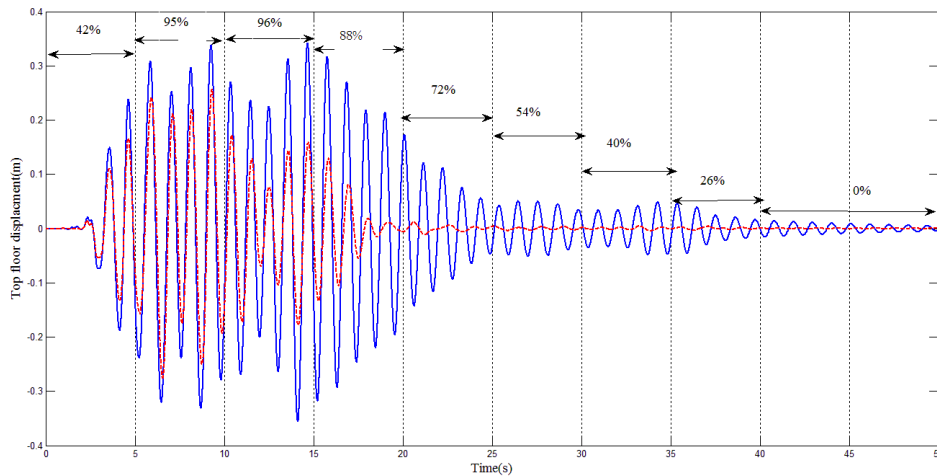
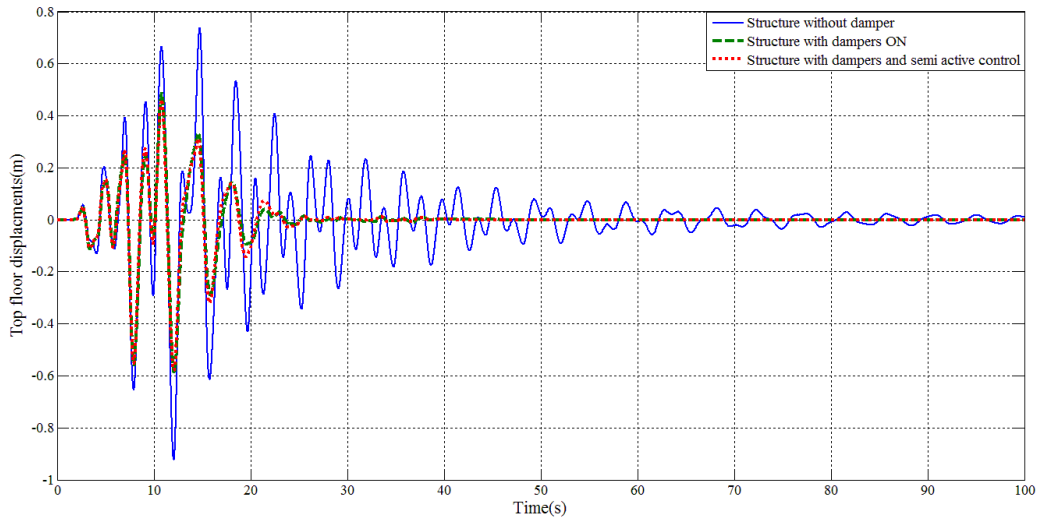


Figure 6-6: Break down of semi active control percentage of ON command for first floor MR damper in five-storey building under Kobe seismic record.

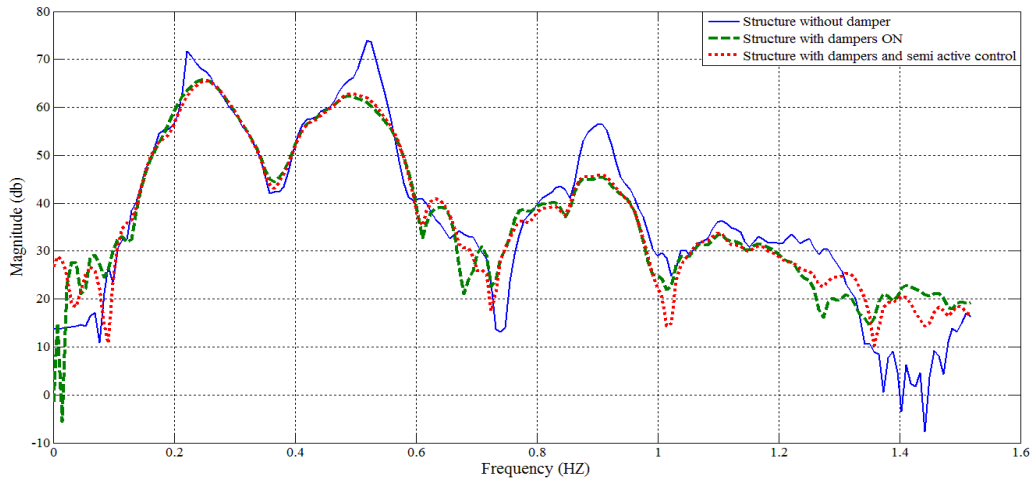
The response of twenty-storey building under Kobe and Irpinia seismic record (scaled to 0.3g) for two different damper arrangements is illustrated in Figure (6-7 & 6-8). The number of the dampers is doubled to investigate if the response of semi-active LQR control system will be modified as compared to the passive ON control mode. From Figure 6-7, the maximum structural deflection with only 10 MR dampers installed in the first floor is 0.8 m.

From Figure (6-7 & 6-8) it can be observed for the twenty-storey building, more than one modes (e.g., modes corresponding to the natural frequencies of 0.22 Hz, 0.55 Hz and 0.9 Hz) contribute

to the structural response of the building. In this case, the MR dampers with semi-active control strategy is found to have insignificant effect as compared to the MR dampers under constant current (MR damper with passive mode on). Nevertheless both systems (i.e., passive mode on and semi-active control) reduce the structural response considerably in 0.22 Hz and 0.55Hz modes as compared to the uncontrolled structure.



a)

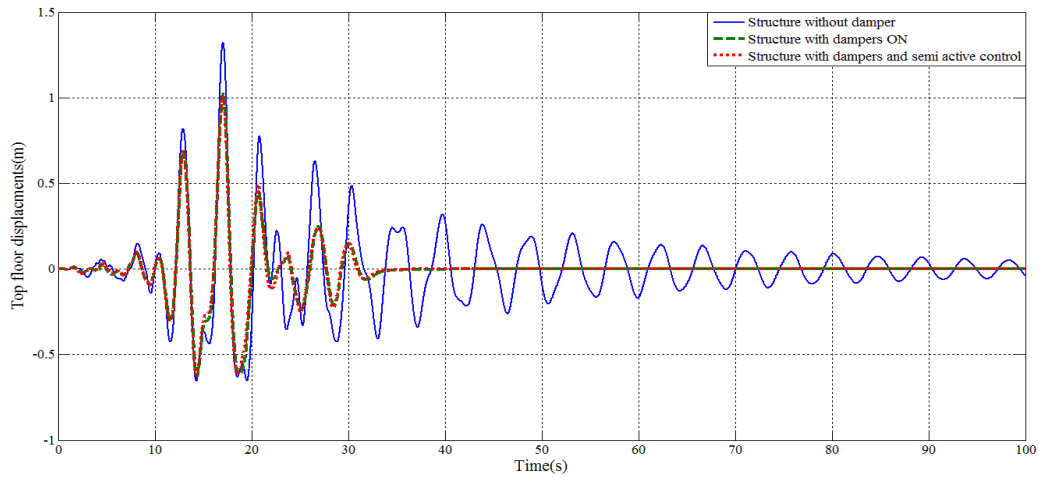


b)

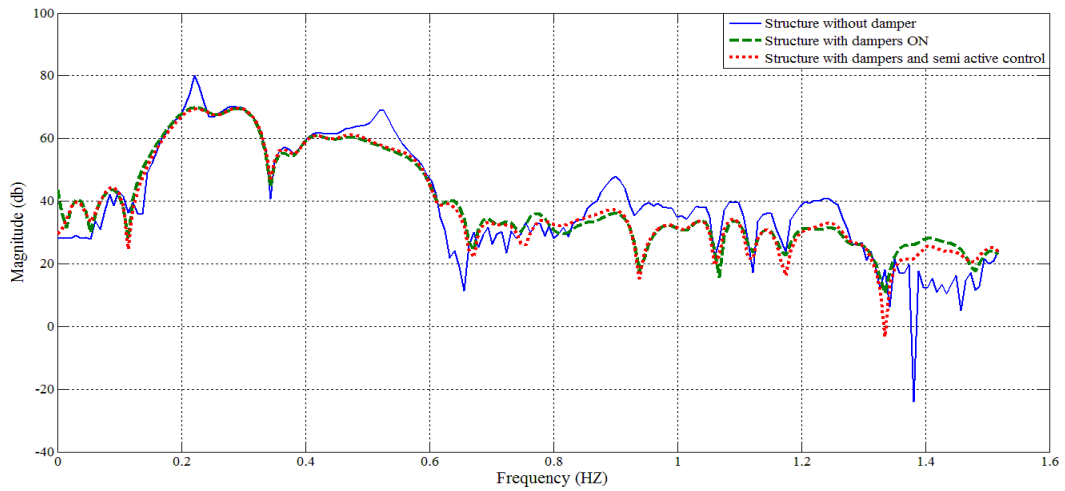
Floor number	Number of dampers
1-7	10
8-14	5
15-20	3

c)

Figure 6-7: Response of twenty storey building under KOBE record ground excitation (1): a) Response in time domain; b) Response in frequency domain; and c) Allocation of dampers



a)



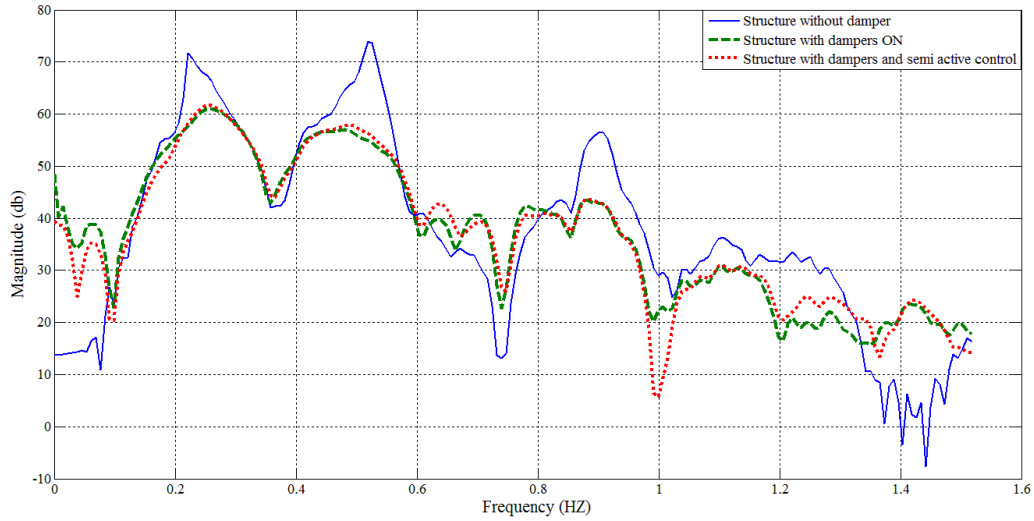
b)

Floor number	Number of dampers
1-7	10
8-14	5
15-20	3

c)

Figure 6-8: Response of twenty storey building under Irpinia record ground excitation (1): a) Response in time domain; b) Response in frequency domain; and c) Allocation of dampers

The response of the structure with increased number of MR damper for LQR control system and passive ON control strategy in frequency domain is illustrated in Figure (6-13 & 6-14). Again, no noticeable advantage is observed in the response of the structure with MR damper utilizing semi-active control strategy in comparison to that using passive ON mode.



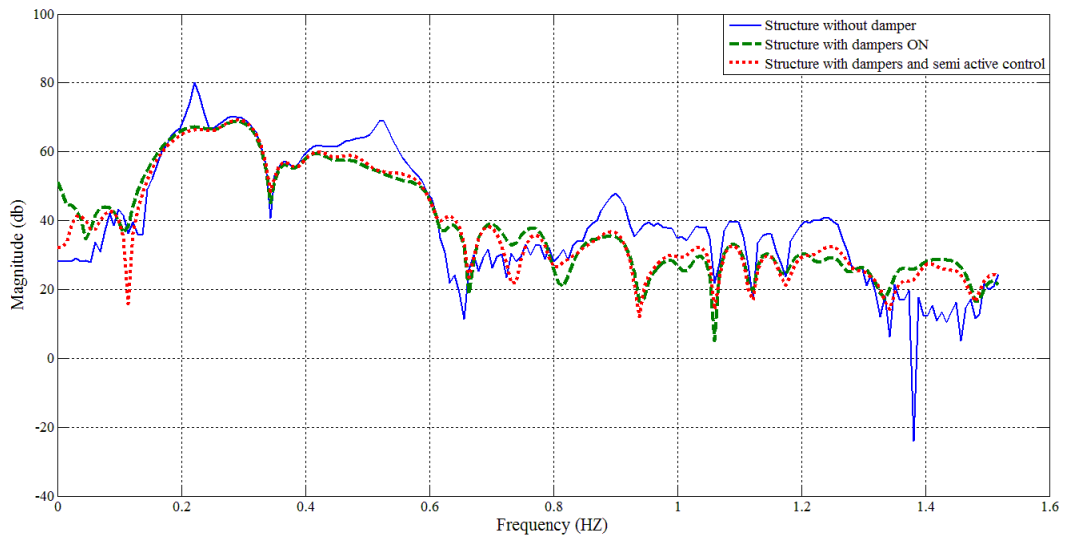
a)

Floor number	Number of damper
1-7	20
8-14	10
15-20	6

b)

Figure 6-9: Response of twenty storey building under KOBE record ground excitation (2): a)

Response in frequency domain; and b) Allocation of dampers



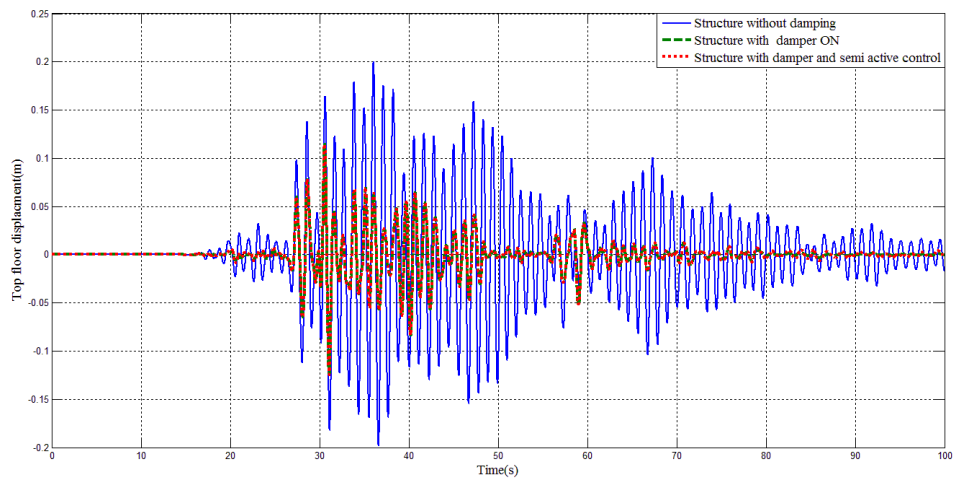
a)

Floor number	Number of damper
1-7	20
8-14	10
15-20	6

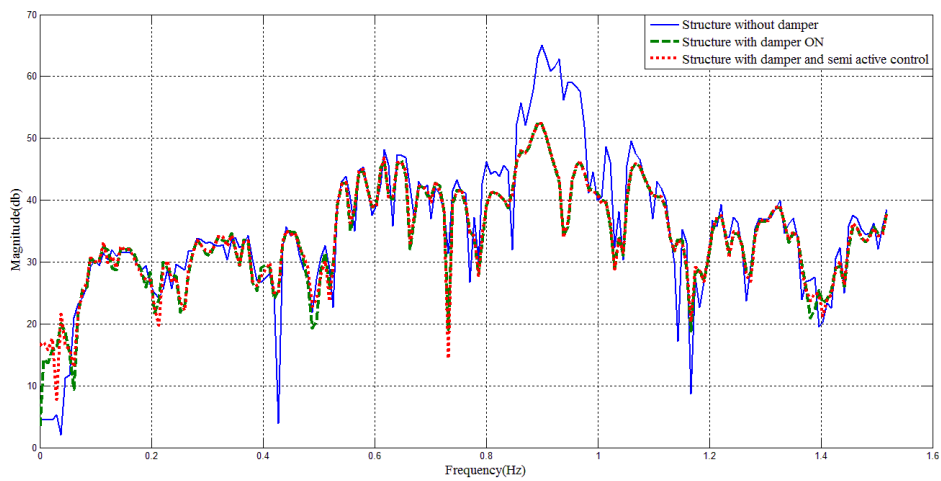
b)

Figure 6-10: Response of twenty storey building under Irpinia record ground excitation (2): a)

Response in frequency domain; and b) Allocation of dampers



a)

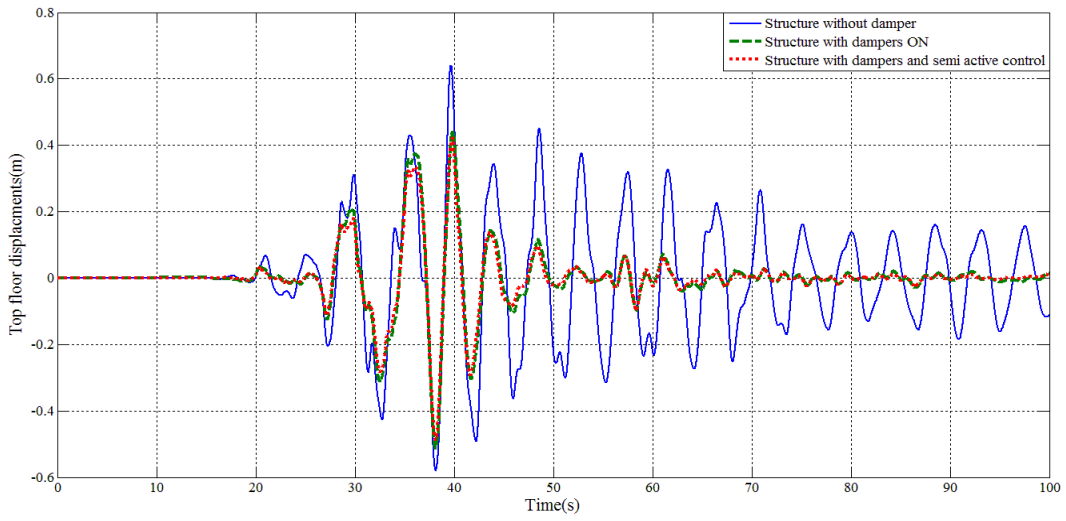


b)

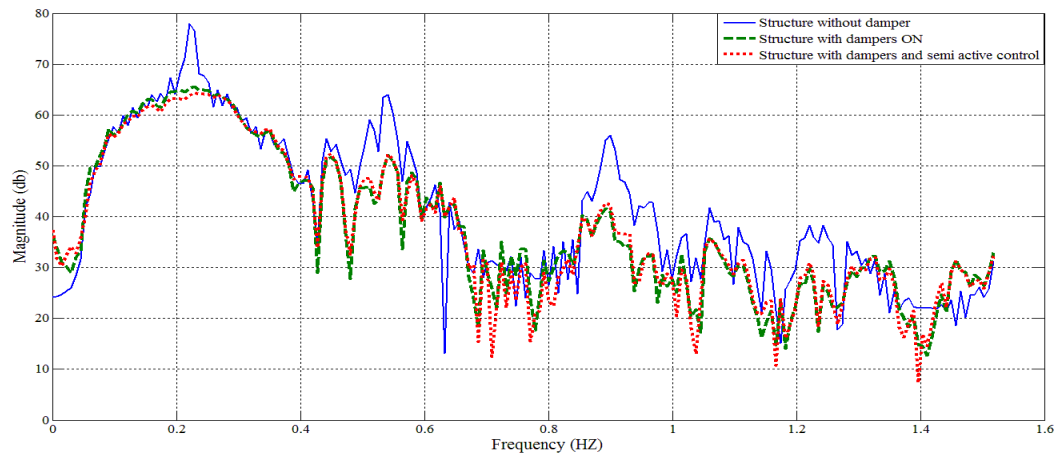
Floor number	Number of dampers
1-3	6
4	3
5	3

c)

Figure 6-11: Response of five storey building under Kocaeli record ground excitation (1): a) Response in time domain; b) Response in frequency domain; and c) Allocation of dampers



a)



b)

Floor number	Number of dampers
1-7	10
8-14	6
15-20	2

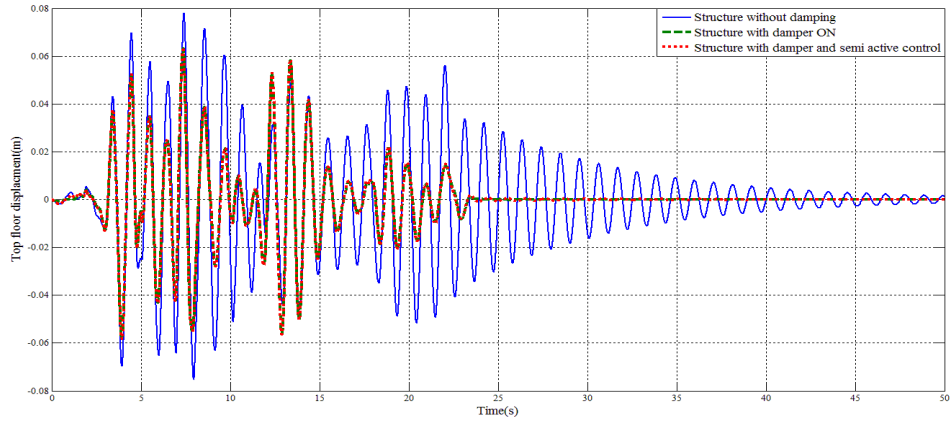
c)

Figure 6-12: Response of twenty storey building under Kocaeli record ground excitation (2): a) Response in time domain; b) Response in frequency domain; and c) Allocation of dampers

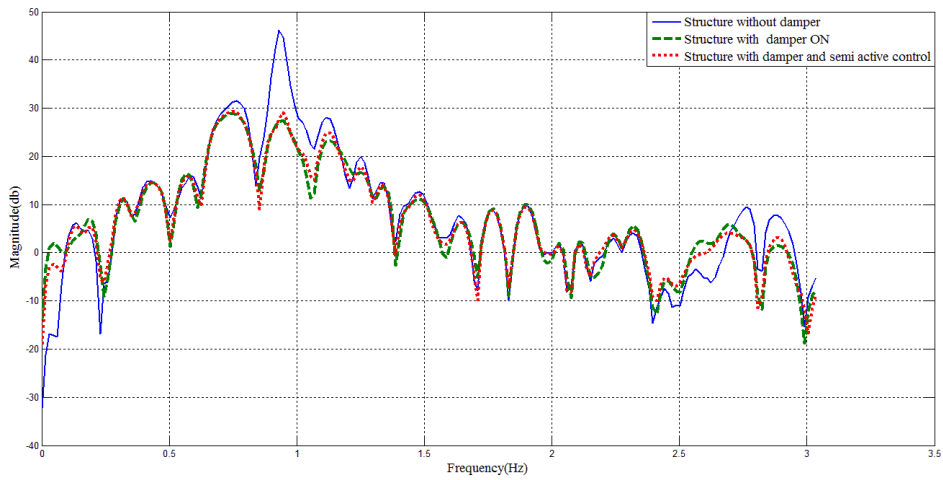
The response of the five and twenty-storey buildings to Kocaeli record ground excitation are shown in Figure (6-11: 6-12). Because of the abrupt fluctuation in time-domain ground acceleration of this record, the Fast Fourier Transform diagrams of the response of the structures are not smooth. In addition, this fluctuation induces smaller response in structure as compared to other seismic records. The MR dampers with semi-active control system demonstrate no superiority over the passive mode ON control strategy in reduction of the structural response for the five and twenty storey buildings under Kocaeli record ground excitation.

The response of the five-storey building structure to Tabas ground acceleration is shown in Figure (6-13). As it can be observed from Figure (6-13), the number of dampers used in the five-storey building structure is half of the number of dampers which is used in the previous part, and in spite of that the top floor displacement is much less under Tabas ground excitation .

The top floor displacement response of the five-storey building to Nahanni and Upland ground excitation are shown in Figures (6-14 & 6-15). It can be seen that maximum response is under 40 mm and semi-active control strategy for MR damper has no obvious advantage to MR damper with passive model on strategy.



a)

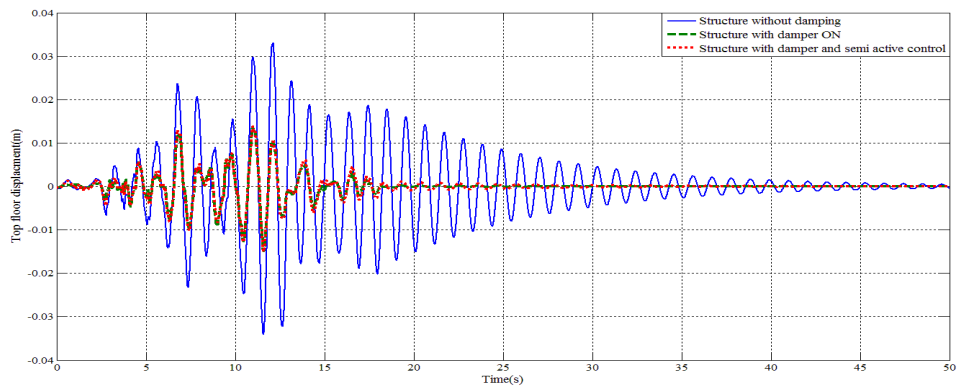


b)

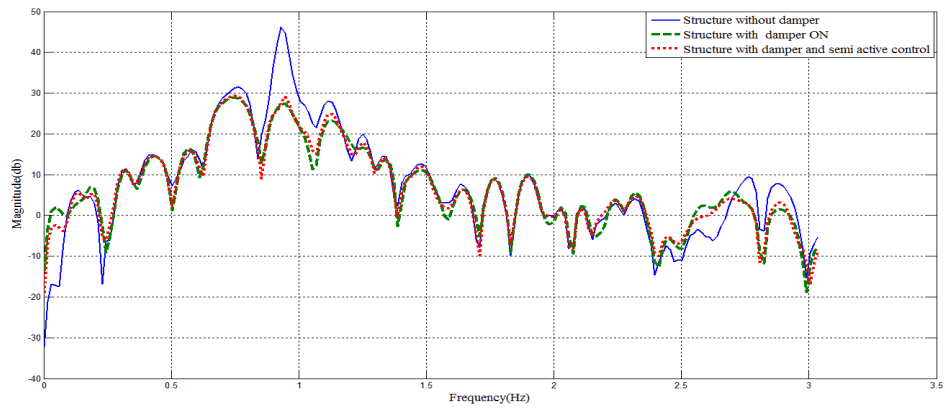
Floor number	Number of dampers
1-2	3
3	3
4	2
5	2

c)

Figure 6-13: Response of five- storey building under Tabas record ground excitation: a) Response in time domain; b) Response in frequency domain; and c) Allocation of dampers



a)

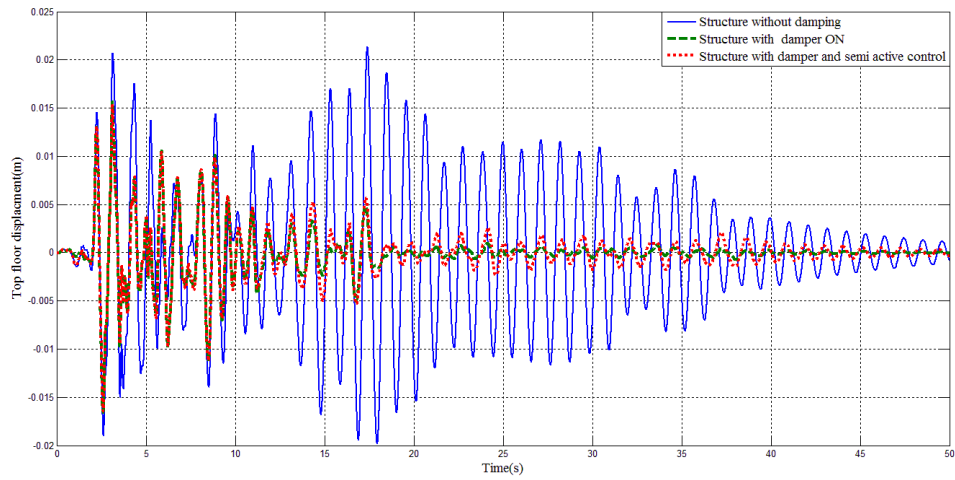


b)

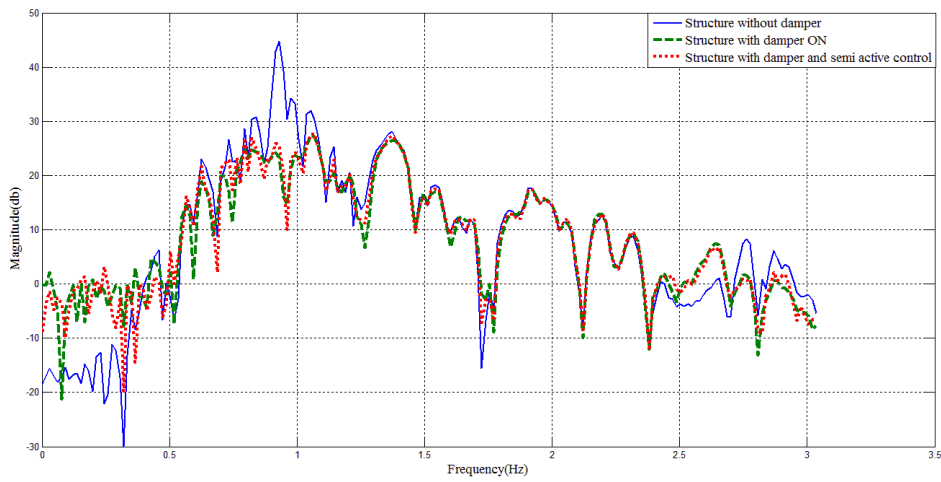
Floor number	Number of dampers
1-2	3
3	3
4	2
5	2

c)

Figure 6-14: Response of five-storey building under Nahanni record ground excitation: a) Response in time domain; b) Response in frequency domain; and c) Allocation of dampers



a)



b)

Figure 6-15: Response of five-storey building under Upland record ground excitation; a)

Response in time domain; b) Response in frequency domain;

6.3. Summary

The effectiveness of implementing LQR control system combined with clipped optimal control strategy in MR damper bracing system as compared to passive mode on control strategy have been investigated in bracing system of a set of building frames excited by ground acceleration. A five-storey building representing short building and a twenty-storey building representing a tall building have been modeled and designed according to the National Building Code of Canada. Two buildings are equipped with MR dampers in all floor and semi-active control passive mode on control strategies have been implemented to control MR dampers during various ground excitations. The response of the structures is studied in both time and frequency domains. The full state LQR control system integrated with clipped optimal control strategy demonstrated insignificant advantage compared to passive on model on strategy.

It should be noted that in this work, MR dampers have been utilized in all floors in accordance to the distribution of the design shear due to earthquake excitation. In the case of large number of MR dampers in the building model the use of the proposed simple MR damper model instead of the Bouc-Wen model is computationally more advantageous.

Chapter 7: Summary and Conclusions

7.1. Summary

The objectives of current research are to develop an accurate physics-based model of MR dampers and to conduct a thorough investigation on their application in controlling the seismic response of building structures. Most previously-developed MR damper models are phenomenological based models which do not provide information on MR damper behaviour in relation to its physical characteristics and MR fluid material properties. The first task of the present research is to develop an accurate mechanistic model of MR /ER dampers considering their geometrical parameters and fluid material properties. A CFD based model has been developed for MR/ER dampers. The model is capable of predicting the damping force generated in MR/ER dampers under any arbitrary excitations. The performance of the developed CFD model has been validated against other methods available in the literature.

Because of the complexity of MR fluid behavior and computational costs, the developed mechanistic model cannot be implemented directly into structural system for the purpose of semi-active vibration control. The complexity of exact dynamic response of MR/ER damper is basically the main reason why most of researchers limited their study in application of MR damper in building to a limited number of MR dampers. Development of a simple MR/ER damper model which can estimate MR/ER damper response in dynamic motion with an acceptable accuracy is the second challenge of this research. Utilizing the developed CFD based model, a simple and efficient phenomenological based model has been developed for MR/ER dampers. The accuracy of the developed model has been verified through comparison of the

obtained results with those obtained based on other phenomenological models (e.g., modified Bouc-Wen model) under both harmonic and random loading.

The application of MR dampers in large size building structures for controlling seismic loadings has been studied in next part of this thesis. Two main applications have been studied: Semi-active tuned mass damper and MR damper in bracing system. Contrary to other researchers which use imaginary or lab scale structures with one or two MR dampers installed in bottom or top floor of their building models, the current research uses real large size MR damper in full-scale building structures integrated with multiple MR dampers. For that purpose, three buildings of 40, 20 and 5 storey height have been designed according to NBCC and relevant standards. Large size MR damper have been implemented in their tuned mass damper system or bracing system. The response of building structures have been investigated under full range of different seismic loadings.

7.2. Conclusions

The conclusions derived from the research conducted in this thesis are summarized as follows:

- Mechanistic model of MR fluid dampers: The developed mechanistic model of MR dampers can accurately predict the generated damping force in MR dampers under any excitation. The developed model can greatly help researchers and engineers to understand how the MR damper works and behaves and how to improve and design better MR damper with desirable characteristic.
- Simplified model of MR dampers: A simple phenomenological based model has been developed based on the developed CFD model to efficiently with reasonable accuracy predict the damping force in a MR damper subjected to an arbitrary dynamic motion. The

model compares very well with Bouc-Wen model which has proved to characterize the hysteresis behavior of MR damper very well. . The proposed model can help researchers to practically investigate and study potential applications of MR damper in building structures.

- MR damper application in tuned mass damper: It is shown that MR based tuned mass damper system can improve the structural response under seismic loading. The improvement has been observed in reduction of both amplitude of the dynamic response and settling time of structural vibration.
- MR damper application in bracing system: No obvious advantages have been observed using semi active controlled MR damper in bracing system over MR dampers in passive off or on modes of operation. This observation has been made for five and twenty storey buildings with different MR damper configurations under different frequency content seismic recodes. Other bracing systems or dampers like friction damper and hydraulic damper are cheaper and perhaps more effective.

7.3. **Contribution and achievements**

Two novel models, namely the high fidelity mechanistic and simplified phenomenological based models have been developed to characterize the behavior of MR dampers.

The developed mechanistic model introduces an alternative numerical method based on CFD to estimate the dynamic behaviour of MR/ER dampers based on their physical nature of the Newtonian and non-Newtonian fluid flow. The method is not only applicable to a wider range of MR dampers with flow mode and mixed mode of operation, but also, to different types of

dynamic motion (e.g., harmonic and random). Available physical models are not capable of estimating the damping force in MR dampers in random motion. The proposed mechanistic model is the only mechanistic model which can estimate damping force in flow mode as well as mix mode MR damper. The proposed Mechanistic model also provides information on how different parameters in damper and MR fluid can affect its behaviour. This information can greatly help the designer optimize the performance of MR dampers at an early stage of the design.

The developed simplified phenomenological based model of MR dampers also provide researchers and engineers with an efficient tool that can be used to estimate the dynamic damping force of MR dampers with reasonable accuracy. Such a model can be easily integrated to a structural model (e.g. a building) to study the dynamic behaviour of an entire system. Proposed simplified phenomenological model may enable researchers to study the behavior of the structure with large number of MR dampers without having any concern about numerical instability of the solution.

In addition, implementing real size MR dampers in high, medium and low rise real structural buildings and study their behaviour in wide range of appropriately scaled seismic records with different frequency contents are another achievements of the present research. Without a simplified phenomenological model as developed here, such studies would be quite cumbersome.

7.4. **Limitation**

The mechanistic model utilizes the Bingham plastic model to simulate MR fluid behavior. Considering this the validation of MR damper model is restricted to MR fluids which follow Bingham model. In addition, the mechanistic model can model the behavior of the MR damper under flow and mixed mode operations. The squeeze mode operation is not considered. It is worth mentioning that large MR dampers with building application are all in mix mode or in flow mode.

In proposed MR damper models, environmental temperature and its effect on modeling of an MR damper has been ignored. For MR damper application in outdoor conditions in extreme cold or extreme heat, environment temperature may play a role which needs to be investigated in the future. Furthermore, increase in temperature of MR fluid during its operation has been ignored. Increase in MR fluid temperature during other loading like wind should be investigated.

In developing mechanistic model it is assumed that MR fluid is incompressible.

The study on the application of MR damper in building structures uses shear building model to simulate structural response under seismic loading. In addition, LQR control system has been implemented as the only control system in semi active control system.

The buildings geometry has been select in a way that torsional modes have negligible participation in the dynamic response of the structures.

The behavior of buildings during an earthquake event is considered to be linear while the damper behaviour is nonlinear. The real behavior of the structure is nonlinear which in this study has been neglected

7.5. Scope for future research

Although this research has established new schemes for modeling MR dampers and their application in real-life large building structures under seismic excitations, the scope of research can be naturally extended to study the response of building structures integrated with MR dampers under wind loading.

This idea is very attractive because high rise building are very vulnerable to dynamic wind loading and thus implementing MR based semi active control system in these structures may be very effective to control vibration response.

Furthermore, implementing more sophisticated control system like sliding mode control system can be useful for future research. The seismic performance of MR dampers should also be compared to equivalent systems with other types of dampers such as friction dampers which are passive, but economical.

Nonlinear analysis of the building equipped with MR damper in bracing system is not consider in current research. Investigating nonlinear behavior of structure with MR damper in bracing system under seismic loading is practical and challenging.

The effects of environmental and operational temperature in MR damper modeling need to be considered and the developed models for MR dampers should be also studied for other structures as in bridges.

References:

Abe, M., Fujino, Y., “Dynamic characterization of multiple tuned mass dampers and some design formulas”, Earthquake Engineering and Structural Dynamics, 1994, vol. 23, Issue.8, pp. 813-835.

Aguirre, N., Ikhouane, F., Rodellar, J., Christenson, R., “Parametric identification of the Dahl model for large scale MR dampers”, Structural Control and Health Monitoring, Vol.19, pp.332–347, 2012.

Bani-Hani, K.A., Sheban, M.A., “Semi-active neuro-control for base-isolation system using magnetorheological (MR) dampers”, Earthquake Engineering & Structural Dynamics ,Vol.35, pp.1119–1144, 2006.

Bass, B. J., Christenson, R. E., “ System identification of a 200 kN Magneto-Rheological fluid damper for structural control in large-scale smart structures”, Proceedings of the 2007 American Control Conference, New York City, USA, July 11-13, 2007.

Bitaraf, M., Ozbulut, O., E., Hurlebaus, S., Barroso, L., “ Application of semi-active control strategies for seismic protection of buildings with MR dampers”, Engineering Structures ,Vol. 32, pp.3040-3047, 2010.

Boada, M.J.L., Calvo, J.A., Boada, B.L., Díaz, V., “Modeling of a magnetorheological damper by recursive lazy learning”, International Journal of Non-Linear Mechanics, Vol. 46, pp.479 – 485, 2011.

Bouc, R. “Modèle mathématique d'hystérésis”. Acustica ,Vol.24, pp. 6-25, 1971.

Cai, C. S., Wu, W. J., Araujo, M., “Cable vibration control with a TMD-MR damper system: experimental exploration”, Journal of Structural Engineering ,Vol.133,pp.629-637,2007.

CAN/CSA-S16-09,Limit States Design of Steel Structures. The Canadian Standards Association.

Casciati,F., Magonette,G., Marazzi,F., “Technology of Semiactive Devices and Applications in Vibration Mitigation”, John Wiley & Sons, Inc,2006.

Chae,Y., Ricles, J. M., Sause,R., “Evaluation of Structural Control Strategies for Improving Seismic Performance of Buildings with MR Dampers Using Real-Time Large-Scale Hybrid Simulation”, 19th Analysis & Computation Specialty Conference , ASCE , pp.335-346,2010.

Chae,Y., Ricles, J. M.,Sause, R., “Modeling of a large-scale magneto-rheological damper for seismic hazard mitigation. Part I: Passive mode”, Earthquake Engineering & Structural Dynamics,Vol.42,pp.669-685, 2012.

Chae,Y., Ricles, J. M.,Sause, R., “Modeling of a large-scale magneto-rheological damper for seismic hazard mitigation. Part II: Semi-active mode”, Earthquake Engineering & Structural Dynamics,Vol.42,pp.687-703, 2012.

Chen,Chun, Chen, Cha –Kuang, Yang ,Yue-Tzu. “Unsteady unidirectional flow of Bingham fluid between parallel plates with different given volume flow rate conditions”. Applied Mathematical Modelling ,pp. 697–709, 2004.

Cheng,F.,Y., Jiang,H., Lou,H., “ Smart Structures Innovative Systems for Seismic Response Control”,CRC Press,2008.

Chey, M.H., Chase, J. G., Mander, J. B., Carr, A. J., “Semi-active tuned mass damper building systems: Design ”, Earthquake Engineering and Structural Dynamics, Vol.39,pp.119–139, 2010.

Chey, M.H., Chase, J. G., Mander, J. B., Carr, A. J., “Semi-active tuned mass damper building systems: Application ”, Earthquake Engineering and Structural Dynamics, Vol.39, pp. 69–89, 2010.

Choi, Seung-Bok and Nguyen,Quoc-Hung . “Dynamic modeling of an electrorheological damper considering the unsteady behaviour of electrorheological fluid flow”. Smart Materials and Structures,Vol.18,No.5,pp. 1-9, 2009.

Chooi, W. W. , Oyadiji, S. O. “Design, modelling and testing of magnetorheological (MR) dampers using analytical flow solutions”. Computers and Structures,Vol.22,No.5,pp. 473–482, 2008.

Chopra, A.K. “Dynamics of Structures”. 4th Edition, Prentice-Hall Inc., NJ, 2012.

CISC, Handbook of Steel Construction, Tenth Edition, Canadian Institute of Steel Construction, 2011.

Connor, J. J. Introduction to Structural Motion Control. Prentice Hall, August 2002.

Dahl, P. R. “Solid friction damping of mechanical vibrations”. AIAA J,Vol.14,No.12, pp.1675–1682, 1976.

Deana, E., J., Roland G. , Giovanna G. ”.On the numerical simulation of Bingham viscoplastic flow:Old and new results”. Journal of Non-Newtonian Fluid Mechanics,Vol.142,pp. 36–62,2007.

Dimock, Yoo And Wereley. “Quasi-steady Bingham Biplastic Analysis of Electrorheological and Magnetorheological Dampers”. Journal of Intelligent Material Systems and Structures,Vol.13,No.9,pp 549-559, 2002.

Dominguez, A., Sedaghati, R., Stiharu, I., “ A new dynamic hysteresis model for Magnetorheological dampers ”, Smart Materials and Structures, Vol. 15, pp.1179–1189, 2006.

Du, H., Lam, J., Zhang, N., “ Modelling of a magneto-rheological damper by evolving radial basis function networks ”, Engineering Applications of Artificial Intelligence, Vol. 19, pp.869–881, 2006.

Duan, Y. F., Ni, Y. Q., Ko, J. M., “ Cable vibration control using magnetorheological dampers ”, Journal of Intelligent Material Systems and Structures, Vol. 17, pp.321-325, 2006.

Dyke, S. J., “ Seismic protection of a benchmark building using magnetorheological dampers ”, Proceedings of the 2nd World Conference on Structural Control, Kyoto, Japan, 1998.

Dyke, S. J., Spencer Jr, B. F., “ A Comparison of Semi-Active Control Strategies for the MR Damper ”, IEEE, Intelligent Information Systems, IIS '97. Proceedings. pp.580-584, 1997.

Dyke, S. J., Spencer Jr, B. F., Sainx, M. K., Carlson, J. D., “ An experimental study of MR dampers for seismic protection ”, Smart Materials and Structures, Vol. 7, pp.693–703, 1998.

Erkus, B., Abe, M., Fujino, Y., “ Investigation of semi-active control for seismic protection of elevated highway bridges ”, Engineering Structures . Vol. 24, pp. 281–293, 2002

Esteki, K., Bagchi, A., Sedaghati, R., “ A new phenomenological model for random loading of MR /ER damper ”, 2nd International Engineering Mechanics and Materials Specialty Conference, Ottawa, Ontario, 2011.

ETABS; Integrated Analysis, Design and Drafting of Building Systems; Computers and Structures, Inc. Berkeley, CA 94704 USA

Filisko, F.E., Gamata, D.R. "Dynamic mechanical studies of electrorheological materials: Moderate frequencies". Journal of Rheology, Vol.35, pp.399-425, 1991.

Frigaarda, I.A. , Nouar, C., 2005, On the usage of viscosity regularization methods for viscoplastic fluid flow computation. Journal of Non-Newtonian Fluid Mechanics, Vol.158, pp.1–26, 2005.

Gattulli, V., Lepidi, M., Potenza, F., "Seismic protection of frame structures via semi-active control: modeling and implementation issues", Earthquake Engineering and Engineering Vibration , Vol.8, pp.627-645, 2009.

Gavin. H. P., " Multi-duct ER dampers", Journal of Intelligent Material Systems and Structures , Vol.12, No.5, 353-366, 2001.

Giuclea, M., Sireteanu, T., Stancioiu, D., Stammers, C.W., "Modelling of Magnetorheological damper dynamic behaviour by genetic algorithms based inverse method", Proceedings of the romanian academy, Series A, Vol.5, 2004.

Gordaninejad, F., Wang, X., Hitchcock, G. , Bangrakulur, K., Ruan, S., Siino, M., "Modular high-force seismic magneto-rheological fluid damper", Journal of Structural Engineering, Vol. 136, pp.135-143, 2010.

Guan, X.C., Guo, P.F., Ou, J.P., "Modeling and analyzing of hysteresis behaviour of magneto rheological dampers", The Twelfth East Asia-Pacific Conference on Structural Engineering and Construction, Hong Kong SAR, China, Vol.14, pp. 2756–2764, 2011.

Guo. D. , Hu. H., " Nonlinear-stiffness of a magnetorheological fluid damper", Nonlinear Dynamics. Vol.40, pp.241–249, 2005.

Guyan, R.J., "Reduction of Stiffness and Mass Matrices," AIAA Journal, Vol. 3, February, 1965.

Hiemenz, G. J., Choi, Y. T., Wereley, N. M., “ Seismic Control of Civil Structures Utilizing Semi-Active MR Braces”, Computer-Aided Civil and Infrastructure Engineering, Vol. 18, pp. 31–44, 2003.

Hiemenz, G. J., Wereley, N. M., “ Seismic Response of Civil Structures Utilizing Semi-Active MR and ER Bracing Systems”, Journal of Intelligent Material Systems and Structures, Vol.10. pp.646-651, 1999.

Hoang, N., Fujino, P., Warnitchai, P.,” “Optimal tuned mass damper for seismic applications and practical design formulas”, Engineering Structures, Vol. 30, Issue.3, pp. 707–715., 2008)

Hong, Wereley, N.M., Choi, S.B and Choi. “ Analytical and experimental validation of a nondimensional Bingham model for mixed-mode magnetorheological dampers”. Journal of Sound and Vibration, Vol.312, pp 399–417, 2008.

Hrovat, D., Barak, F., Rabins, M., “Semi-active versus passive or active tuned mass dampers for structural control”, Journal of Engineering Mechanics, Vol.109, pp.691-705, 1983.

Iskandarani, Y., Karimi, H. R., Hansen, M. R. “An iterative based approach for hysteresis parameters estimation in magnetorheological dampers”, Intelligent Systems (IS), 6th IEEE International Conference, Sofia, Bulgaria, pp. 439 – 444, 2012.

Jagadish KS, Prasad BKR, Rao PV. “Inelastic vibration absorber subjected to earthquake ground motions”. Earthquake Engineering and Structural Dynamics (EESD). Vol 7, No 4, pp.317–326., 1979.

Jansen, L. M., Dyke, S. J., “ Semiactive control strategies for MR dampers: comparative study”, Journal of Engineering Mechanics , Vol. 126, pp.791-803, 2000.

Ji,H.,R., Moon,Y.,J., Kim,C.,H.,Lee,I.,W., “ Structural Vibration Control Using Semiactive Tuned Mass Damper”, The Eighteenth KKCNN Symposium on Civil Engineering-KAIST6,pp.18-20, Taiwan, 2005.

Ji,H.R.,Moon,Y.,J.,Kim,C.H.Lee,I.W., “ Structural vibration control using semi active tuned mass damper”, The Eighteenth KKCNN Symposium on Civil Engineering-KAIST6,Taiwan ,December 18-20, 2005.

Jiang, Z., Christenson, R. E., “A fully dynamic magneto-rheological fluid damper model”, Smart Materials and Structures,Vol. 21, 065002, 2012.

Jiang, Z., Christenson, R., “A comparison of 200 kN magneto-rheological damper models for use in real-time hybrid simulation pretesting”, Smart Materials and Structures, Vol. 20 ,065011, 2011.

Jimenez, Rene and Alvarez-Icaza, Luis. “LuGre friction model for a magnetorheological damper”. Structural Control and Health Monitoring, pp.91–116, 2005.

Johnson, E. A., Ramallo, J. C., Spencer, B. F., Jr., and Sain, M. K., “Intelligent base isolation system”. Proc., 2nd World Conf. on Structural Control, Kyoto, Japan, 1998.

Jung, H.J., Choi, K.M., Spencer Jr, B.F. and Lee, I.W. ,“Application of some semi-active control algorithms to a smart base-isolated building employing MR dampers”, Structural Control and Health Monitoring, Vol.13,pp.693-704,2006.

Jung,H.,J.,Spencer Jr,B.,F., Lee,I.,W., “ Control of seismically excited cable-stayed bridge employing magnetorheological fluid dampers”, Journal of Structural Engineering ,Vol.129,pp.873-883,2003.

Kamath, G., Hurt, M. K., & Wereley, N. M. “Analysis and testing of Bingham plastic behaviour in semi-active electrorheological fluid dampers”.Smart Materials and Structures, Vol.5,576–590, 1996.

Kang, J., Kim, H.S., Lee, D.G., “Mitigation of wind response of a tall building using semi-active tuned mass dampers” ,The Structural Design of Tall and Special Buildings, Vol.20, ,pp.552–565 ,2011.

Kim, H.S., Roschke, P.N., Lin, P.Y., Loh, C.H. , “ Neuro-fuzzy model of hybrid semi-active base isolation system with FPS bearings and an MR damper”, Engineering Structures, Vol. 28,pp. 947–958, 2006.

Kim, Y., Langari, R., Hurlebaus, S., “Seismic response control of a large civil structure equipped with magnetorheological dampers”, Conference on Fuzzy Systems, FUZZ-IEEE , IEEE,2009.

Koo,J.H., “ Using magneto-rheological dampers in semi active tuned vibration absorbers to control structural vibrations”, Dissertation submitted to the Faculty of the Virginia Polytechnic Institute and State University,USA,2003.

Kwan Ahn, K., Quang Truong, D., Aminul Islam, M., “Modeling of a magneto-rheological (MR) fluid damper using a self tuning fuzzy mechanism”, Journal of Mechanical Science and Technology, Vol. 23,pp.1485-1499,2009.

Kwok. N. M., Ha. Q. P., Nguyen. T. H., Li .J. , Samali. B. “A novel hysteretic model for magnetorheological fluid dampers and parameter identification using particle swarm optimization”, Sensors Actuators ,Vol.132, pp.441–51, 2006.

Lee, H.J., Jung, H.J., Moon, S.J., Lee, S.K., Park, E.C., Min, K.W., “ Experimental Investigation of MR Damper-based Semiactive Control Algorithms for Full-scale Five-story Steel Frame Building”, Journal of Intelligent Material Systems and Structures, Vol. 21 ,2010.

Lee, S.H., Min, K.W., Chung, L., Lee,S.K., Lee, M.K., Hwang, J.S., Choi, S.B.,” Bracing Systems for Installation of MR Dampers in a Building Structure”, Journal of Intelligent Material Systems and Structures , Vol. 18,pp.1111-1120, 2007.

Li W.H., Yao G.Z., Chen G., Yeo S.H., Yap F.F., “Testing and steady state modelling of a linear MR damper under sinusoidal loading”, Smart Materials and Structures, Vol.9,No.1,95-102, 2000.

Liedes,T., “ Improving the performance of the semi-active tuned mass damper”, Dissertation submitted to Faculty of technology, department of mechanical engineering, University of Oulu, Finland,2010.

Lin, P. Y., Chung, L. L., “Semiactive control of building structures with semiactive tuned mass damper”, Computer-Aided Civil and Infrastructure Engineering,Vol. 20, pp. 35–51,2005.

Makris, N., Burton, S. A., Taylor, D. P., “Electrorheological damper with annular ducts for seismic protection applications”. Smart Materials and Structures,Vol.5,No.5, pp.551-564,1996.

Marano, G. C., Greco, R., “Optimization criteria for tuned mass dampers for structural vibration control under stochastic excitation”, Journal of Vibration and Control, Vol. 17, No.5, pp.679-688., 2010

Marazzi.F. “Semi-active Control of civil Structures: Implementation Aspects”. Ph.D. Thesis, Università degli Studi di Pavia, 2003.

MATLAB (R2011a), MathWorks Inc, Massachusetts, U.S.A.

Metered, H., Bonello, P., Oyadiji, S.O., “The experimental identification of Magneto-Rheological dampers and evaluation of their controllers”, Mechanical Systems and Signal Processing, Vol.24, pp.976–994,2010.

Miller, R. K., Masri, S. F., Dehghanyar T.J, Caughey, T. K., "Active vibration control of large civil structures." Journal of the Engineering Mechanics Division, ASCE, Vol. 114, No. 9, pp. 1542-1570, 1988.

Miyama T. “Seismic response of multi-story frames equipped with energy absorbing story on its top”. Tenth World Conference of Earthquake Engineering, Madrid, Spain, pp.4201–4206,1992

Mohajer Rahbari, N., Farahmand Azar, B., Talatahari, S., Safari, H.,” Semi-active direct control method for seismic alleviation of structures using MR dampers”, Structural Control and Health Monitoring, Published online in Wiley Online Library,2012.

Nagarajaiah, S., “Adaptive passive, semiactive, smart tuned mass dampers:identification and control using empirical mode decomposition, hilbert transform, and short-term fourier Transform”, Structural Control and Health Monitoring, Vol.16, pp. 800–841, 2009.

National Building Code of Canada 2010, National research council of Canada ,2010.

Ormondroyd, J., Den Hartog J.P., “ The theory of the dynamic vibration absorber”, ASME Journal of Applied Mechanics, pp.9-22, 1928.

Pang, L. and Wereley, N. M. “Nondimensional analysis of semi-active electrorheological and magnetorheological dampers using approximate parallel plate models”. Smart Materials and Structures, Vol. 7, No. 5, pp. 732–743, 1998.

Papanastasiou, T. C. ,”Flows of Materials with Yield”, Journal of Rheology, Vol.31, pp.387-404,1987.

Pinkaew, T., Fujino, Y., “Effectiveness of semi-active tuned mass dampers under harmonic excitation”, Engineering Structures ,Vol.23, pp.850–856, 2001.

Powell, J. A. “ Modelling the oscillatory response of an electrorheological fluid”. Smart Materials and Structures,Vol.3,No.4, pp. 416-438, 1994.

Pozrikidis, C, “Fluid Dynamics:Theory, Computation,and Numerical Simulation”, Springer Science, 2009.

Quang Truong,D., Kwan Ahn,K., “Identification and application of black-box model for a self-sensing damping system using a Magneto-Rheological fluid damper”, Sensors and Actuators ,Vol.161 ,pp. 305–321,2010.

Rana, R., Soong,T., “Parametric study and simplified design of tuned mass dampers”, Engineering Structures,Vol. 20,Issue.3, pp. 193–204., 1998

Renzi,E., Serino,G., “ Testing and modelling a semi-actively controlled steel framestructure equipped with MR dampers”, Structural Control and Health Monitoring , Vol.11,pp.189–221, 2004.

Roffel, A.J., Lourenco, R.,Narasimhan, S., “Experimental Studies on an Adaptive Tuned Mass Damper with Real-time Tuning Capability”, 19th Analysis & Computation Specialty Conference, ASCE, Orlando, Florida,U.S.A.,pp.314-324,2010.

Runlin,Y., Xiyuan,Z., Xihui,L. “ Seismic structural control using semi-active tuned mass dampers”, Earthquake Engineering and Engineering Vibration , Vol.1 ,pp.111-118, 2002.

Runlin,Y., Xiyuan,Z., Xihui,L., “ Seismic structural control using semi-active tuned mass dampers”, Earthquake Engineering and Engineering Vibration,Vol.1,Issue .1,pp. 111-118.2002

Sadek, F., Mohraz, B., Taylor, A., Chung, R., “A method of estimating the parameters of tuned mass dampers for seismic applications”, Earthquake Engineering and Structural Dynamics, Vol. 26, Issue.6, pp. 617-635, 1997.

Sanjay S.S., Nagarajaiah, S., “Semi-active control of sliding isolated bridges using MR dampers: an experimental and numerical study”, Earthquake Engineering and Structural Dynamics, Vol. 34, pp. 965–983, 2005.

Shivaram, A. C. , Gangadharan, K. V. “ Statistical modeling of a Magnetorheological fluid damper using the design of experiments approach ”, Smart Materials and Structures, Vol. 16 ,pp.1310–1314, 2007.

Simulink(R2011a), MathWorks, Inc, Massachusetts, U.S.A.(124)

Sodeyama, H., Suzuki, K., Sunakoda, K.,” Development of large capacity semi-active seismic damper using magneto-rheological fluid”, Journal of Pressure Vessel Technology , Vol.126, pp.105-109, 2004.

Sodeyama, H., Sunakoda, K., Fujitani, H., Soda, S., Iwata, N., Hata, K., “Dynamic tests and simulation of Magneto-Rheological dampers”, Computer-Aided Civil and Infrastructure Engineering, Vol.18, pp.45–57, 2003.

Soeiro, F. J. C. P., Stutz, L.T., Tenenbaum, R. A., Silva Neto, A. J., “Stochastic and hybrid methods for the identification in the Bouc-Wen model for Magneto – Rheological dampers”, 6th International Conference on Inverse Problems in Engineering: Theory and Practice, Journal of Physics: Conference Series, Vol. 135, 012093, 2008.

Spaggiari , A., Dragoni, E., “Efficient dynamic modelling and characterization of a magnetorheological damper”, Meccanica , Vol.47, pp.2041–2054, 2012.

Stanway, R., Sproston, J.L. and Stevens, N.G. "Non-linear modeling of an electro-rheological vibration damper". Journal of Electrostatics, pp.167-184, 1986.

Symans, M.D., Charney, F. A., Whittaker, A.S., Constantinou, M.C., Kircher, C. A., Johnson, M. W., McNamara, R.J., "Energy Dissipation Systems for Seismic Applications: Current Practice & Recent Developments," Journal of Structural Engineering, ASCE, Vol.134.No.1, pp. 3-21, 2008.

Tudon-Martinez, J.C., Lozoya-Santos, J. J., Morales-Menendez, R., Ramirez-Mendoza, R.A., "An experimental artificial-neural-network-based modeling of magneto-rheological fluid dampers", Smart Materials and Structures, Vol. 21, pp.085007, 2012.

United States Geological Survey's (USGS) Earthquake Hazards Program. Earthquakes with 1,000 or More Deaths since 1900. (June 2013) Retrieved from http://earthquake.usgs.gov/earthquakes/world/world_deaths.php

Wang, X., Gordaninejad, F., "A new Magnetorheological fluid-Elastomer mount: phenomenological modeling and experimental study", Smart Materials and Structures, Vol.18, No.9, pp.095045, 2009.

Warburton, G. B., "Optimum absorber parameters for various combinations of response and excitation parameters", Earthquake Engineering and Structural Dynamics, Vol. 10, Issue.3, pp.381-401, 1982

Watakabe, M., Tohdo, M., Chiba, O., Izumi, N., Ebisawa, H., Fujita, T., "Response control performance of a hybrid mass damper applied to a tall building", Earthquake Engineering and Structural Dynamics, Vol.30, Issue.11, pp.1655-1676., 2001

Wen, Y.K. "Method of random vibration of hysteretic systems". ASCE J. Eng. Mech, Vol.102, pp.249-263, 1976

Weng .W. Chooi, S. O. “Design, modelling and testing of magnetorheological (MR) dampers using analytical flow solutions”. Computers and Structures, Vol.86, pp.473–482, 2008.

Wereley, N. M. “Nondimensional Hersche-Bulkley Analysis of Magnetorheological and Electrorheological Dampers”.Journal of Intelligent Material Systems and Structures,Vol.23,pp.257-268,2008.

Wereley, N. M., & Lee, D.Y. “Quasi-Steady Herschel-Bulkley Analysis of Electroand Magneto-Rheological Flow Mode Dampers”. Journal of Intelligent Material Systems and Structures,Vol.10,pp.761-769, 1999.

Wereley, N. M., and Lindler, J. “Quasi-steady Bingham plastic analysis of an electrorheological flow mode bypass damper”. Smart Materials and Structures,Vol.12,pp.305–317, 2003.

Wber, F., Maslanka,M., “Frequency and damping adaptation of a TMD with controlled MR damper”, Smart Materials and Structures, Vol.12, 055011,2012.

Wereley, N. M.and Lindler, J. “Analysis and Testing of Electrorheological Bypass Dampers”. Journal of Intelligent Material Systems and Structures,Vol.10,pp. 363-376, 1999.

Xu, Y. L., Qu, W. L. , Ko, J. M., “Seismic response control of frame structures usingmagnetorheological/electrorheological dampers”, Earthquake Engineering and Structural Dynamics ,Vol. 29,pp. 557-575,2000.

Yang , Spencer, B.F., Carlson ,J.D., Sain, M.K. “Large-scale MR fluid dampers: modeling and dynamic performance considerations”. Engineering Structures,Vol.24,No3,pp. 309–323,2002.

Yang, F., Esmailzadeh, E., Sedaghati, R., “Optimal Vibration Suppression of Structures under Random Base Excitation Using Semi-Active Mass damper”, ASME Transactions, Journal of Vibration and Acoustic, 2010.

Yang, F., Esmailzadeh, E., Sedaghati, R., “Optimal Vibration Suppression of Structures Under Random Base Excitation Using Semi-Active Mass damper” , ASME Transactions, Journal of Vibration and Acoustic, 2010, Vol.132, Issue. 4, 2010.

Yang, G., Jung, H. J., Spencer Jr. B.F., “Dynamic Modeling of Full-Scale MR Dampers for Civil Engineering Applications,” US-Japan Workshop on Smart Structures for Improved Seismic Performance in Urban Region, Seattle, WA., 2001.

Yi, F., Dyke, S. J. , Frech, S., Carlson, J. D., “ Investigation of Magnetorheological Dampers for Earthquake Hazard Mitigation”, Proceedings of the 2nd World Conference on Structural Control,Kyoto,1998.

Yi,F., Dyke, S. J., Caicedo, J. M., “Seismic Response Control Using Smart Dampers”, Proceedings of the American Control Conference , San Diego, California, pp.1022-1026, 1999.

Yoshida,O., Dyke, S. J., “ Response control of full-scale irregular buildings using magnetorheological dampers”, Journal of Structural Engineering, Vol. 131,pp.734–742,2005.

Yoshioka, H., Ramallo, J.C., Spencer Jr,B. F., “ “Smart” base isolation strategies employing magnetorheological dampers”. Journal of Engineering Mechanics,Vol.128,pp. 540–551,2002.

Zemp, R., De la Llera, J. C., Almazán, J. L., “Tall building vibration control using a TM-MR damper assembly”, Earthquake Engineering and Structural Dynamics, Vol.40,pp.339–354,2011.

Zemp, R., De la Llera, J. C., Almazán, J. L., “Tall building vibration control using a TM-MR damper assembly: Experimental results and implementation ”, Earthquake Engineering and Structural Dynamics, Vol.40,pp. 257–271,2011.

Zhou, Q., Nielsena, S.R.K. ,Qu, W.L. “Semi-active control of three-dimensional vibrations of an inclined sag cable with magnetorheological dampers”. Journal of Sound and Vibration, Vol. 296, No. 1-2, pp 1–22, 2006.

Appendix A: List of Publications based on the present thesis

Journal publication

Published:

Kambiz Esteki, Ashutosh Bagchi and Ramin Sedaghati.” Dynamic Analysis of Electro- and Magneto-Rheological Fluid Dampers Using Duct Flow Models”, *Smart Materials and Structures*, Vol 23, 2014.

Submitted to Smart Structures and Systems:

Kambiz Esteki, Ashutosh Bagchi and Ramin Sedaghati.” Semi-Active Control of Seismic Response of a Building using MR Fluid-based Tuned Mass Damper” (revised)

To be submitted to Structural Design of Tall and Special Structures:

Kambiz Esteki, Ashutosh Bagchi and Ramin Sedaghati.” Evaluation of Seismic Response of Building Structures with MR Damper Bracings”

Conference publication

Kambiz Esteki, Ashutosh Bagchi and Ramin Sedaghati.” CFD Analysis of Electro- and Magneto-Rheological Fluid Dampers”, 2nd International Engineering Mechanics and Materials Specialty Conference, Ottawa, Ontario, 2011.

Kambiz Esteki, Ashutosh Bagchi and Ramin Sedaghati.” A New Phenomenological Model for Random Loading of MR /ER Damper”, 2nd International Engineering Mechanics and Materials Specialty Conference, Ottawa, Ontario, 2011.

Kambiz Esteki, Ashutosh Bagchi and Ramin Sedaghati.(2011)” Semi-Active Tuned Mass Damper for Seismic Applications”, Smart Materials, Structures & NDT in Aerospace Conference, Montreal,Quebec,2011.

Appendix B: Analytical model of ER/MR damper

The equation of motion as represented in Equation 3-3 will be solved for three different regions (Figure 3-4) as described below:

Region 1: In Region 1 (post-yield) $R_1 < r < R_{pi}$, $|\tau| > |\tau_y|$, $\frac{du}{dr} > 0$

Shear stress can be calculated from:

$$\tau = \tau_y + \mu \frac{du}{dr} \quad (\text{B-1})$$

Taking the derivatives with respect to r

$$\frac{d\tau}{dr} = \mu \frac{d^2u}{dr^2} \quad (\text{B-2})$$

Recalling Eq.3-2, Plugging Eq. (B-1) and Eq. (B-2) into Eq. (3-2) and solving for u :

$$u_1^B(r) = \frac{\Delta P}{4\mu L} r^2 - \frac{\tau_y}{\mu} r + C_1 \ln(r) + D_1 \quad (\text{B-3})$$

where, C_1 and D_1 are integration constants which depend on the boundary conditions in Region 1.

Region 2: In Region 2 (pre-yield), $R_{pi} < r < R_{po}$, $|\tau| < |\tau_y|$, $\frac{du}{dr} = 0$

This is a plug region; so, the velocity is constant

$$\frac{du}{dr} = 0$$

$$u_2^B = \text{constant} = u_p$$

Integrating Eq. (3-2) with respect to r and solving for τ

$$\tau(r) = \frac{\Delta P}{2L} r + \frac{C_2}{r} \quad (\text{B-4})$$

Region 3: In Region 3 (post-yield), $R_{po} < r < R_{r2}$, $|\tau| > |\tau_y|$, $\frac{du}{dr} < 0$

Like for region 1, one can write

$$u_3^B(r) = \frac{\Delta P}{4\mu L} r^2 + \frac{\tau_y}{\mu} r + C_3 \ln(r) + D_3 \quad (\text{B-5})$$

The quasi-static formulation of MR/ER damper for two different modes of damper; mix mode and flow mode will be discussed below.

Flow mode damper formulation

Region 1: From Figure 3-5 one can deduce that the velocity in flow mode at $R_1=0$ because the duct walls are stationary and acceleration in plug area is zero because the velocity is constant. So it can be written

$$u(R_1) = 0$$

$$\left. \frac{du}{dr} \right|_{r=R_{pi}} = 0$$

Applying these boundary conditions in Eq. (B-3) gives,

$$u_{f,1}^f(r) = \frac{\Delta P}{4\mu L} \left[r^2 - R_1^2 - 2R_{pi}^2 \ln\left(\frac{r}{R_1}\right) \right] - \frac{\tau_y}{\mu} \left[r - R_1 - R_{pi} \ln\left(\frac{r}{R_1}\right) \right] \quad (\text{B-6})$$

Region 2: Transferring from post-yield to pre-yield (from Region 1 to 2) and from pre-yield to post yield (from Region 2 to 3), the shear stress in the boundaries of different regions is τ_y or

$$\tau(R_{pi}) = \tau_y$$

$$\tau(R_{po}) = -\tau_y$$

Plugging these boundary conditions in Eq. (B-4), yields

$$\tau_y R_{pi} = \frac{\Delta P}{2L} R_{pi}^2 + C_2 \quad (\text{B-7})$$

$$-\tau_y R_{po} = \frac{\Delta P}{2L} R_{po}^2 + C_2 \quad (\text{B-8})$$

Subtracting Eq. (B-7) from Eq. (B-8)

$$\tau_y = \frac{\Delta P}{2L} (R_{pi} - R_{po}) \quad (\text{B-9})$$

Solving it for

$$R_{po} - R_{pi} = \frac{\tau_y}{\left(\frac{\Delta P}{2L}\right)} \quad (\text{B-10})$$

Where

$$\Delta P = -\frac{F}{A}$$

$\delta = (R_{pi} - R_{po})$ is flow plug thickness and

$$\delta_p = \frac{2\tau_y}{|\Delta P|} \quad (\text{B-11})$$

Region 3: with the same reasoning for region 1

$$u(R_2) = 0$$

$$\left. \frac{du}{dr} \right|_{r=R_{po}} = 0$$

and

$$u_{f,3}^B(r) = \frac{\Delta P}{4\mu L} \left[r^2 - R_2^2 - 2R_{po}^2 \ln\left(\frac{r}{R_2}\right) \right] - \frac{\tau_y}{\mu} \left[r - R_2 - R_{po} \ln\left(\frac{r}{R_2}\right) \right] \quad (\text{B-12})$$

At this point there two unknown R_{pi} and R_{po}

Recall Eq.(B-10), the velocity equation for Region 1 and 2 should be equal to u_p at the plug location or

$$u_p = u_{f,1}^B(R_{pi}) = u_{f,3}^B(R_{po})$$

or

$$u_{f,1}^B(R_{pi}) - u_{f,3}^B(R_{po}) = 0 \quad (\text{B-13})$$

Eq. (B-10) and Eq. (B-13) can be used to determine R_{pi} and R_{po} . Once they are determined, the velocity profiles for region 1, 2 and 3 can be determined using Eqs. (B-6), (B-12) and (B-13).

On the other hand, the volume flux through the electrode gap is equal to volume flux caused by the piston movement:

$$Q_p = Q_f^B \quad (\text{B-14})$$

$$\text{Or, } Q_f^B = Q_{f,1}^B + Q_{f,2}^B + Q_{f,3}^B \quad (\text{B-15})$$

where, the flux through each region can be computed as

$$Q_{f,1}^B = \int_{R_1}^{R_{pi}} u_{f,1}^B(r) 2\pi r dr \quad (\text{B-16})$$

$$Q_{f,2}^B = \int_{R_{pi}}^{R_{po}} u_{f,2}^B(r) 2\pi r dr \quad (\text{B-17})$$

$$Q_{f,3}^B = \int_{R_{po}}^{R_2} u_{f,3}^B(r) 2\pi r dr \quad (\text{B-18})$$

Plugging Eq. (B-3) into Eq.(B-16) gives

$$Q_{f,1}^B = \frac{\pi \Delta P}{8\mu L} \left[(3R_{pi}^2 - R_1^2)(R_{pi}^2 - R_1^2) - 4R_{pi}^4 \ln\left(\frac{R_{pi}}{R_1}\right) \right] - \frac{\pi \tau_y}{6\mu} \left[(R_{pi} - R_1)(7R_{pi}^2 + R_{pi}R_1 - 2R_1^2) - 6R_{pi}^3 \ln\left(\frac{R_{pi}}{R_1}\right) \right] \quad (\text{B-19})$$

Pre-yield velocity region (plug region) is constant so Eq. (B-17) can be written as

$$Q_{f,2}^B = u_p \pi (R_{po}^2 - R_{pi}^2) \quad (\text{B-20})$$

Substituting Eq. (B-12) into Eq.(B-18) results as

$$Q_{f,3}^B = \frac{\pi \Delta P}{8\mu L} \left[(-3R_{po}^2 + R_2^2)(R_{po}^2 - R_2^2) + 4R_{po}^4 \ln\left(\frac{R_{po}}{R_2}\right) \right] + \frac{\pi \tau_y}{6\mu} \left[-(R_{po} - R_2)(7R_{po}^2 + R_{po}R_2 - 2R_2^2) + 6R_{po}^3 \ln\left(\frac{R_{po}}{R_2}\right) \right] \quad (\text{B-21})$$

It is known that $Q_p = A v_0$; so, one can write

$$v_0 = \frac{Q_{f,1}^B + Q_{f,2}^B + Q_{f,3}^B}{A} \quad (\text{B-22})$$

The equivalent damping coefficient can be computed as

$$C_{eq,f}^B = \frac{F}{v_0} \quad (\text{B-23})$$

Mixed mode damper formulation

For the mixed mode operation (Figure 3-6), the inner duct wall is moves, and the boundary condition can be written as

$$u(R_1) = -v_0 \quad (\text{B-24})$$

$$\left. \frac{du}{dr} \right|_{r=R_{pi}} = 0$$

Inserting the above boundary condition into Eq.(B-3) results in,

$$u_{m,1}^B = u_{f,1}^B(r) - v_0 \quad (\text{B-25})$$

The volume flux through Region 1 is:

$$Q_{m,1}^B = \int_{R_1}^{R_{pi}} u_{m,1}^B(r) 2\pi r dr \quad (\text{B-26})$$

Substituting Eq. (B-25) into Eq. (B-26) results in,

$$Q_{m,1}^B = \int_{R_1}^{R_{pi}} u_{f,1}^B(r) 2\pi r dr - \int_{R_1}^{R_{pi}} v_0 2\pi r dr \quad (\text{B-27})$$

which can be rewrite as,

$$Q_{m,1}^B = Q_{f,1}^B - v_0 \pi (R_{pi}^2 - R_1^2) \quad (\text{B-28})$$

where, $Q_{f,1}^B$ is given by Eq. B-19

Because the boundary conditions in Region 2 and 3 in mixed mode ER/MR damper are the same as boundary conditions in flow mode ER/MR damper, one can write

$$u_{m,2}^B = u_{f,2}^B \quad (\text{B-30})$$

$$u_{m,3}^B = u_{f,3}^B$$

And because the velocity profiles are the same, the volume flux through Regions 2 and 3 in mixed mode damper are the same as for the flow mode damper; or

$$Q_{m,2}^B = Q_{f,2}^B \quad (\text{B-31})$$

$$Q_{m,3}^B = Q_{f,3}^B$$

Equating the volume of fluid displaced by the piston head to the total volume flux through the annular electrode gap,

$$Q_p = Q_m^B$$

$$\text{where, } Q_m^B = Q_{f,1}^B + Q_{f,2}^B + Q_{f,3}^B \quad (\text{B-32})$$

Substitute Eq. B-28 & Eq. B-31 in Eq. B-32, and remembering that $Q_p = Av_0$

$$v_0 = \frac{Q_{f,1}^B + Q_{f,2}^B + Q_{f,3}^B}{A + \pi(R_{pi}^2 - R_1^2)} \quad (\text{B-33})$$

v_0, R_{pi}, R_{po} are unknown; thus, two more equations are needed

Recall Eq B-10 and

$$u_{m,1}^B(R_{pi}) - u_{m,3}^B(R_{po}) = 0 \quad (\text{B-34})$$

which describes the continuity of the velocity profile in mixed mode damper case, and the equivalent damping coefficient can be estimated as,

$$C_{eq,m}^B = \frac{F}{v_0} \quad (\text{B-35})$$

Dynamic model of ER/MR damper

In the previous section ER/MR damper formulations have been established based on the assumption of steady-state behaviour of ER flow in a duct. This assumption is valid only in low frequency motion and small stroke. In high frequency motion and large stroke, dynamic and unsteady flow behaviour of ER/MR fluid should be taken in to account. In this section, the dynamic behaviour of ER/MR damper under harmonic excitation for flow mode damper according to Nguyen and Choi (2009) is presented.

The momentum equation of flow by neglecting fluid weight and compressibility of the MR/ER fluid in annular duct can be written as

$$\rho \frac{\partial u}{\partial t} - \frac{\partial \tau_{yx}}{\partial y} = -\frac{\partial p}{\partial x} = \frac{\Delta P}{L} ; \quad (-h \leq y \leq h) \quad (\text{B-37})$$

where, ρ is density of ER/MR damper fluid. Assuming the one uses Bingham rheological equation for ER/MR fluid as:

$$\tau_{yx} = \tau_y + \mu \frac{du}{dy} \quad (\text{B-38})$$

Substitution of Eq. 3-38 into Eq. 3-37 yields the equation of motion of MR/ER fluid in x direction:

$$\rho \frac{\partial u}{\partial t} - \mu \frac{\partial^2 u}{\partial y^2} = \frac{\Delta P}{L} ; \quad (-h \leq y \leq h) \quad (\text{B-39})$$

A typical shear stress vs. MR/ER fluid profile in an annular duct in flow mode damper is shown in Figure B-1. In Regions I and II shear stress exceeds yield point and fluid flows. In region III, shear stress does not exceed yield stress and fluid acts as rigid body and cannot flow. As shown in Figure B-1, the followings boundary conditions can be deducted:

$$u(h, t) = 0 \quad (\text{B-40})$$

$$\frac{\partial u(h_0, t)}{\partial y} = 0$$

An additional equation can be obtained by equating the inlet flow rate to flow rate through annular duct, as follows

$$W \left(\int_0^{h_0} u_{max}(h_0, t) dy + \int_{h_0}^h u(y, t) dy \right) = Q(t)/2 \quad (\text{B-41})$$

where, Q is inlet flow rate and W is the width of the equivalent duct which is calculated by $W = 2\pi R$ and u_{max} is maximum velocity of the flow and the velocity of the plug region.

The above governing equation, boundary condition and initial condition can be solved by Laplace Transformation technique which yields:

$$\frac{d^2 u(y, s)}{dy^2} - \frac{s}{\vartheta} u(y, s) = \frac{1}{\mu} \frac{dP(x, s)}{dx} \quad (\text{B-42})$$

where, ϑ is the kinematic viscosity coefficient

In this case, the boundary conditions are as follows,

$$u(h, s) = 0 \quad (\text{B-43})$$

$$\frac{du(h_0, s)}{dy} = 0$$

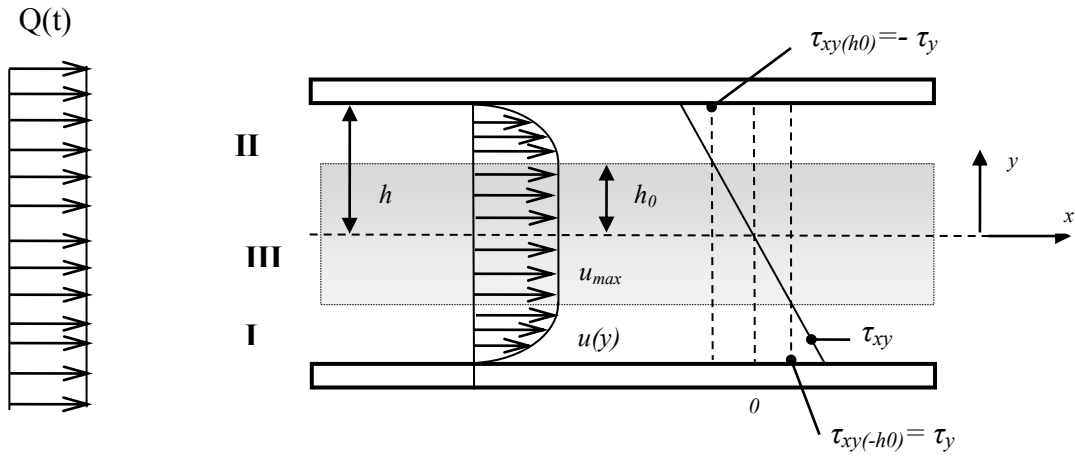


Figure B-1: Shear stress and velocity profile of MR/ER fluid flow in flow mode damper annular duct.

Additionally, the following condition is applicable.

$$\int_0^{h_0} u_{max}(h_0, s) dy + \int_{h_0}^h u(y, s) dy = u_p(s)h \quad (\text{B-44})$$

The general solution of Eq. (B-42) is given by,

$$u(y, s) = C_1 \sinh my + C_2 \cosh my + \Psi_p \quad (\text{B-45})$$

where, Ψ_p is the assumed particular solution and $m = \sqrt{\frac{s}{\nu}}$

The boundary conditions are utilized to determine C_1 and C_2 in Eq. (B-45). Substituting C_1 and C_2 into Eq. B-45

$$u(y, s) = \Psi_p \left(1 + \frac{\cosh mh_0 \cosh my - \sinh mh_0 \sinh my}{\sinh mh \sinh mh_0 - \cosh mh \cosh mh_0} \right) \quad (\text{B-46})$$

By solving the above equation for ΔP ,

$$\Delta P(s) = \rho L s \frac{Q(s)}{2W} \frac{m \Delta}{mh \Delta + mh_0 + \bar{\varepsilon}} \quad (\text{B-47})$$

where,

$$m = \sqrt{\rho s / \mu} \quad (\text{B-48})$$

$$\Delta = \sinh mh \sinh mh_0 - \cosh mh \cosh mh_0 \quad (\text{B-49})$$

$$\bar{\varepsilon} = \cosh mh_0 (\sinh mh - \sinh mh_0) - \sinh mh_0 (\cosh mh - \cosh mh_0) \quad (\text{B-50})$$

In the case of a harmonic motion, of the displacement of the piston head can be stated as:

$$u_p = \begin{cases} 0, & \text{for } t < 0 \\ u_0 \sin \omega t, & \text{for } t \geq 0 \end{cases} \quad (\text{B-51})$$

where, ω is the frequency of the piston movement and u_0 is the amplitude of its motion

Taking the Laplace transform of Eq. (B-50) results in the following:

$$u_p(s) = \frac{u_0 \omega}{s^2 + \omega^2} \quad (\text{B-52})$$

The flow rate of the MR/ER fluid through an annular duct of MR/ER flow mode damper can be stated in Laplace form as:

$$Q(s) = (A_p - A_s)u_{p(s)} = (A_p - A_s) \frac{u_0 \omega}{s^2 + \omega^2} \quad (\text{B-53})$$

Substituting Eq. (B-53) into Eq. (B-47) and then using the residue theorem to find the inverse Laplace transform of $\Delta P(s)$ results in the following equation:

$$\Delta P(t) = \rho L \frac{u_0 \omega (A_p - A_s)}{4W} [e^{i\omega t} \Gamma(i\omega) + e^{-i\omega t} \Gamma(-i\omega)] - \frac{v^2 \rho L u_0 \omega (A_p - A_s)}{W} \sum_{i=1}^{\infty} \left[\frac{\alpha_n^4}{\alpha_n^4 v^2 - \omega^2} \times \frac{(\sin \alpha_n h \sin \alpha_n h_0 + \cos \alpha_n h \cos \alpha_n h_0) e^{\alpha_n^2 v t}}{\Theta} \right] \quad (\text{B-54})$$

where,

$$\Gamma = \frac{m\Delta}{mh\Delta + mh_0 + \varepsilon} \quad (\text{B-55})$$

$$\Theta = h_0 (1 - \sin \alpha_n h_0 \sin \alpha_n h - \cos \alpha_n h_0 \cos \alpha_n h) - \alpha_n h (h - h_0) (\sin \alpha_n h_0 \cos \alpha_n h - \cos \alpha_n h_0 \sin \alpha_n h) \quad (\text{B-56})$$

where, $\alpha_n, n = 1, 2, 3, \dots \dots \infty$ is the zeros of following equation

$$\alpha h_0 - \alpha h (\sin \alpha h_0 \sin \alpha h + \cos \alpha h_0 \cos \alpha h) + \cos \alpha h_0 (\sin \alpha h - \sin \alpha h_0) - \sin \alpha h_0 (\cos \alpha h - \cos \alpha h_0) = 0 \quad (\text{B-57})$$

$$h_0 = \frac{\tau_y L}{\Delta P} \quad \text{and} \quad h_0 \leq h.$$

Calculating the pressure difference in an ER/MR damper will eventually lead to the damping force in it. The closed form solution of the damping force in an unsteady state has its obvious advantages. On the other hand, the closed-form solution is obtained in certain conditions which includes the boundary conditions and predefined strut displacement. In the ER/MR case, which

is considered in this study, the closed-form solution is developed in flow mode and for a harmonic motion.

Appendix C: TMD design

Assume a single degree of freedom structure and its TMD system (Connor, 2002) as shown in Figure C1.

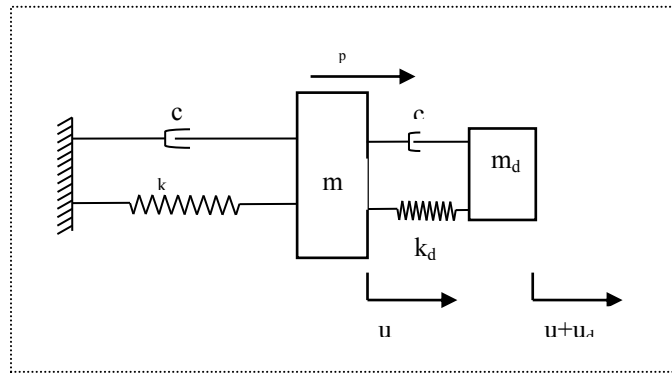


Figure C1: Single degree of freedom:TMD system

For the main structure, it can be stated that

$$\omega^2 = \frac{k}{m} \quad (C-1)$$

$$c = 2\xi\omega m \quad (C-2)$$

And for the TMD system

$$\omega_{TMD}^2 = \frac{k_{TMD}}{m_{TMD}} \quad (C-3)$$

$$c_{TMD} = 2\xi_{TMD}\omega_{TMD}m_{TMD} \quad (C-4)$$

And mass ratio will be defined as

$$\bar{m} = \frac{m_{TMD}}{m} \quad (C-5)$$

The governing equations of motion for the structure and the TMD are given by Eqs. (C-6) and (C-7), respectively, as given below.

Structure

$$(1 + \bar{m})\ddot{u} + 2\xi\omega\dot{u} + \omega^2u = \frac{p}{m} - \bar{m}\ddot{u}_{TMD} \quad (C-6)$$

TMD

$$\ddot{u}_{TMD} + 2\xi_{TMD}\omega_{TMD}\dot{u}_{TMD} + \omega_{TMD}^2u_{TMD} = -\ddot{u} \quad (C-7)$$

The design of the mass damper involves specifying the mass, stiffness, and damping coefficient of TMD system.

Undamped structure - undamped TMD:

The equation of motion of structure(Connor 2002) and its auxiliary mass (Figure C-2) can be written as:

TMD

$$m_{TMD}[\ddot{u}_{TMD} + \ddot{u}] + k_{TMD}u_{TMD} = -m_{TMD}a_g \quad (C-8)$$

Structure

$$m\ddot{u} + ku - k_{TMD}u_{TMD} = -ma_g + p \quad (C-9)$$

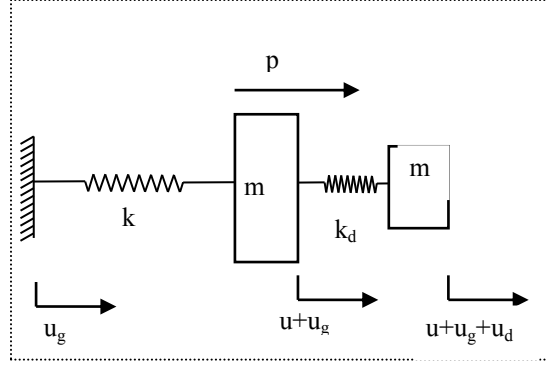


Figure C-2: Structure and its TMD

The excitation is considered to be periodic in frequency Ω

$$a_g = A_g \sin \Omega t \quad (C-10)$$

$$p_g = P \sin \Omega t \quad (C-11)$$

The responses of the structure and TMD can be expressed as

$$u = U \sin \Omega t \quad (C-12)$$

$$u_{TMD} = U_{TMD} \sin \Omega t \quad (C-13)$$

The equation of motion can be re-written as:

$$[-m_{TMD} \Omega^2 + k_{TMD}] U_{TMD} - m_{TMD} \Omega^2 U = -m_{TMD} A_g \quad (C-14)$$

$$-k_{TMD} u_{TMD} + [-m \Omega^2 + k] U = -m A_g + P \quad (C-15)$$

The solution of U and U_{TMD} are given by:

$$U = \frac{P}{k} \left(\frac{1 - \rho_{TMD}^2}{D_1} \right) - \frac{m A_g}{k} \left(\frac{1 - \rho_{TMD}^2 + \bar{m}}{D_1} \right) \quad (C-16)$$

$$U_{TMD} = \frac{P}{k_{TMD}} \left(\frac{1 - \bar{m}\rho^2}{D_1} \right) - \frac{mA_g}{k_{TMD}} \left(\frac{\bar{m}}{D_1} \right) \quad (C-17)$$

where,

$$D_1 = [1 - \rho^2][1 - \rho_{TMD}^2] - \bar{m}\rho^2 \quad (C-18)$$

$$\rho = \frac{\Omega}{\omega} = \frac{\Omega}{\sqrt{\frac{k}{m}}} \quad (C-19)$$

$$\rho = \frac{\Omega}{\omega_{TMD}} = \frac{\Omega}{\sqrt{\frac{k_{TMD}}{m_{TMD}}}} \quad (C-20)$$

Selecting the mass ratio and damper frequency ratio such that

$$1 - \rho_{TMD}^2 + \bar{m} = 0 \quad (C-21)$$

which reduces the solution to

$$U_{TMD} = -\frac{P}{k_{TMD}} \rho^2 + \frac{mA_g}{k_{TMD}} \quad (C-22)$$

$$U = \frac{p}{k} \quad (C-23)$$

Or

$$\omega_{TMD}|opt = \frac{\Omega}{\sqrt{1 + \bar{m}}} \quad (C-24)$$

With this assumption that $1\% \leq \bar{m} \leq 10\%$, $\omega_{TMD}|opt$ is very close to Ω or force frequency.

On the other hand,

$$k_{TMD}|opt = [\omega_{TMD}|opt]^2 m_{TMD} = \Omega^2 \frac{m\bar{m}}{1 + \bar{m}} \quad (C-25)$$